HIGH-THROUGHPUT PROFILING OF ION CHANNEL ACTIVITY IN LYMPHOCYTES FOR QUANTIFYING ACTIVITY OF HUMAN AUTOIMMUNE DISEASE

by

Daniel Joseph Estes

A dissertation submitted in partial fulfillment
of the requirements for the degree of
Doctor of Philosophy
(Biomedical Engineering)
in The University of Michigan
2008

Doctoral Committee:

Assistant Professor Michael Mayer, Chair
Professor David A. Fox
Associate Professor Shuichi Takayama
Assistant Professor Mohamed E. H. El Sayed

DEDICATION

To my parents and brother for always being amazingly supportive and encouraging

ACKNOWLEDGMENTS

The research described in this thesis was funded by a grant from the Michigan Technology Tri-Corridor Fund (now called the Michigan 21st Century Fund), as well as a National Science Foundation CAREER award granted to Michael Mayer. I would like to acknowledge personal funding from a Rackham Pre-Doctoral Fellowship, the Cellular Biotechnology Training Program, and a Rackham Fellowship for first-year graduate students.

Special thanks are extended to the following people, without whom this work would not have been possible:

My research advisor Michael Mayer, who has been a constant source of ideas, support, and inspiration. It is impossible to envision a better mentor or advisor, and I will always be grateful for his direction, his drive, and his friendship.

Kathryn Bennett, R.N., M.S.C.N. for performing almost all blood draws used in this work and for recruiting multiple sclerosis patients and healthy controls.

David A. Fox, M.D. for providing access to patients with rheumatoid arthritis from his clinic. Dr. Fox has also been an invaluable resource; I will always appreciate his vast knowledge of immunology and autoimmune diseases, as well as his willingness to teach me about those subjects.

Mohamed E. H. El Sayed, Ph.D. and Shuichi Takayama, Ph.D., who along with Prof. Mayer and Dr. Fox, comprised my thesis committee. I thank all the members of my committee not only for their helpful insights and suggestions, but also for their patience and support.

Steven K. Lundy, Ph.D., who patiently taught me most of the immunology techniques used in this work. He has also provided invaluable direction and assistance, especially regarding T cell activation and pathways.

Judy Endres for providing blood draws and recruiting patients with osteoarthritis.

Laura Tesmer, Daniel Cepela, and Susan Wallis, M.D., all members of the Fox lab, for their helpful discussions and experimental ideas.

Daniel D. Mikol, M.D., Ph.D. for allowing access to patients with multiple sclerosis from his clinic and for being a constant and early supporter of the technology and research presented in this work.

Sohiel Memarsadeghi, M.S., for early experiments demonstrating the efficacy of the methods used throughout this thesis. Sohiel had the original inspiration to use high-throughput electrophysiology to examine ion channels in cells from human blood, and this work would not have been possible without the early contributions of Sohiel.

Kirk Schroeder, one of the co-founders of Essen Instruments, for being one of the original supporters of high-throughput screening of ion channels in T cells.

John N. Rauch, who skillfully operated and maintained the high-throughput electrophysiology equipment for most experiments performed in this dissertation.

Vince Groppi, Ph.D. and Indu Joshi, Ph.D. from Essen Instruments, for their extremely helpful discussions and ideas for applications of the work presented in this

thesis. Also thanks to Libby Oupicka for helping to operating and maintaining the high-throughput electrophysiology device used in this work.

Jeffrey D. Uram, Ph.D. for being an amazing friend and colleague throughout my Ph.D. experience. Also thanks to the following members of the Biomembrane Lab: Francesc Marti, Ph.D. for his amazing knowledge of immunology and for experiments with γδ T cells; Ricardo Capone, Ph.D. for his creative ideas and fantastic blood cells; and Sheereen Majd, M.S.

Felipe Quiroz, who helped immensely with the quantitative RT-PCR experiments.

Nancy Renner for assistance with clinical laboratory measurements. Also, thanks to Taocong Jin, Ph.D. for assistance with RT-PCR experiments.

And finally, thanks to my parents Robert L. Estes, M.D. and Cassandra Estes for always being supportive and understanding, and also for encouraging me to always do my best. Also, thanks to my brother, Jonathan Estes, for being the most supportive brother this world has ever known, but also for helping me to relax occasionally. This thesis would certainly not have been possible without the help and support of my parents and brother.

TABLE OF CONTENTS

LIST OF TABLES

LIST OF FIGURES

ABSTRACT

HIGH-THROUGHPUT PROFILING OF ION CHANNEL ACTIVITY IN LYMPHOCYTES FOR QUANTIFYING ACTIVITY OF HUMAN AUTOIMMUNE DISEASE

by

Daniel Joseph Estes

Chair: Michael Mayer

The voltage-gated potassium ion channel, Kv1.3, in human lymphocytes is a promising target for treatment of several autoimmune diseases, including multiple sclerosis (MS) and rheumatoid arthritis (RA). Despite the relevance of this ion channel for disease, current techniques to measure Kv1.3 activity are low-throughput, laborious, and require significant expertise. Consequently, studying ion channels in cells of the immune system is not accessible to most clinicians and immunologists.

This thesis describes the development of a high-throughput assay to measure Kv1.3 activity in lymphocytes. The method is automated, specific for Kv1.3 channels, and able to measure Kv1.3 activity in 100-200 lymphocytes within 1 h. This throughput is over 20-fold higher than the throughput of manual patch clamp techniques.

Using this high-throughput assay enabled profiling Kv1.3 activity in T cells from peripheral blood of patients with MS and RA. Patients with chronic progressive (CP)

MS exhibited significantly higher Kv1.3 activity compared to healthy controls or MS patients in remission. Development of metrics to quantify the percentage of T cells with "high" Kv1.3 activity made it possible to distinguish between CP-MS patients and controls with 100% sensitivity and 94% specificity. In addition, patients with an active form of RA exhibited higher Kv1.3 activity than patients with inactive RA. These results suggest that Kv1.3 activity may be a useful clinical marker for quantifying activity of inflammatory autoimmune disorders.

Moreover, the assay developed here enabled immunological experiments to study the changes in Kv1.3 activity upon T cell stimulation. Kv1.3 activity increased ~3-fold in T cells following stimulation. We showed that this upregulation was driven by signaling through the interleukin (IL)-2 receptor. Interestingly, inflammatory cytokines IL-2 and IL-15 increased Kv1.3 activity even in the absence of signaling through T cell receptor pathways. These studies suggest that both direct activation of T cells and inflammatory cytokines lead to high Kv1.3 activity *in vivo*.

High-throughput electrophysiology introduces a promising new strategy for clinical applications such as diagnosis and therapeutic monitoring of autoimmune disease. This work also provides a general methodology that makes the study of ion channels in primary cell types accessible to laboratories not specialized in electrophysiology.

Table X.1. Publications and patent that resulted from the work presented in this thesis

Source	Type	Description
Chapter 2	Publication	Estes D.J., Memarsadeghi S. (D.J.E. and S.M. contributed equally), Marti F., Lundy S.K., Mikol D.D., Fox D.A., Mayer M. "High-throughput profiling of ion channel activity in primary human lymphocytes" *Anal. Chem.*, **2008**, (80): 3728-3735
Chapter 3	Publication	Estes D.J., Lundy S.K., Marti F., Fox D.A., Mayer M. "Functional regulation of Kv1.3 ion channels in human T lymphocytes" *Submitted,* **2008**.
Chapter 4	Publication	Estes D.J., Memarsadeghi S., Lundy S.K., Mikol D.D., Fox D.A., Mayer M. "Quantifying disease activity in patients with multiple sclerosis and rheumatoid arthritis based on Kv1.3 ion channel activity in T cells" *Submitted,* **2008**.
Chapters 2, 4	Patent Application	Memarsadeghi S., Mayer M., Estes D.J. "Potassium channel conductance as a diagnostic marker of disease" *U.S. Patent Application*, **2006**

Table X.2. Additional first author publications achieved during my Ph.D. studies that are not included in this thesis

Description
Estes D.J., Mayer M. "Electroformation of giant liposomes from spin-coated films of lipids" *Colloids and Surf. B.*, **2005**, (42): 115-123.
Estes D.J., Mayer M. "Giant liposomes in physiological buffer using electroformation in a flow chamber" *Biochim. Biophys. Acta*, **2005**, (1712): 152-160.
"Triggering and visualizing the aggregation and fusion of lipid membranes in microfluidic chambers" Estes D.J., Lopez S.R., Fuller A.O., Mayer M. *Biophys. J.*, **2006**, (91): 233-243.
Majd S., Estes D.J. (S.M. and D.J.E. contribued equally), Mayer M. "Assays for studying annexin binding to artificial lipid bilayers" *Calcium Binding Proteins*, **2006**, (1): 26-29.

CHAPTER 1

Potassium Ion Channels in Human T Lymphocytes

Between 15 and 25 million people in the U.S. suffer from some form of chronic autoimmune disorder (1), representing a severe burden both on the quality of life of these patients and on the health care system (with an annual cost of ~$120 billion) (2). While there are many types of autoimmune diseases, several, including multiple sclerosis (MS), rheumatoid arthritis (RA), and type 1 diabetes, arise from abnormal responses of T lymphocytes. Physiologically, T lymphocytes play critical roles in specifically recognizing foreign pathogens and organizing an effective response (typically involving several other cell types) to eliminate these pathogens (3). In many autoimmune disorders, however, T cells abnormally recognize self-antigens as foreign and elicit a damaging response against the body's own cells and tissues. In MS, for example, auto-reactive T cells can cross the blood-brain-barrier and initiate an inflammatory response against the myelin-sheath surrounding axons (4). The resulting damage can cause a range of disabling clinical symptoms common in MS, including blurred vision, loss of coordination, and feelings of numbness.

While significant advances have been made in understanding the pathogenesis of many autoimmune diseases, both treatment and effective diagnosis of these disease remain significant clinical challenges. Current treatments for MS and RA typically include either immunosuppressive drugs or antibodies that neutralize the products of inflammatory cells (5, 6). Many of these treatments, however, lead to significant side-effects or a compromised immune system (7, 8); more importantly, these treatments often have limited efficacy (9). In terms of diagnosis, MS especially presents clinical difficulties, as current diagnostic schemes often take several years to obtain definitive diagnosis (10, 11), well after significant axonal damage has already occurred (12, 13). Because of these challenges, it is critical to identify and characterize new therapeutic targets and drug candidates that may allow for more effective diagnosis, treatment, and monitoring of T cell-mediated autoimmune disease.

One such promising target for both diagnosis and treatment of autoimmune disease is the voltage-gated Kv1.3 ion channel in the plasma membrane of human T cells (14). T cells with high levels of Kv1.3 ion channels have been implicated in the pathogenesis of MS, RA, and type 1 diabetes (15, 16). In addition, drug compounds that specifically inhibit Kv1.3 ion channel activity ameliorated the symptoms of the aforementioned autoimmune diseases in animal models (15, 17).

The work presented here explores the use of Kv1.3 ion channel activity as a quantitative marker of activity of autoimmune disease. In this introduction, I first discuss the different types, roles, and disease-relevance of K^+ ion channels in human T cells. Then I discuss the challenges traditionally associated with measuring functional activity of ion channels. Finally, I outline the goals of this thesis to develop a high-throughput

method to study the immunological roles and clinical relevance of Kv1.3 ion channels in T cells.

1.1. Types of K^+ ion channels in human T cells

Ion channels are integral membrane proteins that regulate flux of ionic species, such as K^+, Na^+, and Ca^{2+}, through biological membranes (18). These proteins, which are typically specific for a single ionic species, undergo conformational changes (e.g. open and close) to regulate the flow of ions through the ion channel, with direction and magnitude determined by the electrochemical gradient for the particular ionic species (19). The mechanisms controlling the opening and closing of ion channels (i.e. gating) include changes in potential across the membrane, binding of intracellular or extracellular ligands, or mechanically-derived signals such as stretching (20-22).

While the importance of ion flux (especially Ca^{2+} and K^+) to the normal functioning of human lymphocytes had been known since the 1970's (23), the first characterization of ion channels in T cells occurred in 1984. The advent of the patch clamping technique (24) allowed the identification of a voltage-gated potassium channel in the plasma membrane of human T cells (~200-300 channels per cell) by the groups of Michael Cahalan and Carol Deutsch (25, 26). Later, genetic studies characterized this channel as the Kv1.3 ion channel (also called KCNA3 or type *n* channels) (27). Key biophysical features of the Kv1.3 ion channel included a single channel conductance of ~12 pS, rapid opening upon depolarization, and slow inactivation upon prolonged depolarization (28). Kv1.3 ion channels have been found in other cells of the immune system, including B lymphocytes, and macrophages; the channel is also expressed in the

following cells: platelets, microglia, osteoclasts, oligodendrocytes, and the olfactory bulb (29).

Since the identification of Kv1.3 ion channels in T cells, various other Ca^{2+}, Cl^-, and Na^+ channels have been characterized in T cells (30). In terms of K^+ channels, the group of Michael Cahalan identified a second type of K^+ channel in the plasma membrane of T cells, a ligand-gated potassium ion channel that is activated by increases in intracellular Ca^{2+} (31, 32). This channel, KCa3.1 (previously called IKCa1), is expressed in low numbers (10-20 channels per cell) on resting human T cells and has a single channel conductance similar to that of Kv1.3 ion channels. While K^+ channels in human T cells primarily include only Kv1.3 and KCa3.1, different human lymphocyte cell lines and T cells from different mammalian species have very different K^+ channel profiles compared to human T cells (Table 1.1). These differences can lead to conflicting accounts in the literature discussing the roles of individual K^+ channels in T cells; they also highlight the importance of using *human* T cells to study K^+ channels in the context of human autoimmune disease.

1.2. Roles of K^+ ion channels in activation of T cells

One of the earliest proposed roles of K^+ ion channels in T cells was that it modulates Ca^{2+}-signaling after stimulation (33). Complex changes in levels of intracellular Ca^{2+} concentrations ($[Ca^{2+}]_i$) are critical for the early stages of T cell activation (34-36). Interestingly, different types of Ca^{2+}-signals during activation, such as oscillations or sustained elevated $[Ca^{2+}]_i$ can lead to different effector functions of T cells

(e.g. variations in the types of secreted cytokines), highlighting the importance of factors that regulate Ca^{2+}-signaling (37, 38).

Table 1.1. Types of K^+ ion channels in T cells from different species and in selected human lymphocytic cell lines.

Source of cells	Description	Voltage-gated K^+ channels (#/cell)	Ca^{2+}-activated K^+ channels (#/cell)	Ref.
Human	$CD4^+$ lymphocytes	Kv1.3 (250)	KCa3.1 (10)	(25, 26, 32)
	$CD8^+$ lymphocytes	Kv1.3 (250)	KCa3.1 (10)	(16)
	B lymphocytes	Kv1.3 (100)	KCa3.1 (5)	(39)
	Class-switched memory B lymphocytes	Kv1.3 (2000)	KCa3.1 (60)	(39)
Jurkat T cells	Human leukemic cell line	Kv1.3 (400)	SKCa2 (400)	(31)
Louckes cells	B cell lymphoma line	Kv3.1 (n.k.)	not determined	(40)
Mouse	$CD4^+$ lymphocytes	Kv1.3 (20), Kv1.1, Kv1.2, Kv1.6	KCa3.1 (50)	(41, 42)
	$CD8^+$ lymphocytes	Kv3.1 (20)	KCa3.1 (50)	(42, 43)
Rat	$CD4^+$ lymphocytes	Kv1.3 (20)	KCa3.1 (10)	(14)
	$CD8^+$ lymphocytes	Kv1.3 (20)	KCa3.1 (10)	(14)

Indicated numbers of specified ion channels in each cell type are approximate numbers in resting (non-activated) cells.

n.k. = not known

To discuss the role of K^+ channels in regulating Ca^{2+}-signaling, I first need to introduce the factors that lead to Ca^{2+}-signaling in T cells upon activation (Fig. 1.1). Briefly, activation of T cells begins with specific recognition of antigen (displayed by major histocompatibility complex (MHC) heterodimers on the surface of antigen presenting cells) by the T cell receptor (TCR) (Fig. 1.1). Engagement of the TCR, as well as other co-stimulatory receptors on the T cell (e.g. cluster of differentiation (CD)-28), with the antigen presenting cell triggers a rearrangement of the T cell membrane and the formation of the immunological synapse (44). The clustering of several protein tyrosine kinases and other adaptor proteins leads to the activation of several proteins (e.g. LAT and ZAP-70), eventually generating inositol 1,4,5-trisphosphate (IP_3), among other second messengers (3).

Generated IP_3 diffuses through the cytosol, eventually binding to IP_3-receptors (IP_3R) on the endoplasmic reticulum (ER). The IP_3R is a ligand-gated Ca^{2+} channel, and the binding of IP_3 opens this channel to release Ca^{2+} from the ER into the cytosol (45). This initial rise in $[Ca^{2+}]_i$, however, is not sufficient to lead to T cell activation (35). Instead, the depletion of the Ca^{2+}-stores in the ER results in the opening of plasma membrane Ca^{2+} release-activated Ca^{2+} (CRAC) ion channels (46, 47). The opening of these channels causes a rapid influx of Ca^{2+} from the extracellular fluid into the cytosol, increasing $[Ca^{2+}]_i$ to >300 nM from a resting level of 100 nM . This rise in free calcium activates calcineurin, which then activates a number of downstream targets including the transcription factor nuclear factor of activated T cells (NF-AT) (48). Activated NF-AT is an important transcription factor for expression of several crucial cytokines, such as IL-2, IL-4, and tumor necrosis factor, which regulate T cell proliferation, differention, and

effector responses (3). For an excellent overview of basic immunology and T cell signaling pathways, see *Cellular and Molecular Immunology* by A. K. Abbas and A. H. Lichtman (3).

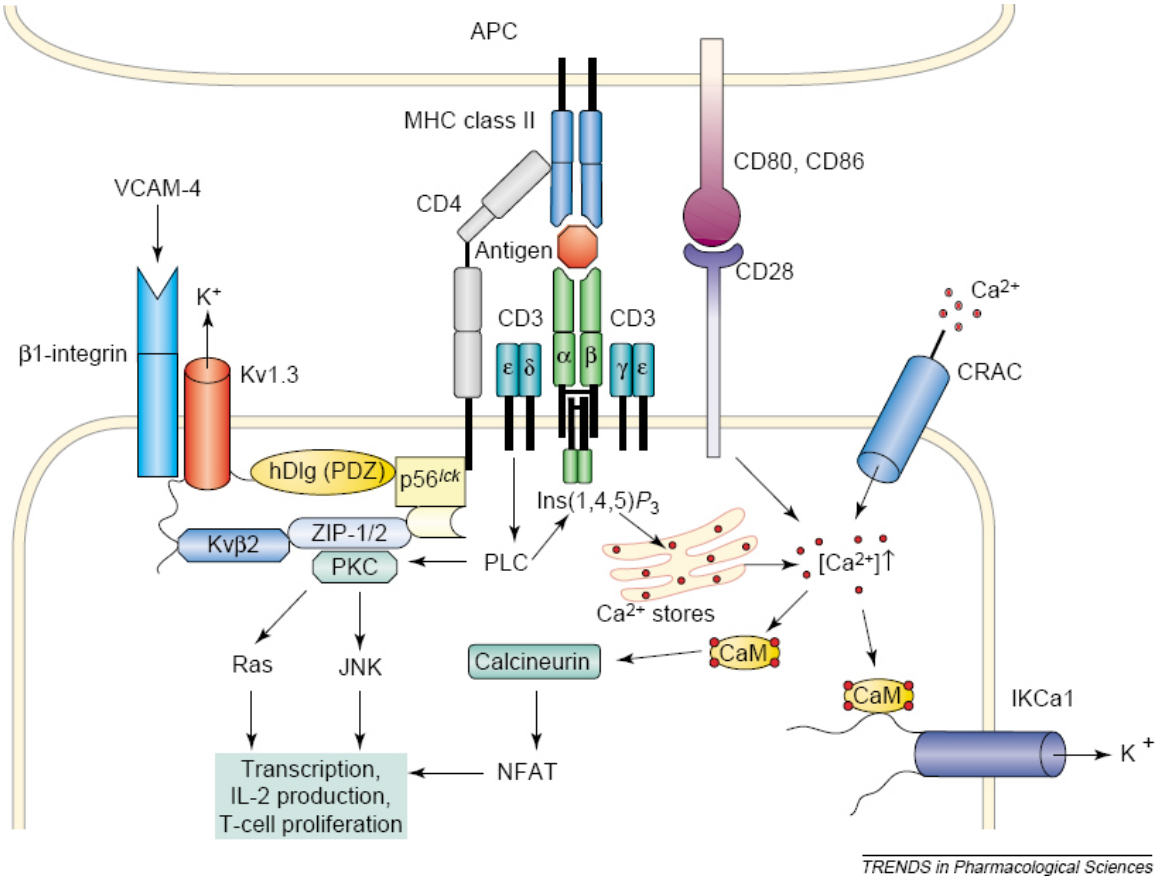

Figure 1.1 | **Overview of pathways leading to Ca^{2+}-signaling in T cells.** Ion channels play several roles in regulating Ca^{2+}-signaling after engagement of the T cell receptor (TCR) with the antigen-MHC complex. IP_3 (labeled $Ins(1,4,5)P_3$ in the figure) generated by phospholipase C (PLC)-γ induces release of Ca^{2+} into the cytosol from stores in the ER through IP_3-gated Ca^{2+} ion channels. This release opens CRAC channels in the plasma membrane to facilitate influx of Ca^{2+} into the cell. Kv1.3 and KCa3.1 (labeled IKCa1) channels facilitate this influx by maintaining a negative membrane potential (30). Efflux of K^+ through these channels counterbalances increased cytosolic Ca^{2+} levels, and allows for sustained Ca^{2+}-signaling. Figure from (49).

K^+ ion channels indirectly regulate the activation of NF-AT by allowing for a sustained increase in $[Ca^{2+}]_i$ after stimulation. The magnitude of the Ca^{2+} influx is

determined solely by the electrochemical gradient of Ca^{2+}, meaning that maximal Ca^{2+}-influx after stimulation requires a negative potential across the plasma membrane (35). K^+ channels allow for this negative membrane potential in T cells (30). Kv1.3 ion channels set the resting membrane potential of T cells (-50 to -60 mV) to allow immediate Ca^{2+}-influx upon opening of CRAC channels (30, 50). During stimulation, both Kv1.3 and KCa3.1 channels contribute to maintaining a negative membrane potential upon increased $[Ca^{2+}]_i$ to allow sustained Ca^{2+}-influx (30). Activation of KCa3.1 channels (by binding of Ca^{2+} to calmodulin sensors on the cytoplasmic side of the channel) or activation of Kv1.3 channels (by membrane depolarization from elevated $[Ca^{2+}]_i$) leads to efflux of K^+ from the cell in order to maintain a negative membrane potential (45).

Drug compounds that block Kv1.3 and KCa3.1 (Table 1.2) alter Ca^{2+}-signaling in T cells (31). Compounds that block Kv1.3 ion channels depolarize the plasma membrane of T cells (by ~+20 mV) and correspondingly reduce the influx of Ca^{2+} after stimulation (51-53). Drugs that block KCa3.1 channels also reduce Ca^{2+} influx after stimulation, although this effect is most pronounced in pre-activated T cells (54). Importantly, these drugs (especially compounds that block Kv1.3 activity) have immunosuppressive effects by affecting processes associated with Ca^{2+}-signaling, including expression of IL-2 mRNA and proliferation of T cells (55-57). As a consequence, development of drugs that block K^+ ion channels is of great interest to pharmaceutical companies and several academic research groups (Table 1.2). Interestingly, drug compounds that block both Kv1.3 and KCa3.1 have a greater effect on reducing Ca^{2+}-influx and suppressing proliferation of T cells from peripheral blood than block of either channel alone (17, 52).

Such studies highlight the importance of the interplay between Kv1.3 and KCa3.1 ion channels in regulating Ca^{2+} flux and T cell activation.

Table 1.2. Sensitivity and specificity of selected drug compounds that block K^+ channels in human T cells

Drug compound	Kv1.3 (IC_{50})	KCa3.1 (IC_{50})	Other channels affected (IC_{50})
ShK	11 pM	30 nM	Kv1.1 (25 pM), Kv1.6 (200 pM), Kv3.2 (2.5 nM)
ShK-F6CA	48 pM	not determined	Kv1.1 (4 nM)
ShK-Dap^{22}	52 pM	> 1 μM	Kv1.1 (1.8 nM), Kv1.2 (39 nM), Kv1.5 (> 1 μM), Kv1.6 (10 nM)
Margatoxin	110 pM	no effect	Kv1.1 (10 nM), Kv1.2 (500 pM)
Noxiustoxin	1 nM	no effect	Kv1.2 (2 nM)
Charybdotoxin	3 nM	5 nM	Kv1.2 (14 nM), Kv1.5 (>100 nM), KCa1.1 (3 nM)
Psora-4	3 nM	> 5 μM	Kv1.1 (62 nM), Kv1.2 (49 nM), Kv1.4 (202 nM), Kv1.5 (8 nM), Kv1.7 (100 nM)
TRAM-34	3 μM	20 nM	
Nifedipine	5 μM	4 μM	L-type Ca^{2+} channels, Kv1.5
Verapamil	6 μM	28 μM	hERG (143 nM), L-type Ca^{2+} channels
TEA	10 mM	24 mM	General blocker of K^+ channels

Abbrevations: ShK, peptide from *Stichodactyla helianthus* toxin; ShK peptide with an attached fluorescein-6-carboxylic acid; ShK-Dap^{22}, ShK peptide with an attached positively charged, non-natural amino acid diaminopropionic acid; TEA, tetraethylammonium chloride

Table adapted from references (29, 49)

1.3. Roles of Kv1.3 ion channels in volume regulation of T cells

In addition to maintaining a negative membrane potential, Kv1.3 ion channels also play important roles in regulating the volume of T cells (30). When lymphocytes are placed in a hypotonic solution, they initially swell due to rapid influx of H_2O; however,

this swelling rapidly reverses, and T cells return to normal cell volume in the hypotonic solution (30, 58). This ability of T cells to regulate their volume in a range of solutions with different osmolarities is known as regulatory volume decrease (RVD), and it is mediated by plasma membrane ion channels (30). The initial swelling of the T cell opens swelling-activated Cl^- channels, leading to efflux of Cl^- and a corresponding depolarization of the plasma membrane (22). This depolarization activates voltage-sensitive Kv1.3 channels, which help to reduce the volume of T cells through two mechanisms: (i) the opening of Kv1.3 channels maintains a negative membrane potential to permit continued Cl^- efflux; and (ii) efflux of K^+ ions combined with efflux of Cl^- ions reduces intracellular osmolarity (towards matching the hypotonic solution) at a normal T cell volume (30, 58). Correspondingly, blocking Kv1.3 ion channels inhibits RVD (58). This ability of T cells to regulate volume is important given variations in osmolarity of microvasculature and during extravasation into tissues (30, 59). Kv1.3 ion channels, therefore, may play a critical role in mediating the migration of T cells after activation through regulation of volume.

1.4. Phenotype-specific regulation of K^+ ion channels upon activation

After stimulation, human T cells upregulate expression of mRNA and increase translation of many proteins that are critical for effector functions, differentiation, and proliferation (3). K^+ ion channels are among these proteins with increased levels after activation. KCa3.1 channels upregulate from ~10 to over ~300 channels per cell through increased expression of mRNA promoted by signaling through protein kinase C (PKC) pathways (54). Activity of Kv1.3 ion channels also increases after stimulation by a factor

of three (60, 61), although Kv1.3 mRNA expression does not change after stimulation (62, 63) and the pathways leading to this functional increase in activity are not known.

Interestingly, the changes in ion channel activity that T cells undergo after stimulation depend on the particular phenotype of T cell (16). There are many different "types" of T cells, which can be differentiated on the basis of their cell surface markers and secreted cytokines (3). Three cell-surface markers that have been used to classify T cells into "memory" and "naïve" subsets are the C-C chemokine-receptor 7 (CCR7, which hones T cells to lymph nodes), CD45RA (an isoform of a tyrosine phosphatase), and CD62L (L-selectin, a cell adhesion molecule that enables migration to lymphoid tissues). The corresponding phenotypes are the following: naïve T cells (T_{naive}, $CCR7^+$, $CD45RA^+$, $CD62L^+$) which have not previously experienced antigenic stimulation; central memory T cells (T_{cm}, $CCR7^+$, $CD45RA^-$, $CD62L^+$), which persist from a previous antigenic response and hone to the lymph nodes for rapid re-activation; effector memory T cells (T_{em}, CCR7-, $CD45RA^-$, $CD62L^-$), which also persist from a previous antigenic stimulation and infiltrate peripheral tissues to exert immediate effector functions after stimulation; and in $CD8^+$ subset of T cells, $CD45RA^+$ effector memory T cells (T_{emra}, $CCR7^-$, $CD45RA^+$, $CD62L^-$) (Fig. 1.2) (64-66).

In a seminal work, Wulff *et al.* found that in vitro-activated T_{em} cells expressed significantly higher levels of Kv1.3 ion channels (~5-fold) than activated T_{naive} or T_{cm} (16). Conversely, T_{naive} and T_{cm} expressed significantly higher levels of KCa3.1 channels than T_{em} (Fig. 1.2) (16). The physiological roles of the selective increase in K^+ channels after activation of T cells are not known but may be related to Ca^{2+}-signaling specific to particular phenotypes (16, 37). Interestingly, proliferation of T_{em} cells (isolated from the

synovial fluid of patients with RA) was suppressed by a 60-fold lower concentration of a specific inhibitor of Kv1.3 ion channels compared to the concentration that blocked proliferation of T_{naive} and T_{cm} cells (42, 67). Drug compounds that block Kv1.3 ion channels, therefore, may offer a selective means for inhibiting activation of T_{em} cells while allowing proliferative and effector responses of naïve cells (42).

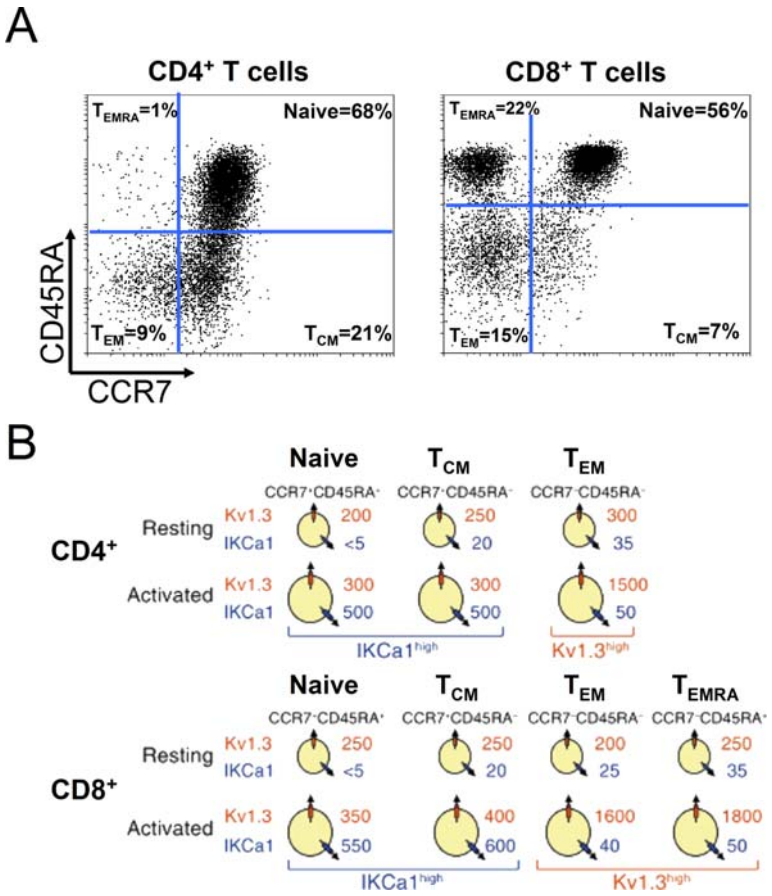

Figure 1.2 | Kv1.3 and KCa3.1 activity in effector and memory subsets of human T cells isolated from peripheral blood. (A) Example of flow cytometric analysis of effector and memory subsets of $CD4^+$ (left) and $CD8^+$ T cells isolated from peripheral blood of a healthy control subject. Naïve, central memory (T_{cm}), effector memory (T_{em}), and $CD45RA^+$ effector memory (T_{emra}) subsets were identified according to surface expression of CCR7 and CD45RA. **(B)** Representation of Kv1.3 and KCa3.1 (identified as IKCa1 above) ion channels in resting and activated human T cells of the various effector and memory subsets. Note that resting subsets have very similar numbers of Kv1.3 ion channels, but that T_{em} cells upregulate Kv1.3 ion channels by a factor of five after activation. Panel (B) figure from (16).

1.5. Links between Kv1.3 ion channels and autoimmune disease

The ability to selectively suppress T_{em} cells with compounds that block Kv1.3 activity offers a promising approach for treating autoimmune disease because T_{em} cells are implicated in the pathogenesis of several autoimmune disorders. In patients with MS, autoreactive, myelin-specific T cells are of the T_{em} phenotype (68, 69). Also, T cells isolated from inflammatory infiltrates from the brains of post-mortem MS patients exhibited characteristics of T_{em} cells (70). In patients with RA, T cells isolated from the synovial fluid of inflamed joints were predominantly T_{em} cells (71). In addition to MS and RA, type 1 diabetes, psoriasis, and uveitis are also among the autoimmune diseases in which T_{em} cells play central roles in initiating a damaging inflammatory response against self-tissues or cells (Table 1.3) (14). The characteristic that T_{em} cells persist from inflammatory responses provides a pathological basis for the chronic nature of these autoimmune disorders.

Extensive animal experiments demonstrated the ability of drug compounds that block Kv1.3 activity (and suppress T_{em} cells) to treat autoimmune disease. The first report of using drug compounds that block Kv1.3 ion channels for treatment of an animal model of disease appeared in 1997 from Koo *et al.*, who used margatoxin to prevent delayed type hypersensitivity and mixed lymphocyte reaction in miniswine (72). In 2001, Beeton *et al.* used the selective blocker of Kv1.3 ion channels, ShK, to prevent the onset of experimental autoimmune encephalomyelitis (EAE), an animal model of MS, in rats (17). Interestingly, this drug compound also improved the course of EAE when administered after onset of disease (17). Later studies showed that treatment with ShK also improved symptoms in animal models of RA, type-1 diabetes, and allergic contact

dermatitis (15, 73). These studies highlighted the promise of drug compounds that block Kv1.3 activity as a general approach for treatment of T_{em}-mediated autoimmune disease; developing compounds that are suitable for use in humans and specifically block Kv1.3 activity is a focus of several research groups and pharmaceutical companies (49, 74).

Table 1.3. Autoimmune diseases in which effector memory T cells are implicated in the pathogenesis

Disease	Target organ	Symptoms
Multiple sclerosis	Central nervous system	vision loss, tremor, speech difficulty, memory loss, loss of coordination
Rheumatoid arthritis	Joints	joint pain and swelling, morning stiffness, gradual erosion of joints
Psoriasis	Skin	dry, scaly skin and inflammation
Type 1 diabetes mellitus	Pancreas	hyperglycemia
Uveitis	Eyes	inflammation of middle layer of eye, blurred vision occasionally progressing to blindness
Chronic graft versus host disease	Various	bone marrow transplant complication, T cells from graft attack host resulting in liver, skin, and gastrointestinal damage
Hashimoto disease	Thyroid	hypothyroidism, slowed metabolism, impaired memory, slowed speech, sensitivity to cold

Table adapted with modifications from reference (14)

In addition to being a promising target for treating T_{em}-mediated autoimmune diseases, Kv1.3 ion channels may also serve as a marker for disease. As mentioned previously, T_{em} cells exhibit high levels of Kv1.3 activity upon activation, thus making Kv1.3 activity a potential marker to identify activated, and possibly pathogenic, T_{em} cells

(14). Studies from the Chandy group at the University of California, Irvine confirmed that the autoreactive disease-specific T cells from patients with MS, RA, and type 1 diabetes exhibited high levels of Kv1.3 activity upon activation (Fig. 1.3) (15, 16). T cells from healthy controls specific for antigens involved in MS-, RA-, or type 1 diabetes-antigens did not have high levels of Kv1.3 ion channels when activated, as these cells were predominantly T_{naive} or T_{cm} (15, 16). In addition, T cells with high Kv1.3 activity were found in the lesions in the brain of post-mortem MS patients (70). These studies suggest that identifying T cells with high Kv1.3 activity (e.g. from peripheral blood or from inflammatory tissues) may offer insight into activity of autoimmune disease.

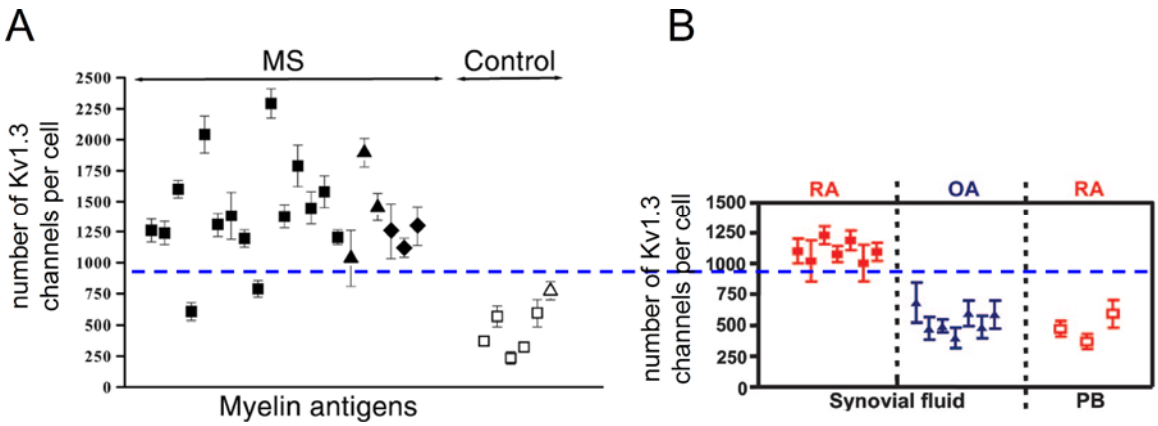

Figure 1.3 | High numbers of Kv1.3 ion channels in auto-reactive, disease-specific T cells from patients with MS and RA. (A) Number of Kv1.3 ion channels per cell in activated myelin-reactive T cell lines derived from the peripheral blood of MS patients (left) and control subjects (right). Each point represents the average ± standard error of Kv1.3 measurements in 20-30 cells from an MS patient or control subject using manual patch clamp. Cells were activated with 50 ng mL^{-1} soluble anti-CD3 antibodies. Figure from Wulff *et al.* (16). **(B)** Number of Kv1.3 ion channels per cell in T cells isolated from the synovial fluid of patients with RA and osteoarthritis (OA), or in T cells from peripheral blood from RA patients. Points represent the average ± standard error of an average of 10-15 cells from an individual RA or OA patient. T cells were activated with anti-CD3 antibodies for 48 h prior to electrophysiology experiments. Figure from Beeton *et al.* (15). Note that the y-axis for panel (B) aligns with the y-axis of panel (A) to afford comparison of Kv1.3 activity between activated MS T cell lines and activated T cells from synovial fluid.

1.6. Techniques to study ion channel activity in T cells

Previous studies of Kv1.3 ion channels in T cells have employed manual patch clamping to measure functional activity (25, 26). This technique was developed by Neher and Sakmann in the 1970's (Nobel Prize award in 1991) and allows the extremely sensitive measurement of ion channel activity in a wide range of cell types (24). Briefly, the technique involves contacting an individual cell with a glass pipette and forming a tight electrical seal between the pipette and the cell (Fig. 1.4). Typically, a "patch" of membrane from the attached cell is removed by suction or a voltage pulse, affording access to the intracellular solution of the cell. Sensitive electronics then detect the flow of ions through ion channels in the plasma membrane of the attached cell (whole-cell patch clamping) after application of a stimulus, usually either a change in voltage across the membrane or addition of a ligand (24). While patch clamping is a versatile technique capable of measuring even single-channel electrical currents, it is also serial, low-throughput, and requires significant expertise (75). A highly-trained operator can typically record whole-cell currents in 20-30 cells per day.

In addition to limitations of manual patch clamping for measuring functional activity of Kv1.3 ion channels in T cells, fluorescence-based approaches to quantifying surface expression of Kv1.3 channels also pose difficulties. The number of Kv1.3 ion channels in human T cells (100-300 channels) is close to the lower limit afforded by flow cytometry due to auto-fluorescence (76). Also, there is currently no commercially available monoclonal antibody to Kv1.3 ion channels. Beeton *et al.* developed a fluorescent analogue of a blocker of Kv1.3 ion channels (ShK-6FAM) that has a high affinity for Kv1.3 channels (77). This molecule, however, displays several positive

charges at neutral pH (74), which can lead to non-specific adsorption on negatively-charged surfaces including all membranes. The combination of non-specific adsorption and low levels of fluorescence leads to significant problems in using ShK-6FAM to evaluate expression of Kv1.3 ion channels in T cells (personal communication with Dr. Christine Beeton, 2007). The low-throughput and difficulties associated with patch clamp combined with the lack of a fluorescent assays to quantify Kv1.3 expression has the consequence that the study of ion channels in cells of the immune system is not accessible to most clinicians and immunologists.

1.7. Development of technology for performing high-throughput electrophysiology

The low throughput of manual patch clamping is primarily associated with the process of using a micromanipulator to attach a glass pipette to individual cells. In the past 10 years, however, advances in micro-fabrication and micro-machining technologies have led to techniques for recording ion channel activity without the use of "patch" pipettes (78, 79). These automated technologies employ planar substrates containing a microfabricated or machined pore (< 2 μm), in which a single cell is positioned over the micropore, typically through the application of suction (Fig. 1.4) (80). The establishing of a tight electrical seal between the cell and the planar substrate then allows for recordings of ion channel activity through ion channels of the attached cell (79). Notably, Schmidt, Mayer, and Vogel performed the first recording of ion channel activity on a planar substrate using giant liposomes as models of cells (81); the first example of ion channel

recordings from cells using planar substrates (glass) was demonstrated by Fertig *et al.* (82).

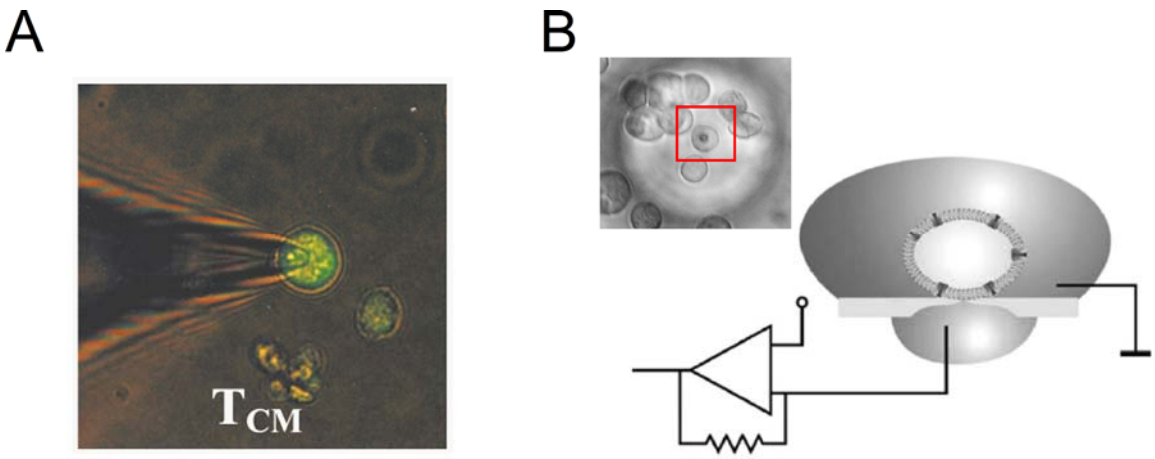

Figure 1.4 | Comparison of traditional patch clamp to recently-developed planar patch clamp techniques. (A) Example of manual (traditional) patch clamp of a T cell. Under a microscope, a single T cell is selected and attached to a glass pipette with the aid of a micromanipulator. The serial process of selecting T cells and achieving stable seals limits the throughput of this technique. Panel from (16). **(B)** Planar patch clamp technology, in which cells are added to a planar substrate containing a micropore (inset depicts the micropore region). One single cell attaches to the micropore, affording a stable electrical seal for patch clamp experiments. Because there are no moving pipettes or manual techniques involved with planar patch clamp, the process can be automated and carried out in a parallel format. Panel from (83).

Based on the concept of planar patch clamp, several commercial technologies have emerged that allow automated and parallel recordings of ion channel activity in cells (75, 83-86). These medium- to high-throughput electrophysiology devices vary in throughput (from 16 - 384 cells per experiment) and types of planar substrates (polyimide, glass, and silicon-nitride) (see Table 1.4 for a comparison of different technologies). Typically, these devices have been used for high-throughput screening of drug compounds, either to select for drugs that target certain ion channels or to ensure that other drugs do not inadvertently affect ion channel activity (86). Importantly, these

studies employed cell lines with a single recombinantly expressed ion channel type (85, 86); there have been no reports of using high-throughput patch clamp technology to examine ion channel activity in a primary cell type such as T cells.

Table 1.4. Comparisons of commercially available platforms for performing medium- to high-throughput electrophysiology experiments

Platform (Company)	Seals (MΩ)*	Format	Comments
IonWorks HT (MDS)	~100	384 well substrate, one micropore per well, 48-parallel electrodes, perforated patch	Highest throughput, automated compound addition, low seals, no intracellular perfusion
IonWorks Quattro (MDS)	30-50	384 well substrate, 64 micropores per well, perforated patch	High percentage of success for each well, does not provide distributions of current from single cells
Patchliner (Nanion)	> 1000	2, 4, or 8 wells in parallel, one micropore per well	Intracellular and extracellular perfusion, high seals, low throughput
QPatch (Sophion)	>1000	16-48 wells in parallel, one micropore per well	Multiple compound additions, laminar solution flow, no intracellular perfusion
PatchXpress (MDS)	>1000	16 wells in parallel, one micropore per well	Multiple compound additions, no intracellular perfusion

* "Seals" refers to the typical seal resistance between cells and the micropore of the planar substrate of the specified technology.

Table adapted from reference (86)

1.8. Overview of thesis

In this thesis, we use high-throughput electrophysiology technology to develop an automated assay for measuring Kv1.3 activity in human T cells. In Chapter 2, we present the details and validations of this method. In Chapter 3, we apply the high-throughput

assay to study the immunological pathways that regulate Kv1.3 activity in T cells. In Chapter 4, we profile Kv1.3 activity in T cells from patients with MS and RA to study the relationship between disease activity and Kv1.3 activity in T cells from peripheral blood. In Chapter 5, we evaluate the potential and feasibility of the high-throughput assay for measuring Kv1.3 activity for clinical and immunological studies and discuss potential future applications. This work provides an enabling and general technique to measure voltage-gated ion channels in a range of primary cell types, and it provides a new tool that may be useful for diagnosis and therapeutic monitoring of human autoimmune disease.

Chapter 1 References

1. National Institutes of Health. **2005**. Progress in Autoimmune Diseases Research.
2. Nakazawa, D. J., **2008**, *The Autoimmune Epidemic: Bodies Gone Haywire in a World Out of Balance--and the Cutting-Edge Science that Promises Hope*; Touchstone: New York.
3. Abbas, A. K., and A. H. Lichtman, **2005**, *Cellular and Molecular Immunology*, 5th Ed. ed.; Elsevier Saunders: Philadelphia, PA.
4. Sospedra, M., and R. Martin, **2005**, Immunology of multiple sclerosis, *Annu. Rev. Immunol.*, 23: 683-747.
5. Frohman, E. M., M. K. Racke, and C. S. Raine, **2006**, Multiple sclerosis--the plaque and its pathogenesis, *N. Engl. J. Med.*, 354: 942-955.
6. Steinman, L., **2004**, Immune therapy for autoimmune diseases, *Science*, 305: 212-216.

7. Rudick, R. A., W. H. Stuart, P. A. Calabresi, C. Confavreux, S. L. Galetta, E. W. Radue, F. D. Lublin, B. Weinstock-Guttman, D. R. Wynn, F. Lynn, M. A. Panzara, and A. W. Sandrock, **2006**, Natalizumab plus interferon beta-1a for relapsing multiple sclerosis, *N. Engl. J. Med.*, 354: 911-923.

8. Lipsky, P. E., D. M. van der Heijde, E. W. St Clair, D. E. Furst, F. C. Breedveld, J. R. Kalden, J. S. Smolen, M. Weisman, P. Emery, M. Feldmann, G. R. Harriman, and R. N. Maini, **2000**, Infliximab and methotrexate in the treatment of rheumatoid arthritis. Anti-Tumor Necrosis Factor Trial in Rheumatoid Arthritis with Concomitant Therapy Study Group, *N. Engl. J. Med.*, 343: 1594-1602.

9. Wolinsky, J. S., P. A. Narayana, P. O'Connor, P. K. Coyle, C. Ford, K. Johnson, A. Miller, L. Pardo, S. Kadosh, and D. Ladkani, **2007**, Glatiramer acetate in primary progressive multiple sclerosis: results of a multinational, multicenter, double-blind, placebo-controlled trial, *Ann. Neurol.*, 61: 14-24.

10. Dalton, C. M., P. A. Brex, K. A. Miszkiel, S. J. Hickman, D. G. MacManus, G. T. Plant, A. J. Thompson, and D. H. Miller, **2002**, Application of the new McDonald criteria to patients with clinically isolated syndromes suggestive of multiple sclerosis, *Ann. Neurol.*, 52: 47-53.

11. Whiting, P., R. Harbord, C. Main, J. J. Deeks, G. Filippini, M. Egger, and J. A. Sterne, **2006**, Accuracy of magnetic resonance imaging for the diagnosis of multiple sclerosis: systematic review, *BMJ*, 332: 875-884.

12. Filippi, M., M. Bozzali, M. Rovaris, O. Gonen, C. Kesavadas, A. Ghezzi, V. Martinelli, R. I. Grossman, G. Scotti, G. Comi, and A. Falini, **2003**, Evidence for

widespread axonal damage at the earliest clinical stage of multiple sclerosis, *Brain*, 126: 433-437.

13. Kuhlmann, T., G. Lingfeld, A. Bitsch, J. Schuchardt, and W. Bruck, **2002**, Acute axonal damage in multiple sclerosis is most extensive in early disease stages and decreases over time, *Brain*, 125: 2202-2212.

14. Beeton, C., and K. G. Chandy, **2005**, Potassium channels, memory T cells, and multiple sclerosis, *Neuroscientist*, 11: 550-562.

15. Beeton, C., H. Wulff, N. E. Standifer, P. Azam, K. M. Mullen, M. W. Pennington, A. Kolski-Andreaco, E. Wei, A. Grino, D. R. Counts, P. H. Wang, C. J. LeeHealey, S. A. B, A. Sankaranarayanan, D. Homerick, W. W. Roeck, J. Tehranzadeh, K. L. Stanhope, P. Zimin, P. J. Havel, S. Griffey, H. G. Knaus, G. T. Nepom, G. A. Gutman, P. A. Calabresi, and K. G. Chandy, **2006**, Kv1.3 channels are a therapeutic target for T cell-mediated autoimmune diseases, *Proc. Natl. Acad. Sci. U. S. A.*, 103: 17414-17419.

16. Wulff, H., P. A. Calabresi, R. Allie, S. Yun, M. Pennington, C. Beeton, and K. G. Chandy, **2003**, The voltage-gated Kv1.3 K+ channel in effector memory T cells as new target for MS, *J. Clin. Invest.*, 111: 1703-1713.

17. Beeton, C., H. Wulff, J. Barbaria, O. Clot-Faybesse, M. Pennington, D. Bernard, M. D. Cahalan, K. G. Chandy, and E. Beraud, **2001**, Selective blockade of T lymphocyte K(+) channels ameliorates experimental autoimmune encephalomyelitis, a model for multiple sclerosis, *Proc. Natl. Acad. Sci. U. S. A.*, 98: 13942-13947.

18. Aidley, D. J., and P. R. Stanfield, **1996**, *Ion Channels: Molecules in Action*; Cambridge University Press: Cambridge, UK.

19. Jiang, Y., A. Lee, J. Chen, M. Cadene, B. T. Chait, and R. MacKinnon, **2002**, The open pore conformation of potassium channels, *Nature*, 417: 523-526.

20. Jiang, Y., A. Lee, J. Chen, M. Cadene, B. T. Chait, and R. MacKinnon, **2002**, Crystal structure and mechanism of a calcium-gated potassium channel, *Nature*, 417: 515-522.

21. Jiang, Y., V. Ruta, J. Chen, A. Lee, and R. MacKinnon, **2003**, The principle of gating charge movement in a voltage-dependent K+ channel, *Nature*, 423: 42-48.

22. Lewis, R. S., P. E. Ross, and M. D. Cahalan, **1993**, Chloride channels activated by osmotic stress in T lymphocytes, *J. Gen. Physiol.*, 101: 801-826.

23. Lewis, R. S., and M. D. Cahalan, **1990**, Ion channels and signal transduction in lymphocytes, *Annu. Rev. Physiol.*, 52: 415-430.

24. Sakmann, B., and E. Neher, **1995**, *Single-Channel Recording*; Plenum Press: New York.

25. DeCoursey, T. E., K. G. Chandy, S. Gupta, and M. D. Cahalan, **1984**, Voltage-gated K+ channels in human T lymphocytes: a role in mitogenesis?, *Nature*, 307: 465-468.

26. Matteson, D. R., and C. Deutsch, **1984**, K channels in T lymphocytes: a patch clamp study using monoclonal antibody adhesion, *Nature*, 307: 468-471.

27. Grissmer, S., B. Dethlefs, J. J. Wasmuth, A. L. Goldin, G. A. Gutman, M. D. Cahalan, and K. G. Chandy, **1990**, Expression and chromosomal localization of a lymphocyte K+ channel gene, *Proc. Natl. Acad. Sci. U. S. A.*, 87: 9411-9415.

28. Panyi, G., **2005**, Biophysical and pharmacological aspects of K+ channels in T lymphocytes, *Eur. Biophys. J.*, 34: 515-529.

29. Chandy, G., H. Wulff, C. Beeton, P. Calabresi, G. A. Gutman, and M. Pennington, **2006**, The Kv1.3 potassium channel: physiology, pharmacology, and therapeutic indications, In: *Voltage-Gated Ion Channels as Drug Targets*; Triggle, D. J., M. Gopalakrishnan, D. Rampe, and W. Zheng, Eds.; Wiley-VCH: Weinheim, Germany, pp 214-252.

30. Cahalan, M. D., H. Wulff, and K. G. Chandy, **2001**, Molecular properties and physiological roles of ion channels in the immune system, *J. Clin. Immunol.*, 21: 235-252.

31. Grissmer, S., R. S. Lewis, and M. D. Cahalan, **1992**, Ca(2+)-activated K+ channels in human leukemic T cells, *J. Gen. Physiol.*, 99: 63-84.

32. Grissmer, S., A. N. Nguyen, and M. D. Cahalan, **1993**, Calcium-activated potassium channels in resting and activated human T lymphocytes. Expression levels, calcium dependence, ion selectivity, and pharmacology, *J. Gen. Physiol.*, 102: 601-630.

33. Chandy, K. G., T. E. DeCoursey, M. D. Cahalan, and S. Gupta, **1985**, Ion channels in lymphocytes, *J. Clin. Immunol.*, 5: 1-6.

34. Agrawal, N. G. B., and J. J. Linderman, **1995**, Calcium Response of Helper T-Lymphocytes to Antigen-Presenting Cells in a Single-Cell Assay, *Biophys. J.*, 69: 1178-1190.

35. Lewis, R. S., **2001**, Calcium signaling mechanisms in T lymphocytes, *Annu. Rev. Immunol.*, 19: 497-521.

36. Lewis, R. S., and M. D. Cahalan, **1989**, Mitogen-induced oscillations of cytosolic Ca2+ and transmembrane Ca2+ current in human leukemic T cells, *Cell Regul.*, 1: 99-112.

37. Dolmetsch, R. E., R. S. Lewis, C. C. Goodnow, and J. I. Healy, **1997**, Differential activation of transcription factors induced by Ca2+ response amplitude and duration, *Nature*, 386: 855-858.

38. Dolmetsch, R. E., K. Xu, and R. S. Lewis, **1998**, Calcium oscillations increase the efficiency and specificity of gene expression, *Nature*, 392: 933-936.

39. Wulff, H., H. G. Knaus, M. Pennington, and K. G. Chandy, **2004**, K+ channel expression during B cell differentiation: Implications for immunomodulation and autoimmunity, *J. Immunol.*, 173: 776-786.

40. Grissmer, S., S. Ghanshani, B. Dethlefs, J. D. McPherson, J. J. Wasmuth, G. A. Gutman, M. D. Cahalan, and K. G. Chandy, **1992**, The Shaw-related potassium channel gene, Kv3.1, on human chromosome 11, encodes the type l K+ channel in T cells, *J. Biol. Chem.*, 267: 20971-20979.

41. Liu, Q. H., B. K. Fleischmann, B. Hondowicz, C. C. Maier, L. A. Turka, K. Yui, M. I. Kotlikoff, A. D. Wells, and B. D. Freedman, **2002**, Modulation of Kv channel expression and function by TCR and costimulatory signals during peripheral CD4(+) lymphocyte differentiation, *J. Exp. Med.*, 196: 897-909.

42. Beeton, C., M. W. Pennington, H. Wulff, S. Singh, D. Nugent, G. Crossley, I. Khaytin, P. A. Calabresi, C. Y. Chen, G. A. Gutman, and K. G. Chandy, **2005**, Targeting effector memory T cells with a selective peptide inhibitor of Kv1.3 channels for therapy of autoimmune diseases, *Mol. Pharmacol.*, 67: 1369-1381.

43. Lewis, R. S., and M. D. Cahalan, **1988**, Subset-specific expression of potassium channels in developing murine T lymphocytes, *Science*, 239: 771-775.

44. Grakoui, A., S. K. Bromley, C. Sumen, M. M. Davis, A. S. Shaw, P. M. Allen, and M. L. Dustin, **1999**, The immunological synapse: a molecular machine controlling T cell activation, *Science*, 285: 221-227.

45. Panyi, G., Z. Varga, and R. Gaspar, **2004**, Ion channels and lymphocyte activation, *Immunol. Lett.*, 92: 55-66.

46. Zweifach, A., and R. S. Lewis, **1993**, Mitogen-regulated Ca2+ current of T lymphocytes is activated by depletion of intracellular Ca2+ stores, *Proc. Natl. Acad. Sci. U. S. A.*, 90: 6295-6299.

47. Zhang, S. L., Y. Yu, J. Roos, J. A. Kozak, T. J. Deerinck, M. H. Ellisman, K. A. Stauderman, and M. D. Cahalan, **2005**, STIM1 is a Ca2+ sensor that activates CRAC channels and migrates from the Ca2+ store to the plasma membrane, *Nature*, 437: 902-905.

48. Rao, A., C. Luo, and P. G. Hogan, **1997**, Transcription factors of the NFAT family: regulation and function, *Annu. Rev. Immunol.*, 15: 707-747.

49. Chandy, K. G., H. Wulff, C. Beeton, M. Pennington, G. A. Gutman, and M. D. Cahalan, **2004**, K+ channels as targets for specific immunomodulation, *Trends Pharmacol. Sci.*, 25: 280-289.

50. Lewis, R. S., and M. D. Cahalan, **1995**, Potassium and calcium channels in lymphocytes, *Annu. Rev. Immunol.*, 13: 623-653.

51. Leonard, R. J., M. L. Garcia, R. S. Slaughter, and J. P. Reuben, **1992**, Selective blockers of voltage-gated K+ channels depolarize human T lymphocytes:

mechanism of the antiproliferative effect of charybdotoxin, *Proc. Natl. Acad. Sci. U. S. A.*, 89: 10094-10098.

52. Rader, R. K., L. E. Kahn, G. D. Anderson, C. L. Martin, K. S. Chinn, and S. A. Gregory, **1996**, T cell activation is regulated by voltage-dependent and calcium-activated potassium channels, *J. Immunol.*, 156: 1425-1430.

53. Lin, C. S., R. C. Boltz, J. T. Blake, M. Nguyen, A. Talento, P. A. Fischer, M. S. Springer, N. H. Sigal, R. S. Slaughter, M. L. Garcia, and et al., **1993**, Voltage-gated potassium channels regulate calcium-dependent pathways involved in human T lymphocyte activation, *J. Exp. Med.*, 177: 637-645.

54. Ghanshani, S., H. Wulff, M. J. Miller, H. Rohm, A. Neben, G. A. Gutman, M. D. Cahalan, and K. G. Chandy, **2000**, Up-regulation of the IKCa1 potassium channel during T-cell activation. Molecular mechanism and functional consequences, *J. Biol. Chem.*, 275: 37137-37149.

55. Price, M., S. C. Lee, and C. Deutsch, **1989**, Charybdotoxin inhibits proliferation and interleukin 2 production in human peripheral blood lymphocytes, *Proc. Natl. Acad. Sci. U. S. A.*, 86: 10171-10175.

56. Hu, L., M. Pennington, Q. Jiang, K. A. Whartenby, and P. A. Calabresi, **2007**, Characterization of the functional properties of the voltage-gated potassium channel Kv1.3 in human CD4(+) T lymphocytes, *J. Immunol.*, 179: 4563-4570.

57. Freedman, B. D., M. A. Price, and C. J. Deutsch, **1992**, Evidence for voltage modulation of IL-2 production in mitogen-stimulated human peripheral blood lymphocytes, *J. Immunol.*, 149: 3784-3794.

58. Grinstein, S., and J. D. Smith, **1990**, Calcium-independent cell volume regulation in human lymphocytes. Inhibition by charybdotoxin, *J. Gen. Physiol.*, 95: 97-120.

59. Mao, J. W., L. W. Wang, T. Jacob, X. R. Sun, H. Li, L. Y. Zhu, P. Li, P. Zhong, S. H. Nie, and L. X. Chen, **2005**, Involvement of regulatory volume decrease in the migration of nasopharyngeal carcinoma cells, *Cell Res.*, 15: 371-378.

60. Estes, D. J., S. Memarsadeghi, S. K. Lundy, F. Marti, D. D. Mikol, D. A. Fox, and M. Mayer, **2008**, High-throughput profiling of ion channel activity in primary human lymphocytes, *Anal. Chem.*, 80: 3728-3735.

61. Lee, S. C., D. E. Sabath, C. Deutsch, and M. B. Prystowsky, **1986**, Increased voltage-gated potassium conductance during interleukin 2-stimulated proliferation of a mouse helper T lymphocyte clone, *J. Cell Biol.*, 102: 1200-1208.

62. Cai, Y. C., P. B. Osborne, R. A. North, D. C. Dooley, and J. Douglass, **1992**, Characterization and functional expression of genomic DNA encoding the human lymphocyte type n potassium channel, *DNA Cell Biol.*, 11: 163-172.

63. Attali, B., G. Romey, E. Honore, A. Schmid-Alliana, M. G. Mattei, F. Lesage, P. Ricard, J. Barhanin, and M. Lazdunski, **1992**, Cloning, functional expression, and regulation of two K+ channels in human T lymphocytes, *J. Biol. Chem.*, 267: 8650-8657.

64. Lanzavecchia, A., and F. Sallusto, **2000**, Dynamics of T lymphocyte responses: Intermediates, effectors, and memory cells, *Science*, 290: 92-97.

65. Sallusto, F., C. R. Mackay, and A. Lanzavecchia, **2000**, The role of chemokine receptors in primary, effector, and memory immune responses, *Annu. Rev. Immunol.*, 18: 593-+.

66. Geginat, J., F. Sallusto, and A. Lanzavecchia, **2001**, Cytokine-driven proliferation and differentiation of human naive, central memory, and effector memory CD4(+) T cells, *J. Exp. Med.*, 194: 1711-1719.

67. Wulff, H., C. Beeton, and K. G. Chandy, **2003**, Potassium channels as therapeutic targets for autoimmune disorders, *Curr. Opin. Drug Discov. Devel.*, 6: 640-647.

68. Scholz, C., K. T. Patton, D. E. Anderson, G. J. Freeman, and D. A. Hafler, **1998**, Expansion of autoreactive T cells in multiple sclerosis is independent of exogenous B7 costimulation, *J. Immunol.*, 160: 1532-1538.

69. Burns, J., B. Bartholomew, and S. Lobo, **1999**, Isolation of myelin basic protein-specific T cells predominantly from the memory T-cell compartment in multiple sclerosis, *Ann. Neurol.*, 45: 33-39.

70. Rus, H., C. A. Pardo, L. N. Hu, E. Darrah, C. Cudrici, T. Niculescu, F. Niculescu, K. M. Mullen, R. Allie, L. P. Guo, H. Wulff, C. Beeton, S. I. V. Judge, D. A. Kerr, H. G. Knaus, K. G. Chandy, and P. A. Calabresi, **2005**, The voltage-gated potassium channel Kv1.3 is highly expressed on inflammatory infiltrates in multiple sclerosis brain, *Proc. Natl. Acad. Sci. U. S. A.*, 102: 11094-11099.

71. Ezawa, K., M. Yamamura, H. Matsui, Z. Ota, and H. Makino, **1997**, Comparative analysis of CD45RA- and CD45RO-positive CD4+T cells in peripheral blood, synovial fluid, and synovial tissue in patients with rheumatoid arthritis and osteoarthritis, *Acta Med. Okayama*, 51: 25-31.

72. Koo, G. C., J. T. Blake, A. Talento, M. Nguyen, S. Lin, A. Sirotina, K. Shah, K. Mulvany, D. Hora, Jr., P. Cunningham, D. L. Wunderler, O. B. McManus, R. Slaughter, R. Bugianesi, J. Felix, M. Garcia, J. Williamson, G. Kaczorowski, N.

H. Sigal, M. S. Springer, and W. Feeney, **1997**, Blockade of the voltage-gated potassium channel Kv1.3 inhibits immune responses in vivo, *J. Immunol.*, 158: 5120-5128.

73. Azam, P., A. Sankaranarayanan, D. Homerick, S. Griffey, and H. Wulff, **2007**, Targeting effector memory T cells with the small molecule Kv1.3 blocker PAP-1 suppresses allergic contact dermatitis, *J. Invest. Dermatol.*, 127: 1419-1429.

74. Pennington, M. W., V. M. Mahnir, D. S. Krafte, I. Zaydenberg, M. E. Byrnes, I. Khaytin, K. Crowley, and W. R. Kem, **1996**, Identification of three separate binding sites on SHK toxin, a potent inhibitor of voltage-dependent potassium channels in human T-lymphocytes and rat brain, *Biochem. Biophys. Res. Commun.*, 219: 696-701.

75. Chiu, D. T., and O. Orwar, **2004**, Functional cell-based high throughput drug screening, *Drug Disc. World*, 5: 45-51.

76. Shapiro, H. M., **2005**, *Practical Flow Cytometry*; Alan R. Liss, Inc.: New York.

77. Beeton, C., H. Wulff, S. Singh, S. Botsko, G. Crossley, G. A. Gutman, M. D. Cahalan, M. Pennington, and K. G. Chandy, **2003**, A novel fluorescent toxin to detect and investigate Kv1.3 channel up-regulation in chronically activated T lymphocytes, *J. Biol. Chem.*, 278: 9928-9937.

78. Uram, J. D., K. Ke, A. J. Hunt, and M. Mayer, **2006**, Label-free affinity assays by rapid detection of immune complexes in submicrometer pores, *Angew. Chem. Int. Ed. Engl.*, 45: 2281-2285.

79. Mayer, M., S. Terrettaz, L. Giovangrandi, T. Stora, and H. Vogel, **2003**, Functional analysis of ion channels: Planar patch clamp and impedance

spectroscopy of tethered lipid membranes, In: *Biosensors - A practical Approach,* 2nd ed.; Cass, A. E. G., Ed.; Oxford University Press: Oxford, UK, pp 153-184.

80. Behrends, J. C., and N. Fertig, Planar Patch Clamping, In: *Patch Clamp Analysis: Advanced Techniques*; W., W., Ed.; Humana Press, Inc.: Totowa, NJ, pp 411-433.

81. Schmidt, C., M. Mayer, and H. Vogel, **2000**, A Chip-Based Biosensor for the Functional Analysis of Single Ion Channels *Angew. Chem. Int. Ed. Engl.*, 39: 3137-3140.

82. Fertig, N., R. H. Blick, and J. C. Behrends, **2002**, Whole cell patch clamp recording performed on a planar glass chip, *Biophys. J.*, 82: 3056-3062.

83. Bruggemann, A., S. Stoelzle, M. George, J. C. Behrends, and N. Fertig, **2006**, Microchip technology for automated and parallel patch-clamp recording, *Small*, 2: 840-846.

84. Kiss, L., P. B. Bennett, V. N. Uebele, K. S. Koblan, S. A. Kane, B. Neagle, and K. Schroeder, **2003**, High throughput ion-channel pharmacology: planar-array-based voltage clamp, *Assay Drug Dev. Technol.*, 1: 127-135.

85. Schroeder, K., B. Neagle, D. J. Trezise, and J. Worley, **2003**, IonWorks (TM) HT: A new high-throughput electrophysiology measurement platform, *J. Biomol. Screen.*, 8: 50-64.

86. Dunlop, J., M. Bowlby, R. Peri, D. Vasilyev, and R. Arias, **2008**, High-throughput electrophysiology: an emerging paradigm for ion-channel screening and physiology, *Nat. Rev. Drug Discov.*, 7: 358-368.

CHAPTER 2

High-Throughput Profiling of Ion Channel Activity in Primary Human Lymphocytes

We present a high-throughput method to quantify the functional activity of potassium (K^+) ion channels in primary human lymphocytes. This method is rapid, automated, specific (here for the voltage-gated Kv1.3 ion channel), and capable of measuring, in parallel, the electrical currents of over 200 individual lymphocytes isolated from freshly drawn blood. The statistics afforded by high-throughput measurements allowed direct comparison of Kv1.3 activity in different subsets of lymphocytes, including $CD4^+$ and $CD8^+$ T cells, γδ T cells, and B cells. High-throughput measurements made it possible to quantify the heterogeneous, functional response of Kv1.3 ion channel activity upon stimulation of $CD4^+$ and $CD8^+$ T cells with mitogen. These experiments enabled elucidation of time-courses of functional Kv1.3 activity upon stimulation as well as studies of the effects of the concentration of mitogenic antibodies on Kv1.3 levels. The results presented here suggest that Kv1.3 ion channel activity can be used as a functional activation marker in T cells, and that it correlates to cell size and levels of a surface antigen, CD25. Moreover, this work presents an enabling methodology that can be

applied widely, allowing high-throughput screening of specific voltage-gated ion channels in a variety of primary cells.

2.1. Introduction

Ion channels in cells of the immune system serve important roles in generating an effective response to pathogens (1). The plasma membranes of lymphocytes contain a variety of calcium (Ca^{2+}), potassium (K^{+}), and chloride (Cl^{-}) ion channels that help to regulate at least four cellular properties, including: (i) the membrane potential; (ii) signal transduction, especially in the activation of different cell types; (iii) cell volume; and (iv) cell motility (2).

One of the best studied ion channels in immune cells is the voltage-gated K^{+} ion channel, Kv1.3, in human T cells (3, 4). Kv1.3 ion channels regulate the resting potential of T cells and help to regulate Ca^{2+}-signaling after activation of T cells (5, 6). This Ca^{2+}-signaling leads to the expression of cytokines that mediate proliferation and differentiation of effector T cells as well as regulation of the inflammatory response (7). Interestingly, T cells with high Kv1.3 ion channel activity have been implicated in the pathogenesis of human autoimmune diseases including multiple sclerosis, type I diabetes, and rheumatoid arthritis (8-10). Therapeutic compounds that specifically block Kv1.3 activity have led to amelioration of the symptoms of the above diseases in animal models (9, 11). The Kv1.3 ion channel is, therefore, a promising therapeutic target for autoimmune diseases (12-15), and studying the roles and functions of Kv1.3 channels in primary human T cells, as well as other cells of the immune system, is critical for understanding the consequences of therapies that involve blocking Kv1.3 channels.

A significant challenge in studying Kv1.3 ion channels in primary lymphocytes is the lack of an accessible and high-throughput technique to conduct parallel recordings of functional ion channel activity in various subpopulations of cells. Previous studies have employed manual patch-clamping (8, 16), which involves contacting a single cell with a glass micropipette to gain electrical access to the inside of the cell followed by measuring the flow of ions through the plasma membrane of the entire cell (17). While this manual whole-cell patch clamping technique is extremely sensitive and versatile, the technique is serial, has low throughput, and requires significant expertise (18). As a result, quantifying ion channel activity in primary cells of the immune system under various conditions has thus far not been a feasible approach for most immunologists and clinicians.

Here, we present an automated, high-throughput method capable of measuring functional Kv1.3 ion channel activity in over 200 individual lymphocytes within one hour. In recent years, several new technologies have emerged that automate the patch-clamp method, using different strategies (19-22) and offering varying degrees of throughput (typically 16 – 384 cells per run). In the present study, we used a high-throughput patch clamp device capable of measuring up to 384 cells per experiment (23, 24) to implement an automated assay that is: (i) capable of measuring voltage-gated ion channels in a primary cell type, specifically different subsets of lymphocytes; (ii) specific for endogenous, wild-type levels of Kv1.3 ion channels from human subjects; and (iii) able to compare different T cell populations in parallel. We applied this assay to elucidate time-courses of Kv1.3 activity after T cell stimulation as well as the effects of different stimulation conditions on the regulation of the activity of this ion channel. This study presents the first example of functional high-throughput screening of ion channels in a

primary cell type and makes it possible to place the upregulation of Kv1.3 activity into the context of the signaling cascade during activation of human T cells.

2.2. Experimental Section

Human subjects. We obtained peripheral venous blood from 12 healthy subjects without history of autoimmune disease. We obtained multiple blood samples from six subjects. The Institutional Review Board at the University of Michigan approved blood draws and protocols.

High-throughput electrophysiology assay. We used an IonWorks HT high-throughput electrophysiology instrument (MDS Analytical Technologies, Sunnyvale, CA) made available via collaboration with the original developers of the technology (Essen Instruments, Ann Arbor, MI) to measure Kv1.3 currents in lymphocytes. Separated lymphocytes were suspended in Dulbecco's phosphate buffered saline (D-PBS, with Ca^{2+} and Mg^{2+}) at a concentration of 5×10^5 cells mL^{-1} and stored at room temperature for 30 min prior to electrophysiology experiments. A typical experiment required 2.2 mL of cell suspension. Integrated fluidics within the IonWorks instrument then automatically dispensed cells into the single-use 384-well "patch plate". The bottom of these plates consisted of microfabricated polyimide that contained one micropore in each well. For experiments with lymphocytes, we typically used only patch plates with an open hole resistance (i.e. before adding cells) of at least 3.0 MΩ (corresponding to hole diameters below 1.8 μm, measured in D-PBS with Ca^{2+} and Mg^{2+}). In each experiment, $CD4^+$ T cells occupied half of the patch-plate (192 microwells), and the other half was occupied by either $CD8^+$ T cells, B cells, or γδ T cells, allowing for direct comparisons

between subsets of lymphocytes. The IonWorks HT instrument applied and maintained suction from below each well to seal a single lymphocyte over the hole in each well of the patch plate. The intracellular recording solution consisted of 100 mM K^+ D-gluconic acid, 50 mM KCl, 3 mM $MgCl_2$, 5 mM EGTA pH 7.3 (all from Sigma-Aldrich). To gain electrical access to the interior of the sealed cells, automated fluidics introduced a pore-forming peptide (amphotericin B, 100 μg mL^{-1} with 0.2% DMSO) in the intracellular recording solution. Recordings started 5 min after introduction of the peptide.

To record Kv1.3 ion channel currents, T cells were first voltage-clamped at a holding potential of -80 mV for 30 s before applying a depolarizing step pulse from -80 mV to +40 mV for 300 ms. This voltage-step opened voltage-gated channels, and the resulting current was recorded in parallel using an array of 48 Ag/AgCl electrodes. After performing this process in all of the 384 wells, the integrated fluidics array added a specific blocker of Kv1.3 channels, 6-FAM-AEEAc-*Stichodactyla helianthus* neurotoxin peptide (ShK-F6CA, Bachem Biosciences, King of Prussia, PA), to a final concentration of 72 nM to each well of the patch plate (25). After an incubation time of 3 min to specifically block all Kv1.3 ion channels, electrical currents from the attached cells were then measured again using the same voltage protocols as described above. We defined Kv1.3 current as the difference between the pre- and post-compound currents (see Figure 2-App.3 for detailed information on data processing algorithms as well as Supporting Methods in section 2-App.Methods for details on wash protocols, cell separations and culture, flow cytometry assays, and statistical analyses).

2.3. Automated high-throughput profiling of Kv1.3 ion channels in human lymphocytes

To establish a method that enables rapid profiling of Kv1.3 ion channel activity in different subtypes of lymphocytes from human blood, we adopted a high-throughput patch-clamp technology that had previously been developed for drug-screening in the pharmaceutical industry (Fig. 2.1) (23, 24). This technology is based on 384 microwells with a single micropore at the bottom of each well (Fig. 2.1A). Cells in suspension are automatically positioned onto these micropores by suction, enabling up to 384 whole-cell patch clamp recordings within one hour. An integrated microfluidics array dispenses cells, drugs, or other molecules in solution to each of the 384 wells, while keeping the cells attached to the micropore. Previous applications of this high-throughput electrophysiology technology employed cell lines (diameter typically > 15 μm) that over-expressed one particular, recombinant ion channel protein (26). To the best of our knowledge, there have been no published manuscripts of high-throughput measurements of ion channels in primary cells, possibly because of difficulties in isolating primary cell types in large numbers and possibly because the number of a particular endogenous ion channel in wild-type primary cells may have been considered too low to detect. We chose lymphocytes as examples of primary cell types because: (i) the molecular mechanisms of activation of these cell is fundamentally important for an effective immune response; (ii) these cells can be obtained in high yield from peripheral blood; (iii) they can be easily activated *ex vivo*; and (iv) emerging evidence identifies ion channels in lymphocytes as potential drug targets for treatment of autoimmune disease. These cells, however, offer several challenges to high-throughput screens because of their small sizes (~8 μm

diameter for T cells from blood (27)) and diversity with respect to endogenous ion channels in their plasma membranes (2).

To adapt high-throughput patch clamp technology for a specific ion channel (here the voltage-gated potassium channel Kv1.3) in subsets of lymphocytes without over-expressing the channel protein, implemented the following four strategies. First, we isolated specific lymphocyte subsets ($CD4^+$ T cells, $CD8^+$ T cells, γδ T cells, and B cells) using commercially-available magnetic beads coated with an antibody against particular surface markers (e.g. CD4) which are expressed on the blood cell subset of interest. Second, we specifically selected 384-well "patch-plates" with micropore sizes below 1.8 μm (Fig. 2.1*A*). Third, we developed a differential measurement of electrical current through individual cells before and after application of a highly specific blocker of Kv1.3 ion channels (the ShK-F6CA peptide) (25, 28). This strategy ensured specificity for the Kv1.3 ion channel while subtracting possible "leak" currents (Fig. 2.1*B,C*). We confirmed specificity, as well as efficacy of block, by testing additional compounds that either block Kv1.3 ion channels (margatoxin and Psora-4) (12) or have minimal effect (TRAM-34) (12) on these channels (Figs. 2-App.1, 2-App.2). And fourth, we used data processing algorithms (i) to exclude cells that did not remain attached to the micropore throughout the experiment and (ii) to compute the magnitude of Kv1.3-specific currents after the differential measurements (Fig. 2-App.3).

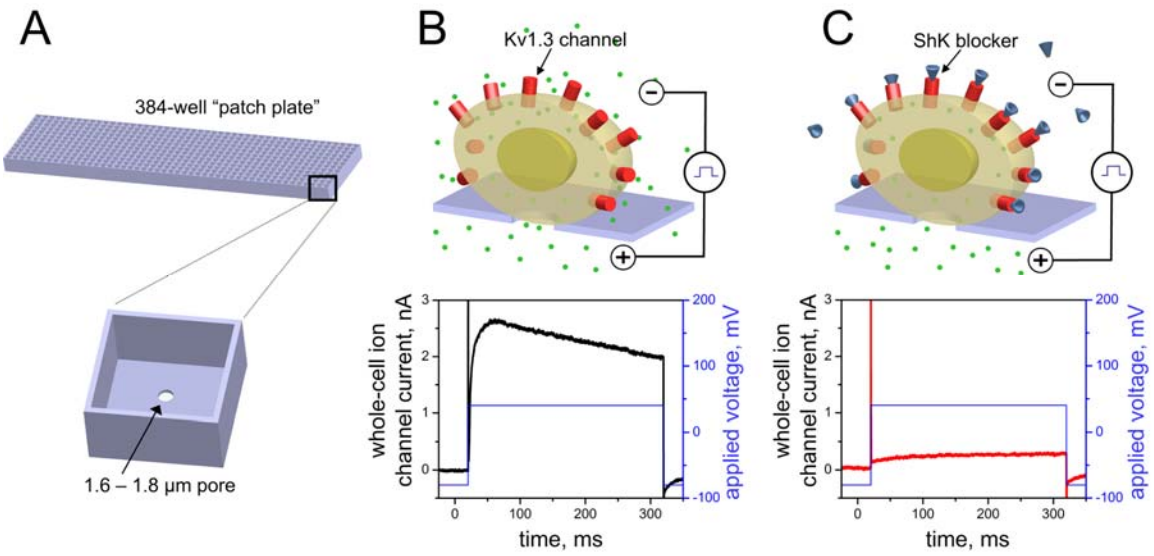

Figure 2.1 | High-throughput method for measuring Kv1.3 ion channel activity in lymphocytes. (A) Isolated lymphocytes in suspension (5×10^5 mL^{-1}) were dispensed into a 384-well patch plate (~2,500 cells per well). The bottom of each well contained a micropore with a diameter of 1.6 – 1.8 µm. Suction resulted in positioning of a single lymphocyte over the hole in each well to form a stable electrical seal (>75 MΩ) with the "patch plate". **(B)** After electrical access to the cytoplasm was obtained, a depolarizing voltage step function from -80 mV to +40 mV was applied across the cell membrane. This depolarization opened voltage-gated ion channels, and the resulting whole-cell current through the plasma membrane was recorded. **(C)** While the same cell was still attached, a specific blocker of Kv1.3 channels was added to each microwell. A second depolarizing step was applied to the cell, and the resulting whole-cell current was recorded. The Kv1.3-specific current was defined as the difference between the pre-blocker (B) and post-blocker (C) electrical currents.

This high-throughput assay enabled us to profile Kv1.3 activity rapidly in four different subsets of lymphocytes isolated directly from fresh blood (Fig. 2.2). In each experiment, we measured two subsets on the same patch plate (all cells were seeded at the same concentrations), with $CD4^+$ T cells on one half (192 wells) and either $CD8^+$ T cells, γδ T cells, or B cells on the other half (see 2-App.Table for comparisons and discussions of throughput, which can depend on lymphocyte subtype). Examining Kv1.3 currents, we found that although the mean Kv1.3 currents of each of the four lymphocyte subtypes were similar, histograms representing the distribution of Kv1.3 currents through

78 – 1220 individual cells showed significant differences between subtypes (Fig. 2.2). $CD4^+$ and $CD8^+$ T cells displayed similar distributions of Kv1.3 currents; for both of these T cell types, more than 98% of whole-cell currents had a magnitude between 0 and 0.5 nA (Fig. 2.2*A*,*B*). In contrast, the majority of B cells displayed Kv1.3 currents below 0.2 nA; however ~5% of B cells exhibited very high Kv1.3 activity (currents > 1.25 nA) (Fig. 2.2*C*). These rare, large currents in B cells were the largest Kv1.3 currents that we observed from all subsets of primary cells isolated from freshly drawn blood. These cells presumably represented activated class-switched IgD^- $CD27^+$ B cells that express large numbers of Kv1.3 channels.(29) γδ T cells, which previously had not been characterized with respect to Kv1.3 ion channel activity, displayed distributions of Kv1.3 currents more similar to B cells than $CD4^+$ or $CD8^+$ T cells (Fig. 2.2*D*). The majority of γδ T cells displayed little or no Kv1.3 current, while ~10% of γδ T cells displayed currents larger than 0.5 nA. These results demonstrate that the high-throughput assay presented here makes it possible to characterize rapidly cells with heterogeneous phenotypes (e.g. B cells) as well as to elucidate differences in Kv1.3 activity among various subsets of lymphocytes.

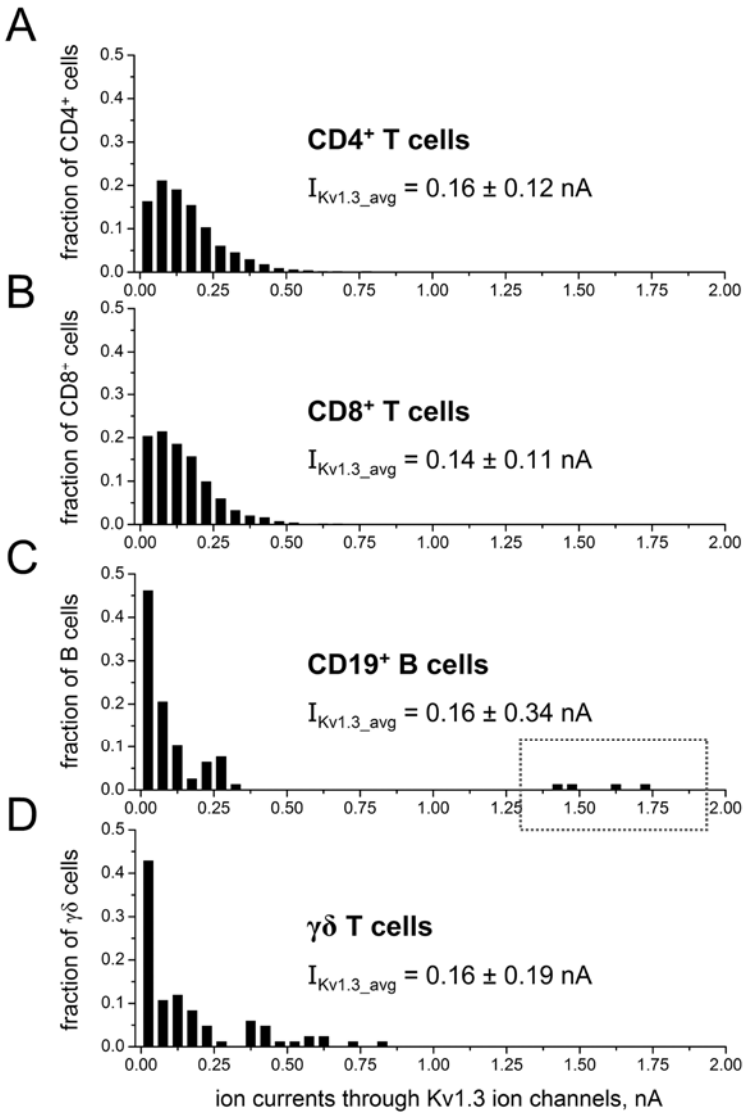

Figure 2.2 | Histograms of current through Kv1.3 ion channels in lymphocyte subsets isolated directly from human blood. Histograms represent the combined totals of Kv1.3 measurements on individual cells isolated from 3 or more independent blood draws for each subtype. **(A)** $CD4^+$ T cells, $N = 1220$ total cells measured from 17 independent experiments. **(B)** $CD8^+$ T cells, $N = 556$ cells from 10 independent experiments. **(C)** $CD19^+$ B cells, $N = 78$ cells from 3 independent experiments. The dashed blue box indicates the ~5% of measurements with large Kv1.3 currents above 1.25 nA. These B cells with large Kv1.3 currents were present in two out of the three subjects examined. **(D)** γδ T cells, $N = 84$ cells from 3 independent experiments. All histograms were constructed with a bin-size of 0.05 nA, and all y-axes display the fraction of cells of that subtype (e.g. $CD4^+$ T cells) with Kv1.3 currents in the specified bin. Average Kv1.3 currents ($I_{Kv1.3\_avg}$) for each subtype are listed within each histogram as mean ± standard deviation and were computed using the total number of cells for that cell type.

2.4. Quantification of ion current through Kv1.3 ion channels in activated T cells

To validate the high-throughput assay presented here, we measured the increase of Kv1.3 activity in $CD4^+$ and $CD8^+$ T cells after immunologic stimulation. Wulff *et al.* indicated that T cells increased the number of functional Kv1.3 ion channels after mitogen stimulation with anti-CD3 antibodies, although the degree of upregulation depended on the phenotype of T cell (8). Naïve and central memory T cells modestly increased Kv1.3 activity 1.5-fold, while effector memory T cells (T_{em}) upregulated Kv1.3 channels 5-fold (8). The reasons for this increase in functional activity of Kv1.3 ion channels are not well understood but may be related to regulation of cytokine-specific Ca^{2+} signals in activated T cells (8).

Using the high-throughput method to compare $CD4^+$ and $CD8^+$ T cells in parallel, we found that the mean whole cell currents through Kv1.3 channels in T cells isolated from 10 independent blood draws increased significantly after 72 h of mitogen stimulation with anti-CD3 antibodies (Fig. 2.3). The mean Kv1.3 activity from individual subjects increased by a factor of 3.0 ± 1.5 in $CD8^+$ T cells (mean ± standard deviation) after mitogenic stimulation compared to currents from freshly drawn blood (p = 0.00001). Correspondingly, mean Kv1.3 activity increased by a factor of 2.5 ± 0.8 in $CD4^+$ T cells (p = 0.00001). The mean Kv1.3 activities in $CD4^+$ and $CD8^+$ T cells increased to similar extents upon stimulation (p = 0.20). Figure 2.3 shows histograms of Kv1.3 currents from individual cells combined from all 10 experiments from T cells from freshly drawn blood (797 $CD4^+$ and 541 $CD8^+$ T cells) and from T cells after stimulation (823 $CD4^+$ and 888 $CD8^+$ T cells). These histograms show an increased dispersion in

Kv1.3 currents after stimulation and highlight the advantages of using high-throughput methods to profile the heterogeneous response of primary T cells to stimulation.

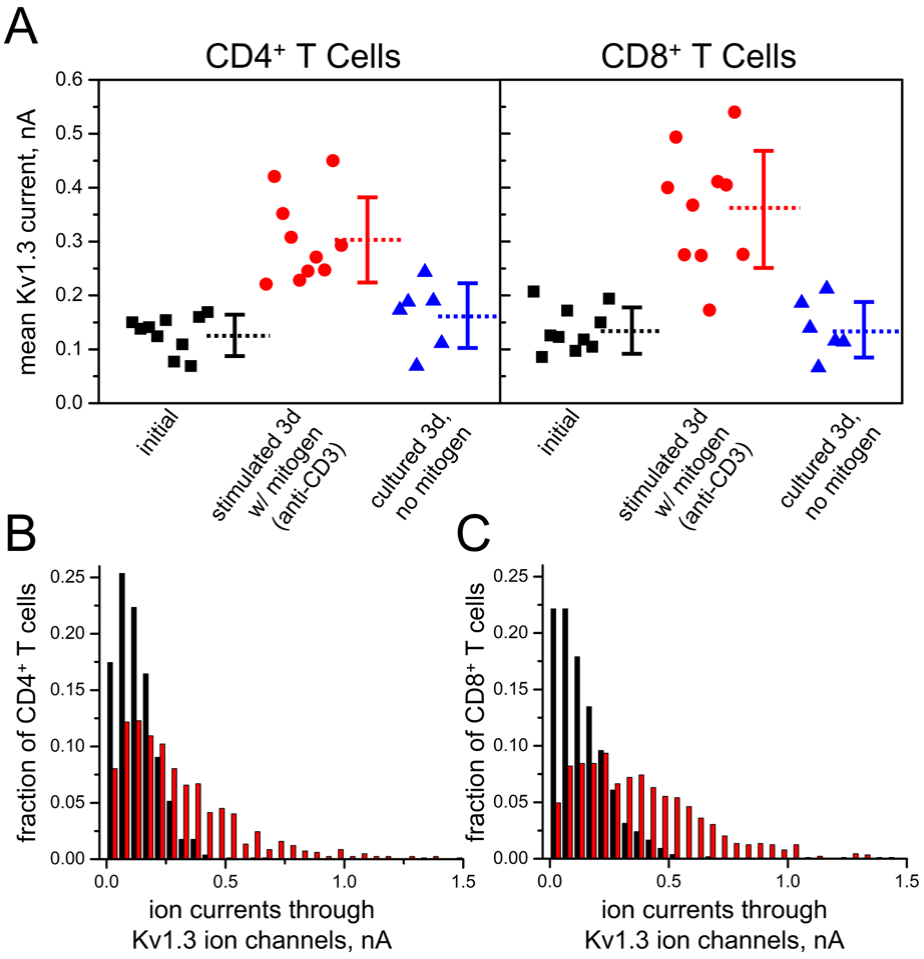

Figure 2.3 | Functional increase of Kv1.3 ion channel activity in stimulated T cells from 10 independent blood draws. (A) Kv1.3 activity was quantified from freshly drawn blood (labeled "initial", ■), after 72 h culture in the presence of 150 ng mL^{-1} anti-CD3 antibody (●), and after 72 h culture without added antibody (no stimulation, ▲). Each point represents mean Kv1.3 current in CD4$^+$ (left) or CD8$^+$ (right) T cells from an individual subject. Dashed lines represent averages of the 10 experiments (N = 6 for T cells cultured without stimulation), and the error bars show standard deviation. **(B)** Histograms of Kv1.3 currents from 797 CD4$^+$ T cells before (black bars) and from 823 CD4$^+$ T cells after 72 h culture with anti-CD3 antibody (red bars). Plots depict the fraction of cells in each histogram bin (bin-size = 0.05 nA). **(C)** Histograms of Kv1.3 currents from 541 CD8$^+$ T cells before (black bars) and from 888 CD8$^+$ T cells after stimulation (red bars).

In addition to heterogeneity of responses of individual cells with respect to Kv1.3 activity, high-throughput functional ion channel recording revealed that blood samples

from different individuals (i.e. different human subjects) exhibited surprisingly varied Kv1.3 responses to mitogen stimulation (Fig. 2.3*A*). The largest increase in mean Kv1.3 activity that we found in a sample from one human subject was a 5.7-fold increase in $CD8^+$ T cells; the same subject exhibited a 3-fold increase in $CD4^+$ T cells. In contrast, another subject actually exhibited a slight decrease in Kv1.3 activity in $CD8^+$ T cells after stimulation. T cells from this subject did not exhibit other characteristics of stimulation such as an increase in cell size or upregulation of CD25 or CD26 cell surface markers, indicating a deficient response to the activating mitogen.

Control experiments with blood samples from all subjects in which we cultured T cells without stimulation (i.e. without addition of anti-CD3 antibody) showed no significant increase in Kv1.3 activity in either $CD4^+$ or $CD8^+$ T cells ($N = 6$, $p = 0.19$ for $CD4^+$ T cells, $p = 0.97$ for $CD8^+$ T cells) (Fig. 2.3*A*). In summary, these results demonstrate three interesting points: (i) the increase in Kv1.3 activity is a direct result of T cell stimulation; (ii) $CD4^+$ and $CD8^+$ T cells responded similarly to stimulation despite differences in clonality and phenotypes (30, 31); and (iii) the magnitude of Kv1.3 increase measured using high-throughput electrophysiology varies by individual but generally agrees with previous measurements using traditional patch clamping.

2.5. Time-course of Kv1.3 ion channel regulation after T cell stimulation

To demonstrate the benefits of the assay presented here, we elucidated time-courses of the functional Kv1.3 ion channel activity in T cells after stimulation. Previous studies have employed manual patch clamping to study the time-dependent changes of Kv1.3 activity after mitogenic stimulation in a variety of cell types (25, 32-34). Here,

high-throughput screening provided additional insight into the time-courses of Kv1.3 activity in stimulated human lymphocytes by providing a large number of measurements within one hour for statistical analyses and by comparing directly $CD4^+$ and $CD8^+$ subsets during the same experiment (i.e. on the same patch plate). We conducted time-course studies of three subjects who responded strongly to stimulation with anti-CD3 antibodies (these three subjects are shown in Figure 2.3 with the highest Kv1.3 activity in $CD8^+$ T cells). We measured Kv1.3 activity in $CD4^+$ and $CD8^+$ T cells before, as well as 2 h, 24 h, 48 h, 72 h, and 96 h after stimulation with anti-CD3 antibodies (Fig. 2.4*A*).

Three aspects of this time-course are remarkable. First, 2 h after stimulation, the mean Kv1.3 currents decreased by ~50% compared to initial values from blood. This reduction in activity possibly resulted from phosphorylation of Kv1.3 channels immediately after activation which has been reported to decrease activity (35). Second, maximum Kv1.3 activity occurred 48 h after stimulation for two subjects and after 72 h for the third subject (mean $CD8^+$ activity increased 4.3 ± 1.2 fold, $CD4^+$ activity increased 3.6 ± 0.5 fold). Third, we observed no significant differences between $CD4^+$ and $CD8^+$ T cells in average Kv1.3 currents at any time-point (comparing mean values obtained from the three subjects at each time-point, minimum p value = 0.19).

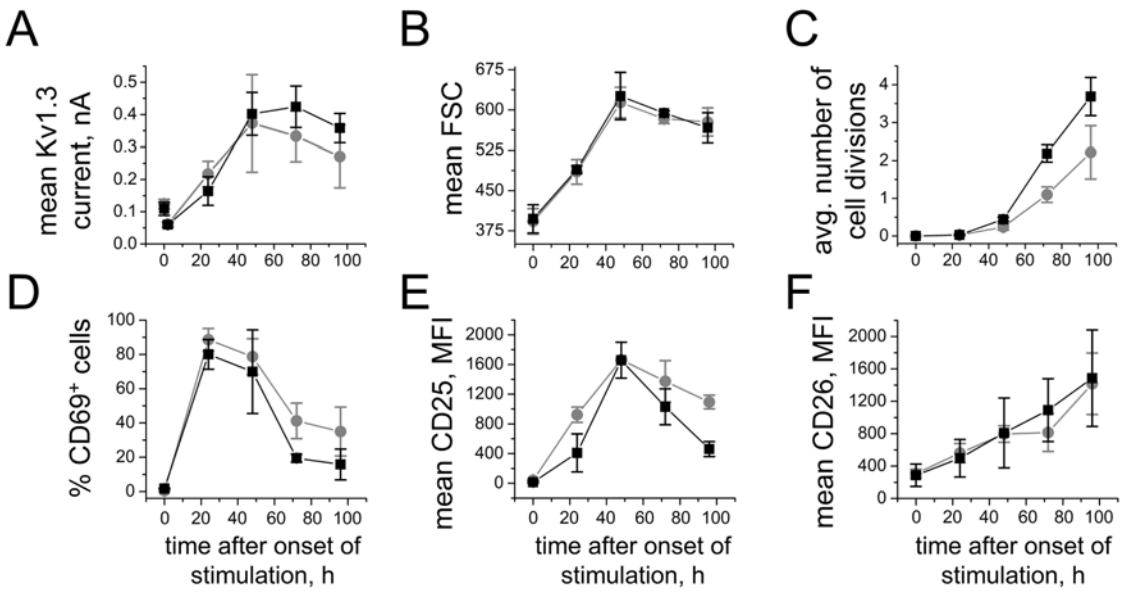

Figure 2.4 | Time-courses of functional Kv1.3 activity, as well as other T cell parameters, following stimulation with anti-CD3 antibody averaged from 3 subjects. $CD4^+$ T cells are depicted as red circles, and $CD8^+$ T cells are depicted as black squares. **(A)** High-throughput measurements of mean Kv1.3 currents in T cells from freshly drawn blood (0 h) and 2 h, 24 h, 48 h, 72 h, and 96 h after the onset of mitogenic stimulation of PBMCs with 150 ng mL^{-1} anti-CD3 antibody. At least 40 $CD4^+$ and 35 $CD8^+$ T cells were averaged at each time point for each subject. **(B through F)** Flow cytometric analysis of other lymphocyte properties following stimulation. **(B)** Mean forward scatter (related to cell volume) **(C)** Average number of cell divisions quantified by CFSE dilution. **(D)** Percentage of cells with high expression of CD69. **(E)** Mean fluorescence intensity (MFI) of CD25 expression. **(F)** MFI of CD26 expression. All points represent averages of three independent experiments (each experiment was performed on a blood sample from a different subject), and the error bars show standard deviation.

To compare the changes in Kv1.3 ion channel activity with changes in other parameters of T cells, we measured levels of cell surface markers, proliferation, and cell size at each time-point (Fig. 2.4*B*-*F* and Fig. 2-App.4). The cell surface marker that correlated most strongly with Kv1.3 was CD25, i.e. the α-chain of the IL-2 receptor. Peak expression of CD25 occurred at the same time-point as peak Kv1.3 activity, although CD25 was upregulated to a greater extent than Kv1.3 ion channels (~30 fold increase in mean fluorescence intensity). Forward scatter, which is related to cell volume, also correlated strongly with the time-course of Kv1.3 activity. The time-courses of other cell

surface markers that are commonly used as activation markers, such as CD69, CD26, and CD62L, all displayed distinctly different kinetics of regulation compared to Kv1.3 (Fig. 2.4*D*,*F* and Fig. 2-App.4). Proliferation data, measured in a parallel assay using CFSE to quantify the number of divisions of T cells, indicated that T cell proliferation of both $CD4^+$ and $CD8^+$ T cells initiated between 48−72 h after the onset of stimulation. Hence, proliferation started shortly after the cells reached maximum Kv1.3 activity (Fig. 2.4*C*). The high-throughput assay presented here, therefore, made it possible to place Kv1.3 activity in the chronology of events during T cell activation.

2.6. Effects of co-stimulation on levels of functional Kv1.3 ion channel activity

As mentioned previously, the data shown in Figure 2.4 summarized the response in Kv1.3 activity of three subjects who responded strongly to stimulation with anti-CD3 antibodies alone. We also observed subjects who responded weakly to this stimulation (Fig. 2.3*A*). A reason for these differences may be that T cells require two signals for effective stimulation, one through the T cell receptor (TCR) and the second through a co-stimulatory molecule such as CD28 (36). In experiments without co-stimulatory anti-CD28 antibodies (Figs. 2.3, 2.4), T cells presumably received co-stimulatory signals from other cells in culture. We hypothesize that the heterogeneity of Kv1.3 activity in T cells upon stimulation may in part be due to varying efficiencies of co-stimulation by other cells in the PBMC population. An advantage of the presented method is that the effects of different stimulation conditions on Kv1.3 activity can be elucidated rapidly and reliably.

To explore the effects of co-stimulation, we acquired time-courses of Kv1.3 activity after onset of stimulation with and without added anti-CD28 antibodies from a subject who responded weakly to stimulation with anti-CD3 antibodies alone (Fig. 2.5*A,B*). Without added anti-CD28 antibodies, Kv1.3 currents increased gradually after stimulation; $CD4^+$ currents peaked 72 h after stimulation, and $CD8^+$ currents peaked 96 h after stimulation. When we added anti-CD28 antibodies during stimulation of T cells from the same subject, we observed markedly accelerated kinetics of Kv1.3 activity. The Kv1.3 current peaked 48 h after stimulation for both $CD4^+$ and $CD8^+$ T cells (Fig. 2.5*A,B*), and the time-dependent profiles in Kv1.3 activity were now similar to those changes of subjects who responded strongly to mitogen stimulation alone (Fig. 2.4*A*). Changes in other T cell properties, such as kinetics of expression of cell surface markers, cell size, and proliferation with added anti-CD28 also showed similar correlations to Kv1.3 activity as those of subjects that responded strongly to stimulation by anti-CD3 antibodies alone (Fig. 2.4 and Fig. 2-App.5).

To explore the effects of co-stimulation on upregulation of Kv1.3 further, we investigated the effects of the concentration of added anti-CD3 antibodies on functional Kv1.3 increase after 48 h of stimulation in the presence or absence of a fixed concentration of anti-CD28 antibodies (Fig. 2.5*C,D*). The subject examined had previously responded strongly to stimulation with anti-CD3 antibodies alone (Fig. 2.3). We observed that maximum Kv1.3 activity occurred at intermediate concentrations of added anti-CD3 antibodies (50 and 150 ng mL^{-1}), and that adding anti-CD28 antibodies increased Kv1.3 currents by ~30% at these concentrations of anti-CD3 antibodies (Fig. 2.5*C,D*). Stimulation with 150 ng mL^{-1} anti-CD28 antibodies alone did not result in

increases in Kv1.3 activity (Fig. 2.5*C,D*). Interestingly, $CD4^+$ T cells exhibited smaller increases in Kv1.3 activity than $CD8^+$ T cells after stimulation with low (5 ng mL^{-1}) and high (1000 ng mL^{-1}) concentrations of anti-CD3 antibodies. These results suggest that the increase in Kv1.3 channel activity after stimulation depends strongly on the type and intensity of this stimulation. These results also identify stimulation conditions (antibody concentrations, time-course) for obtaining T cells with maximum Kv1.3 activity. Such T cells might be useful to examine potential drug candidates that block Kv1.3 channels (37).

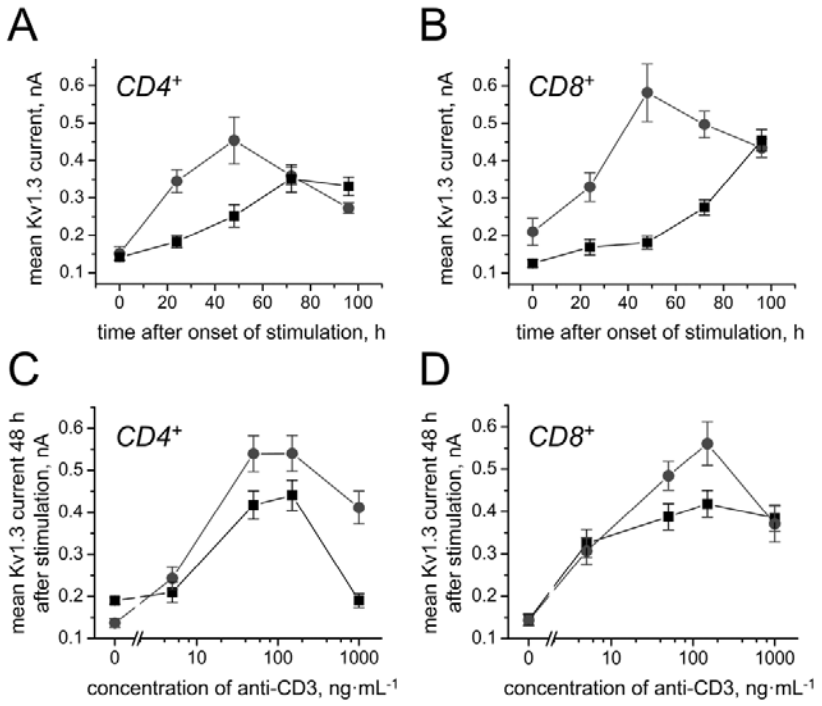

Figure 2.5 | Functional increase of Kv1.3 ion channel activity in mitogen stimulated T cells with or without a co-stimulatory molecule (anti-CD28 antibody). (A) For a subject with a previously observed weak response to stimulation with anti-CD3 antibodies alone, time-courses of Kv1.3 activity in $CD4^+$ T cells were obtained after stimulation of PBMCs with 150 ng mL^{-1} anti-CD3 antibodies alone (■) or with anti-CD3 plus 150 ng mL^{-1} anti-CD28 antibodies (●). **(B)** Time-courses of Kv1.3 activity in $CD8^+$ T cells in the same experiment as described in (A). **(C)** For a subject with previously measured strong response to anti-CD3 stimulation alone, Kv1.3 activity in $CD4^+$ T cells was measured after 48 h of stimulation of PBMCs in the presence of increasing concentrations of anti-CD3 antibodies with (●) and without (■) 150 ng mL^{-1} anti-CD28 antibody. **(D)** Kv1.3 activity in $CD8^+$ T cells in the same experiment described in (C). All points represent averages of Kv1.3 currents from at least 60 T cells; error bars show standard error of the mean.

2.7. Discussion

The expression and function of ion channels in lymphocytes is not only dependent on the phenotype of cells but also on their activation status. This characteristic makes ion channels especially attractive as selective pharmaceutical targets. In this context, growing evidence supports that the activity of ion channels is compromised in different immune-related pathologies (10, 38); there are, however, inherent difficulties to measure their functional activity in freshly isolated cells. Here, we introduce a novel high-throughput method that makes the study of specific ion channels in cells of the immune system accessible to biochemists, clinicians, and immunologists who often lack the equipment and expertise for measuring ion channel activity.

This high-throughput assay offers at least three advantages over traditional patch clamp techniques. First, it affords a significantly increased number of measurements of electrical whole-cell ion currents through individual cells compared to existing techniques. We measured as many as 974 lymphocytes within 10 h, a throughput which is 10 to 50-fold higher than what is possible with manual patch clamp techniques. Large numbers of measurements are particularly important in profiling ion channel activity in cell populations with heterogeneous phenotypes such as activated $CD4^+$ and $CD8^+$ T cells. Moreover, high-throughput measurements allow the detection of small subsets of cells within a population that possess high ion channel activity (e.g. B cells or γδ T cells directly isolated from blood).

Second, the high-throughput assay presented here is rapid (< 1 h) and proceeds in a completely automated fashion, including dispensing of cells, establishing seals, performing whole-cell voltage-clamp recordings, and processing data. Third, this assay

allows direct comparisons of subsets of lymphocytes under the same experimental conditions and at the same time-points by examining multiple subsets of cells on the same patch plate. By examining Kv1.3 ion channel activity in $CD4^+$ T cells, $CD8^+$ T cells, and B cells isolated from human blood by magnetic bead separations, we found that the results obtained from the high-throughput electrophysiology method agreed well with previously reported data (Fig. 2.2), confirming the reliability and robustness of this method. These experiments also revealed that γδ T cells display a different distribution of Kv1.3 activity than do $CD4^+$ or $CD8^+$ T cells (Fig. 2.2). These γδ T cells had previously not been characterized with respect to the expression of active Kv1.3 channels. γδ T cells display specific signaling events that differ from other subsets of lymphocytes (39, 40). The results presented here suggest that altered K^+ signaling may be one of these different signaling events.

With respect to immunological implications, we demonstrate the feasibility of measuring Kv1.3 ion channel activity as a functional activation marker of T cells. We demonstrated that levels of ion currents through Kv1.3 ion channels in human T cells peaked between 48 h and 72 h after the onset of mitogenic stimulation and more than tripled compared to baseline levels in both $CD4^+$ and $CD8^+$ T cells (Fig. 2.4, 2.5, and Figs. 2-App.4, 2-App.5). This increase in Kv1.3 activity depended on both the primary stimulatory signal through the TCR as well as co-stimulatory signals. The time-course of Kv1.3 activity upon stimulation correlated strongly with expression of CD25 and the sizes of T cells (Fig. 2.6). Maximum Kv1.3 levels also occurred shortly before significant proliferation of T cells (Fig. 2.6). The immunological basis for the functional increase in Kv1.3 activity after stimulation is not well-understood; however, the results presented

here, especially the coupling of maximum Kv1.3 activity to the onset of proliferation, suggest that the increase in functional levels of Kv1.3 may be cell-cycle related, perhaps to ensure proper regulation of the resting potential in daughter cells after division (33).

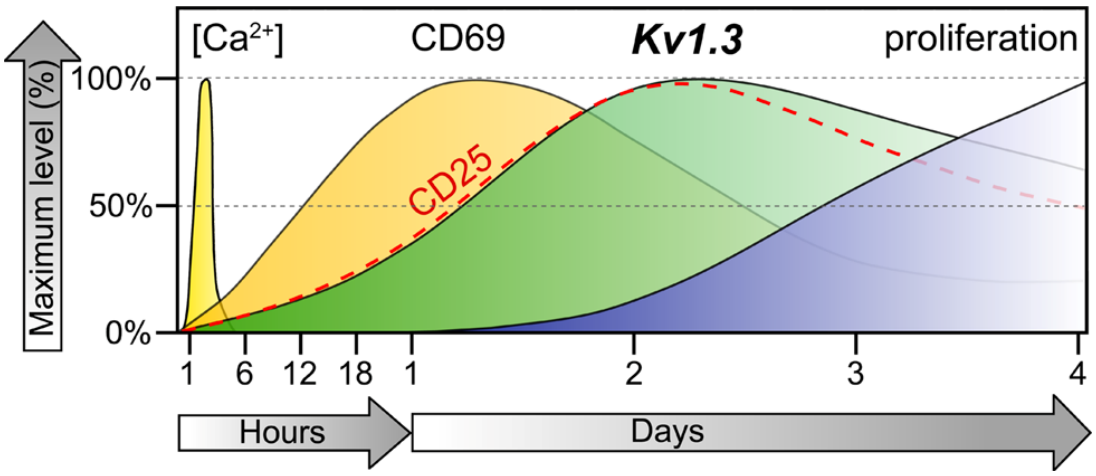

Figure 2.6 | Time-course of functional Kv1.3 activity in the context of increases of other activation markers in T cells. The time-course for Ca^{2+}-signaling (here represented as a spike in the intracellular concentration of Ca^{2+}) was inferred from Lewis (7). Data for CD69 expression, Kv1.3 activity, CD25 expression, and T cell proliferation were averaged from the three time-courses shown in Figure 2.4 and from the time-course with added anti-CD28 antibodies in Figure 2.5. For each individual time-course, values were first averaged between $CD4^+$ and $CD8^+$ T cells and normalized between 0% and 100% to account for differences in peak levels between different subjects. Figure inspired by Abbas and Lichtman (27).

While the present study focused on lymphocytes, the developed high-throughput methodology could in principle be used to screen functional activity of voltage-gated ion channels in a range of cell types (e.g. other primary cell types or malignant cells, such as lymphoma cells, etc.). For instance, we performed pilot experiments that profiled ion channel activity in regulatory T cells (T_{reg}) and dendritic cells (Fig. 2-App.6). The requirements for such assays are: (i) preparing a primary cell type in suspension that seals well to the planar substrate of the high-throughput patch-clamp device, and (ii) identifying a specific blocker of the voltage-gated channel of interest. Several factors

affect the sealing of cells to the substrate (41), most notably cell size in relation to the size of micropore in the patch plate (small cells require small pores). In addition, surface properties of the planar substrate may contribute; modifying the pore size or coating the substrate with adhesive molecules, may further increase the number of primary cells that can be analyzed successfully in each experimental run. With regards to blockers of ion channels, a selection of compounds are available that specifically block various K^+, Na^+, Cl^-, and Ca^{2+} channels (12).

High-throughput profiling of ion channels has three limitations compared to traditional techniques. First, patch clamping allows for measurements of electrical currents through single ion channels (so-called single-channel recordings), mainly because of the tight electrical "seals" between the tip of a glass pipette and the attached cell (e.g. giga-ohm seal) (17). In contrast, the instrument used in this work typically operates with seal resistances between 75-300 MΩ. Potential leak currents are, however, subtracted by the leak current compensation of the instrument and by taking differential measurements before and after addition of an ion channel blocker (23). Second, the high-throughput instrument used in this work is not configured to perform measurements of ligand-gated ion channels (some existing automated patch clamp technologies do allow for measurements of this channel type, albeit at lower throughput (42)). Finally, automated patch clamp instruments are currently not widely accessible and are typically expensive. Rapid advances in microfabrication (43), microfluidics, and automated patch-clamp recordings are likely to reduce cost and increase the accessibility to these instruments in the near future (42, 44, 45).

2.8. Conclusions

The functional, high-throughput assay presented here provides a tool to investigate the role of ion channels in primary cells, under conditions with different degrees of activation, and in physiological or pathological conditions. Importantly, this method makes it possible to elucidate profiles of the distribution of ion channel activity. We expect this method to serve as a useful and accessible tool for biochemists, cell biologists, immunologists, and clinicians to study rapidly and conveniently ion channel activity in a range of primary cell types. The ensuing insight based on functional activities of ion channel proteins that are involved in cell signaling and immune cell activation may lead to a better understanding of the role of ion channels in physiology, immune responses, and human disease.

Chapter 2 Appendix

2-App.Methods. Supporting Methods

Cell culture and separations. To separate subsets of lymphocytes from whole blood, we first isolated peripheral blood mononuclear cells (PBMCs). We centrifuged whole blood at 700 × *g* for 20 min to isolate the intermediate "buffy coat" layer containing white blood cells. A subsequent density gradient centrifugation (Histopaque, Sigma-Aldrich, St. Louis, MO) at 700 × *g* for 20 min allowed separation of PBMCs from this buffy coat layer. Isolated PBMCs were washed twice in wash buffer, defined here as Dulbecco's modified phosphate buffered saline without Ca^{2+} or Mg^{2+} (D-PBS, Invitrogen, Carlsbad, CA) and supplemented with 2% (v/v) fetal bovine serum (FBS,

Mediatech, Herndon, VA). To select for particular subsets of lymphocytes, we separated PBMCs using magnetic beads coated with antibodies against either CD4, CD8, CD19 (for B cells), or the γδ T cell receptor (Miltenyi Biotec, Auburn, CA). Briefly, we added 50 μL of bead solution to 350 μL of PBMCs suspended in wash buffer and incubated for 15 min at room temperature. We then passed labeled cells through a paramagnetic column (Miltenyi Biotec) and collected positively-labeled cells which were retained in the column. After magnetic separations in columns, we stored cells either at 4° C for flow cytometry analysis or prepared them immediately for high-throughput electrophysiology measurements.

To culture and stimulate cells, we first washed the separated PBMCs in culture media, here defined as RPMI-1640 medium (ATCC, Manassas, VA) supplemented with 10% (v/v) FBS, 150 U mL^{-1} penicillin, 150 μg mL^{-1} streptomycin (pen-strep, Invitrogen), and 55 μM 2-mercaptoethanol (Invitrogen). To stimulate T cells, we added soluble monoclonal mouse anti-human CD3 antibody (clone UCHT1, BD Biosciences, San Jose, CA) at indicated concentrations in culture media. For co-stimulation experiments, we additionally added 150 ng mL^{-1} soluble monoclonal anti-CD28 antibody from mouse (clone CD28.2, BD Biosciences) to PBMCs in suspension. Cells with added antibodies for stimulation were seeded in tissue culture flasks (8 mL into T25 flasks, BD Biosciences) at a concentration of 1×10^6 cells mL^{-1} and cultured at 37° C in an atmosphere of 5% CO_2, for 72 h unless otherwise noted. After culture, we washed PBMCs twice in wash buffer and then used magnetic bead separations to isolate stimulated $CD4^+$ and $CD8^+$ T cells. These stimulated cells were either stored at 4° C for flow cytometry or prepared immediately for high-throughput electrophysiology.

Wash protocols for the high-throughput electrophysiology instrument. After measuring Kv1.3-specific currents in all 384 wells of the patch plate, we used the automated wash protocols of the IonWorks HT system to flush the internal fluidics and microfluidics array for dispensing drugs to each well of the "patch plate". The sequence of wash steps consisted of a flush with 5% Hellmanex II (Hellma GmbH & Co. KG, Müllheim, Germany) in H_2O followed by a flush with distilled H_2O (repeat sequence twice). We also washed the electrode array by soaking the electrode tips in 2.5% Hellmanex II in H_2O for 60 s followed by a final soak in D-PBS for 120 s.

Algorithms to quantify Kv1.3-specific currents. We developed custom computer software using the PERL language to quantify specifically the ion current passing through Kv1.3 ion channels. The algorithm first automatically filtered out cells that did not maintain stable seals with the micropore in each well of the patch plate. For a cell to be considered "stable" and to yield a valid whole-cell recording, we imposed two criteria: (i) the cell had to maintain a seal resistance with the micropore of the patch plate of at least 75 MΩ throughout the experiment (including after addition of the compound); and (ii) the magnitude of the seal resistance had to be constant within ± 25% from pre-compound to post-compound measurements.

For cells with valid seals, we quantified Kv1.3-specific currents by subtracting the post-compound (i.e. post blockage with ShK-F6CA) current from the pre-compound current (Fig. 2-App.3*B*). The PERL computer algorithms computed the pre-compound current by determining the maximum current (averaged during a 1-ms "time-window") after the depolarizing pulse and subtracting an average of the current before the depolarizing pulse (baseline current). The post-compound current consisted of

quantifying, again, the average current over a 1 ms interval. This interval was taken at the exact same time after applying the depolarizing pulse as the time interval from the pre-compound recording. The algorithm then, again, subtracted an average of the current before the depolarizing voltage pulse (baseline current). Finally, the algorithm computed the Kv1.3-specific current from the difference between the pre- and post-compound currents (Fig. 2-App.3). We confirmed the accuracy of these algorithms in each experiment by viewing the largest currents in each experiment graphically, but all computations of currents were performed automatically by the PERL programs to ensure unbiased, reliable, and automated data analysis.

Flow cytometry assays. We performed flow cytometry analysis using a four-color flow cytometer (FACScalibur, Becton Dickinson, Franklin Lakes, NJ) with CellQuest software. Cells were stained with antibodies against the following antigens (all from BD Biosciences) conjugated to either the fluorophore allophycocyanin (APC) or phycoerythrin (PE): CD4-APC, CD8-APC, CD8-PE, CD19-PE, CD25-PE, CD26-PE, CD62L-PE, CD69-PE, and CD69-APC. All staining, incubation (for 30 min), and wash procedures occurred at 4°C using wash buffer. For each type of surface marker, we measured forward scatter, side scatter, and fluorescence intensity from at least 5,000 cells (typically from over 10,000 cells). All cytometer settings (compensation and detector voltages) remained constant for all experiments. We typically quantified mean fluorescence intensity (MFI) for all cells gated (i.e. selected) as lymphocytes based on size (forward scatter) and complexity (side scatter) using analysis software (WEASEL, The Walter and Eliza Hall Institute, Parkville, Australia). For cells stained with CD69, we determined the percentage of cells with "high" levels of CD69 ($CD69^+$) by computing

the percentage of cells with fluorescence intensities above the background fluorescence levels of unstained cells.

CFSE assays to quantify proliferation in $CD4^+$ and $CD8^+$ T cells. To quantify the proliferation of T cells, we measured the levels of carboxyfluorescein diacetate succinimidyl ester (CFSE) in individual T cells. Labeling cells with CFSE made it possible to determine T cell proliferation by flow cytometry, as cells evenly split their concentration of CFSE when they divided. We performed experiments with cells labeled with CFSE in parallel to experiments with unlabeled cells for high-throughput electrophysiology measurements because electrophysiology experiments required a significantly higher number of cells than CFSE experiments. We stained cells with 0.25 μM CFSE according to instructions from the manufacturer (Invitrogen). Stained populations of cells were seeded into flat-bottom 96-well plates using the same cell density, media, and stimulation conditions as the corresponding cultures for Kv1.3 measurements.

Before analysis, we labeled CFSE-stained cells with either anti-CD4-APC or anti-CD8-APC antibodies to observe specifically the proliferation in those subsets. We used APC-labeled antibodies to avoid "interference" between APC and CFSE (measured using the FITC excitation and detection settings) during the detection by flow cytometry. To quantify proliferation from the resulting flow cytometry data, we performed the following three steps: first, we selected (or gated) for lymphocytes based on the size (forward scatter) and complexity (side scatter) of the cells in the cytometer; second, among gated-lymphocytes, we selected for cells with high levels of APC fluorescence, representing $CD4^+$ or $CD8^+$ T cells; and third, for gated $CD4^+$ or $CD8^+$ T cells, we determined the

percentage of cells in each of the clearly-defined CFSE "peaks". Each peak corresponded to cells that divided 0×, 1×, 2×, 3×, 4×, etc., respectively. Determining the percentages of cells that divided a known number of times allowed calculation of the average number of cell divisions for a specific cell population.

Statistical Analyses. We calculated all *P*-values using a two-sample Student's *t*-test (Origin, Northampton, MA). Means and standard deviations are clearly indicated throughout the text, with all standard deviations calculated using sample standard deviation. In indicated cases, we used standard error of the mean (defined as standard deviation divided by $\sqrt{N}$) to depict potential errors in mean values of Kv1.3 activity determined from individual high-throughput electrophysiology experiments.

2-App.Table. Throughput of automated ion channel experiments using lymphocyte subsets isolated from human blood.

lymphocyte subset	percentage of wells in the "patch-plate" with successful Kv1.3 measurements, %	average seal resistance of successful cells, MΩ	main reason for unsuccessful wells
$CD4^+$ T cells	42 ± 9	134 ± 21	lost/low seals after compound addition
$CD8^+$ T cells	32 ± 9	124 ± 23	lost/low seals after compound addition
B cells	15 ± 6	123 ± 6	lost/low seals after compound addition
γδ T cells	25 ± 3	116 ± 4	low seal resistance between cell and microwell
stimulated $CD4^+$ T cells*	46 ± 12	152 ± 23	no seal between cell and microwell
stimulated $CD8^+$ T cells*	50 ± 13	146 ± 23	no seal between cell and microwell

All subsets measured using half of a 384-well patch-plate.
Values represent average ± standard deviation of mean values from individual subjects involving the indicated subtype (N = 17 for $CD4^+$ T cells, N = 10 for $CD8^+$ T cells, N = 3 for B cells, N = 3 for γδ T cells, N = 10 for stimulated $CD4^+$ T cells, and N = 10 for stimulated $CD8^+$ T cells).
* T cells stimulated for 3 d with 150 ng mL^{-1} anti-CD3 antibodies.

There may be several reasons for the different throughputs of the various subsets of lymphocytes using the IonWorks HT high-throughput electrophysiology system. Cell size may affect the stability of lymphocytes attached to the micropores of the "patch plate". Stimulated T cells, with an average of ~1.5 times the diameter of resting T cells from blood, exhibited higher average seal resistances than resting T cells ($p < 0.05$ for both $CD4^+$ and $CD8^+$ T cells). These stimulated T cells were also ~20% less likely than

resting T cells to lose their seals after addition of the ShK-F6CA compound to block Kv1.3 channels ($p < 0.01$ for both $CD4^+$ and $CD8^+$ T cells).

A second reason for the different throughputs may be related to surface morphology of the lymphocyte subset. $CD4^+$ and $CD8^+$ T cells isolated from blood, which have very similar sizes and which were always measured in parallel on the same patch plate, exhibited different throughputs in high-throughput electrophysiology experiments. $CD4^+$ T cells showed ~10% higher throughput than $CD8^+$ T cells ($p < 0.01$), as $CD4^+$ T cells were 15% more likely to contact the micropore and 10% more likely to have sufficiently high seals after initially contacting the micropore than $CD8^+$ T cells. $CD4^+$ and $CD8^+$ T cells were equally likely to lose seals after compound addition. Properties of $CD4^+$ and $CD8^+$ T cells that may contribute to the initial sealing to the micropore might include differences in phenotypes, expression of certain cell surface molecules, and perhaps differences in mechanical properties.

An interesting finding in the analysis of throughputs of different lymphocyte subsets is that B cells and γδ T cells isolated from blood had significantly lower throughput than $CD4^+$ or $CD8^+$ T cells. γδ T cells were especially likely to form low and insufficient seals with the micropores but otherwise behaved similarly to $CD4^+$ T cells. B cells, which exhibited the lowest throughput of all cell types measured, were the least likely subset to initially contact the micropore and was the most likely subset to lose seals after addition of compound. The reasons for this instability may be related to morphological or mechanical properties of B cells. Modifications to the patch plates, either by having smaller diameters of micropores or by coating the plates with adhesive molecules, may help to increase seal resistances and stability and increase throughputs

for all cell types. The observed differences in behavior of different lymphocytes attached to micropores may, however, allow insights into the mechanical properties of lymphocytes and may provide a platform for rapid screening of drug compounds or molecules that affect the cytoskeleton and mechanical stability of primary cells.

2-App.1. Confirming full blockage of Kv1.3 ion channels

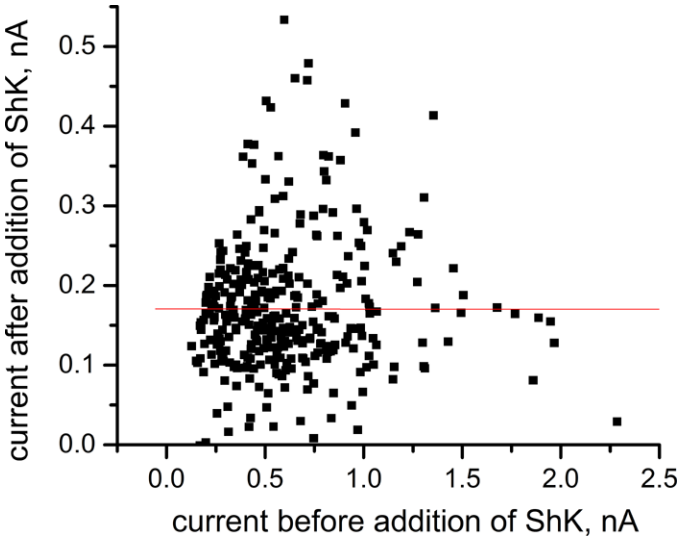

Figure 2-App.1 | Confirming full blockage of Kv1.3 ion channels. This graph quantifies the correlation of the recorded whole-cell ion current after addition of ShK-F6CA (post-compound currents) as a function of the ion current before addition of the blocker (pre-compound currents). The recorded currents were obtained from $CD8^+$ T cells from the time-course shown in Figure 2.5B in the main text (stimulation with both anti-CD3 and anti-CD28 antibodies, number of $CD8^+$ T cells, $N = 342$ from the five time-points). The red line represents a linear best fit of to the data (slope = −0.0001, $R^2 = 2 \times 10^{-7}$). The slope of this line was zero, and the absence of correlation of the data indicates that the magnitude of the post-compound currents was not dependent on the magnitude of the pre-compound currents. This absence of correlation demonstrates full-block of Kv1.3 ion channels.

2-App.2. Specificity of the high-throughput electrophysiology method for Kv1.3 ion channel activity

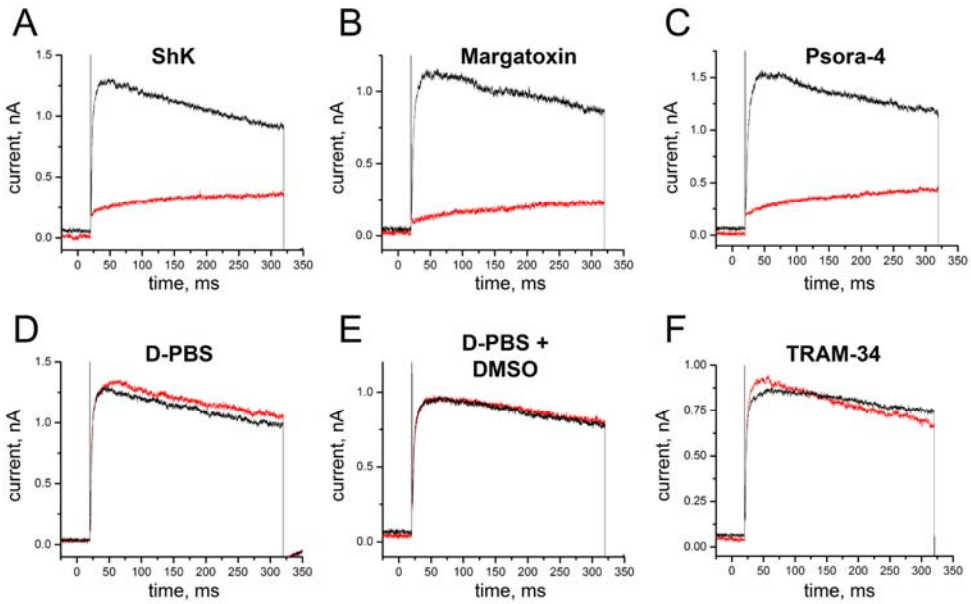

Figure 2-App.2 | Specificity of the high-throughput electrophysiology method for Kv1.3 ion channel activity. This figure depicts the blockage of ion current through stimulated $CD8^+$ T cells by different drug compounds. Electrical currents recorded before addition of the drug compound (black line) were compared to currents through the same cell after 3 min incubation with the respective drug compound (red lines). Compounds tested included the following known blockers of Kv1.3 ion channels at concentrations well above their IC_{50} value for Kv1.3 ion channels: **(A)** 72 nM ShK-F6CA (IC_{50}=48 pM); **(B)** 160 nM margatoxin (IC_{50}=110 pM); **(C)** 250 nM Psora-4 (IC_{50}=3 nM), which was initially dissolved in DMSO before dilution in D-PBS. For these compounds, the residual electrical current after addition of the compound (i.e. in the presence of the blocker) was severely attenuated and did not display the time-dependent de-activation that is characteristic of Kv1.3 ion channels.[3] These residual currents after addition of blocker were mostly due to a "leak" current from imperfect electrical seals between the cell and the micropore in the patch plate. A part of these currents may have also been due to the presence of other voltage-gated ion channels than Kv1.3 channels. The following compounds and solutions that are known not to block Kv1.3 ion channels were also tested: **(D)** D-PBS; **(E)** 0.33% DMSO in D-PBS; **(F)** 150 nM TRAM-34, which was initially dissolved in DMSO before dilution in D-PBS. The example of TRAM-34 is particularly important because TRAM-34 blocks the calcium-gated potassium ion channel KCa3.1 (IC_{50}=20 nM), which is the other significant potassium ion channel in T cells (besides Kv1.3). For each of these conditions, the electrical current after addition of the compounds (or solution) was not attenuated and still displayed time-dependent de-activation of Kv1.3 channels. The observation that TRAM-34 did not block the electrical current through T cells in this assay suggests that most of the K^+ current measured in this assay was due to Kv1.3 ion channels. This result, in combination with using the ShK peptide, a blocker highly specific for Kv1.3 channels, confirms that the high-throughput assay presented here is specific for Kv1.3 ion channels. Note that all compounds were dispensed using the integrated fluidics of the high-throughput electrophysiology device, and all concentrations of compounds refer to final concentrations in the microwells. All graphs are representative of measurements from at least 20 cells for each compound or solution.

2-App.3. Algorithms to quantify Kv1.3-specific currents

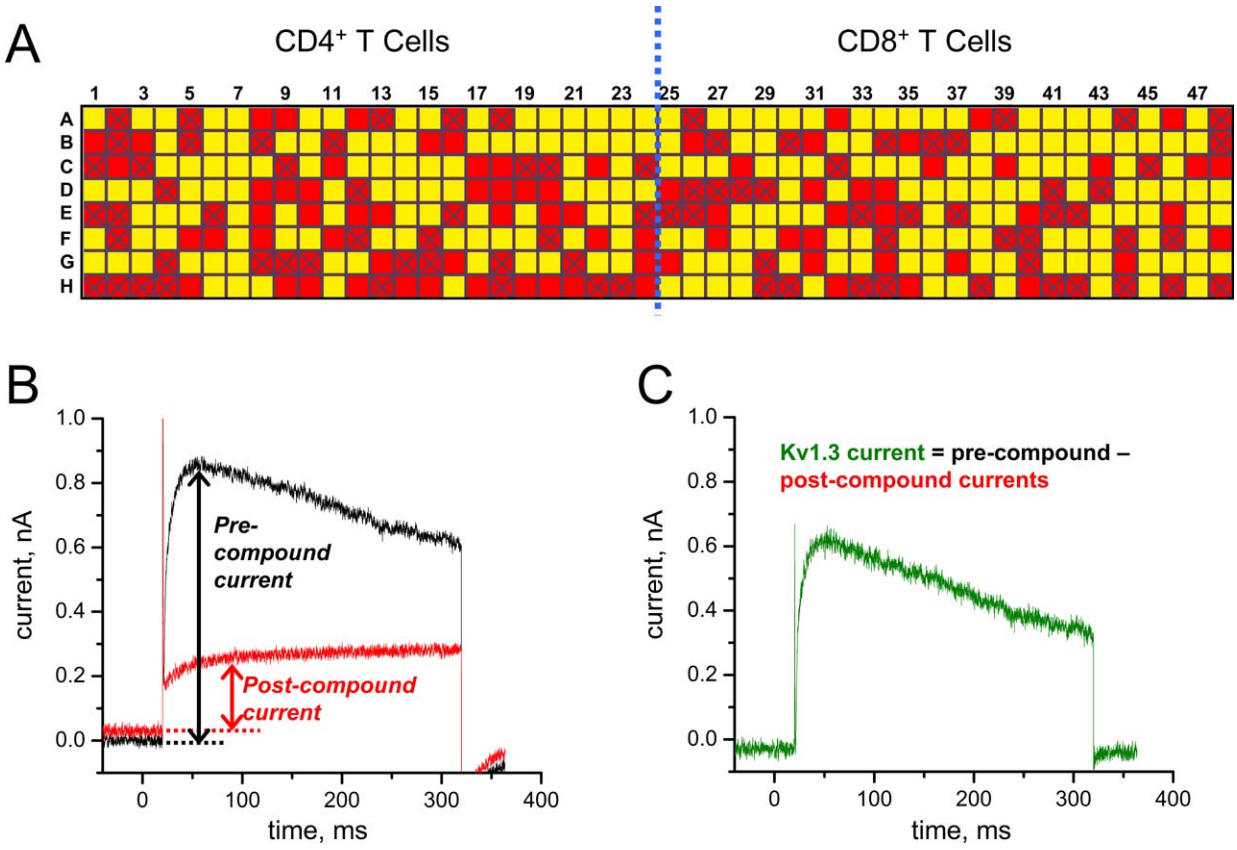

Figure 2-App.3 | Algorithms to quantify Kv1.3-specific currents. This figure shows a graphical representation of the data processing algorithms used to quantify Kv1.3-specific currents. **(A)** Schematic of the patch-plate with $CD4^+$ T cells measured on the left half (192 wells) and $CD8^+$ T cells measured on the right half of the plate. Only cells with sufficiently high (>75 MΩ) and stable seals between the cell and micropore were included for analysis (such wells of the micropore are depicted in yellow). Wells in which no cell sealed to the micropore (red squares without an "×") or wells in which cells did not have sufficiently high or stable seals (red squares with an "×") were excluded from further analysis. **(B)** Application of a voltage-pulse to quantify the ion currents before (pre-compound current) and after addition of a highly-specific blocker (ShK) of Kv1.3 ion channels (post-compound current). All current amplitudes (represented by the vertical arrows) were obtained by subtracting the current before application of the pulse from the maximum current after addition of the pulse (all current values were obtained by averaging over a 1-ms window). **(C)** Graphical example of a "Kv1.3-speicific" current trace, obtained by subtracting the post-compound current from the pre-compound current at each time-point. The values displayed throughout the text, however, represent the pre-compound current minus the post-compound current, as computed in panel (B). All determinations of sufficiently high and stable seals as well as quantifying of amplitudes of Kv1.3-specific currents were computed automatically using custom-written PERL algorithms.

2-App.4. Time-courses of Kv1.3 activity using three human subjects.

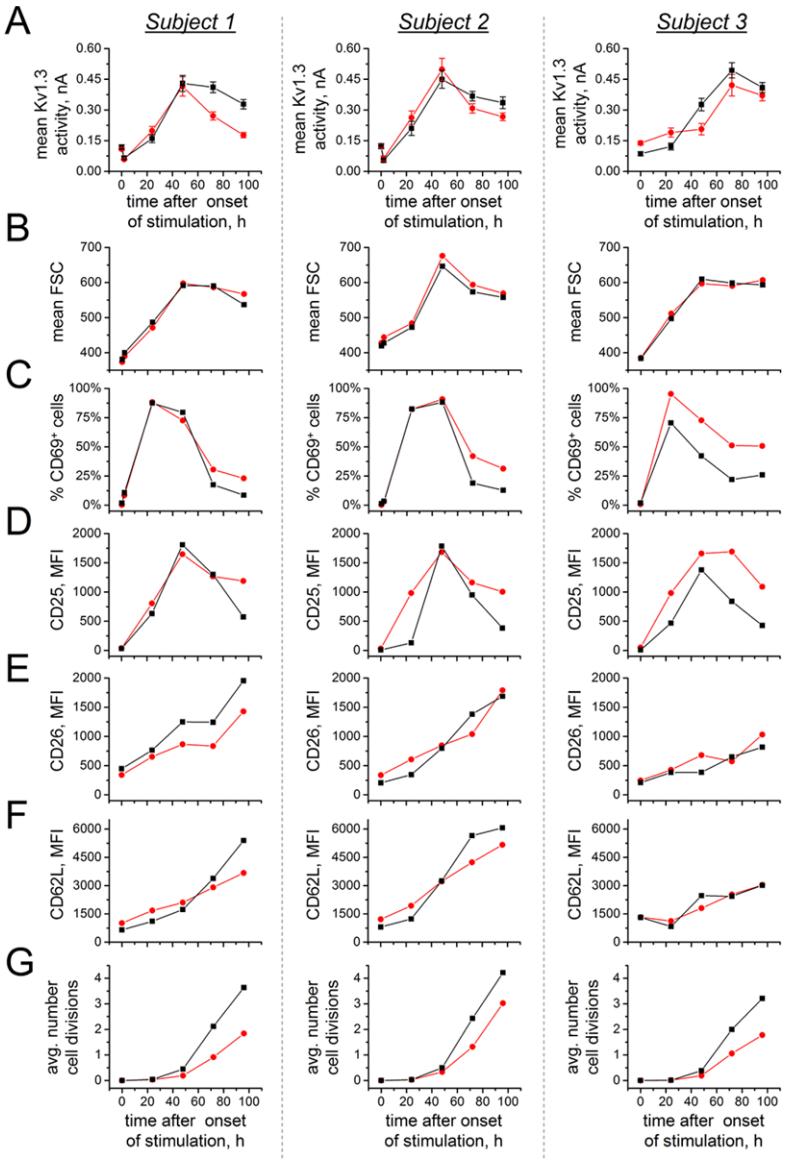

Figure 2-App.4 | Individual time-courses of functional Kv1.3 activity after mitogenic stimulation in three different subjects. This figure shows individual time-courses of functional Kv1.3 activity, as well as other T cell parameters, for three subjects following mitogenic stimulation with anti-CD3 antibodies (Fig. 2.4 in main text). $CD4^+$ T cells are depicted as red circles, and $CD8^+$ T cells are depicted as black squares. Time-courses for each of the three individual subjects are separated into three columns (all time-courses in the same column are from the same subject), with each row depicting a time-course of a single T cell parameter. **(A)** High-throughput measurements of mean Kv1.3 currents in T cells from freshly drawn blood (0 h) and 2 h, 24 h, 48 h, 72 h, and 96 h after the onset of mitogenic stimulation of isolated PBMCs with 150 ng mL^{-1} anti-CD3 antibody. Error bars represent standard error of the mean. **(B through G)** Flow cytometric analysis of other lymphocyte properties following stimulation. **(B)** Mean forward scatter (related to cell volume). **(C)** Percentage of cells expressing high levels of CD69. **(D)** Mean fluorescence intensity (MFI) of CD25 expression. **(E)** MFI of CD26 expression. **(F)** MFI of CD62-L expression. **(G)** Average number of cell divisions quantified by CFSE dilution.

2-App.5. Time-course of functional Kv1.3 activity after stimulation with both anti-CD3 and anti-CD28 antibodies

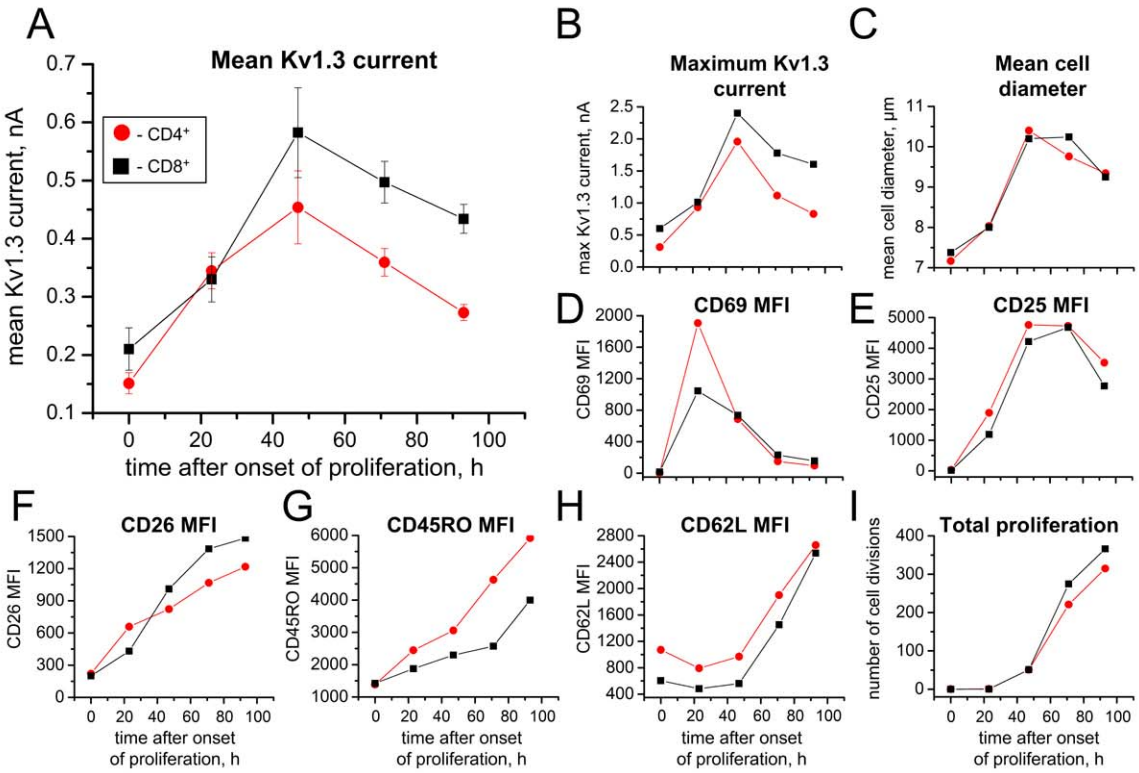

Figure 2-App.5 | Time-course of functional Kv1.3 activity after stimulation with both anti-CD3 and anti-CD28 antibodies. This figure shows time-courses of functional Kv1.3 activity, as well as other T cell parameters, following stimulation with both anti-CD3 and anti-CD28 antibodies (Fig. 2.5*A,B* in the main text). $CD4^+$ T cells are depicted as red circles, and $CD8^+$ T cells are depicted as black squares. **(A)** High-throughput measurements of mean Kv1.3 currents in T cells from freshly drawn blood (0 h) and 2 h, 24 h, 48 h, 72 h, and 96 h after the onset of mitogenic stimulation of isolated PBMCs with 150 ng mL^{-1} anti-CD3 antibody and 150 ng mL^{-1} anti-CD28 antibody. Error bars represent standard error of the mean. **(B)** Largest single Kv1.3 current measured, here denoted as "maximum Kv1.3 current". **(C)** Average cell diameter, measured immediately prior to high-throughput electrophysiology experiments using a Coulter counter. **(D through I)** Flow cytometric analysis of other lymphocyte properties following stimulation. **(D)** Percentage of cells expressing high levels of CD69. **(E)** Mean fluorescence intensity (MFI) of CD25 expression. **(F)** MFI of CD26 expression. **(G)** MFI of CD45-RO expression. **(H)** MFI of CD62-L expression. **(I)** Average number of cell divisions quantified by CFSE dilution.

2-App.6. Distribution of Kv1.3 ion currents in regulatory T cells and dendritic cells

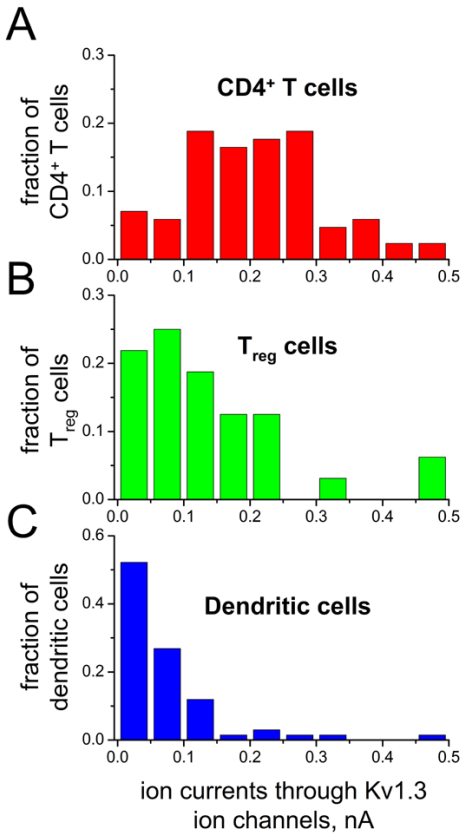

Figure 2-App.6 | Distribution of Kv1.3 ion currents in regulatory T cells and dendritic cells. This figure displays histograms of ion current from pilot experiments that measured Kv1.3 activity in $CD4^+$ T cells, regulatory $CD4^+$ T cells (T_{reg}) isolated from human peripheral blood and cultured for 24 h, as well as dendritic cells cultured for 7 d. **(A)** Cultured $CD4^+$ T cells, N = 85 total cells measured from one experiment (mean ion current through Kv1.3 ion channels = 0.21 ± 0.11 nA, mean ± standard deviation). **(B)** Cultured T_{reg} cells, N = 32 (mean Kv1.3 ion current = 0.13 ± 0.12 nA). Note that the $CD4^+$ T cells in panel (a) and the T_{reg} cells in panel (b) were isolated from the same individual and separated and cultured under the same conditions. T_{reg} cells and $CD4^+$ T cells were initially separated from freshly isolated PBMCs using magnetic bead kits (Miltenyi Biotec, using the $CD4^+/CD25^+/CD127^{dim/-}$ kit for T_{regs}). $CD4^+$ T cells and T_{reg} cells, with magnetic beads still attached, were cultured for 24 h in culture media supplemented with IL-2 (20 U mL^{-1}, Sigma), TGF-beta (2 ng mL^{-1}, Sigma), IL-10 (5 µg ml^{-1}, eBioscience, Inc., San Diego, CA), and anti-CD3 antibodies (clone OKT3, 50 ng mL^{-1}, eBioscience). Note that the culture conditions for the $CD4^+$ T cells shown here and the T_{reg} cells shown here were significantly different from the culture conditions for cells in the main text. Here conditions were used to sustain cells rather than activate them. **(C)** Dendritic cells, N = 67 cells from one experiment (mean Kv1.3 ion current = 0.06 ± 0.09 nA). Dendritic cells were prepared by culturing monocytes isolated by a magnetic bead kit (Miltenyi Biotec) in culture media for 7 d in the presence of 20 ng mL^{-1} GMC-SF (Sigma) and 20 ng mL^{-1} IL-4 (eBioscience).

Chapter 2 References

1. Panyi, G., **2005**, Biophysical and pharmacological aspects of K+ channels in T lymphocytes, *Eur. Biophys. J.*, 34: 515-529.
2. Cahalan, M. D., H. Wulff, and K. G. Chandy, **2001**, Molecular properties and physiological roles of ion channels in the immune system, *J. Clin. Immunol.*, 21: 235-252.
3. DeCoursey, T. E., K. G. Chandy, S. Gupta, and M. D. Cahalan, **1984**, Voltage-gated K+ channels in human T lymphocytes: a role in mitogenesis?, *Nature*, 307: 465-468.
4. Matteson, D. R., and C. Deutsch, **1984**, K channels in T lymphocytes: a patch clamp study using monoclonal antibody adhesion, *Nature*, 307: 468-471.
5. Panyi, G., Z. Varga, and R. Gaspar, **2004**, Ion channels and lymphocyte activation, *Immunol. Lett.*, 92: 55-66.
6. Lewis, R. S., and M. D. Cahalan, **1995**, Potassium and calcium channels in lymphocytes, *Annu. Rev. Immunol.*, 13: 623-653.
7. Lewis, R. S., **2001**, Calcium signaling mechanisms in T lymphocytes, *Annu. Rev. Immunol.*, 19: 497-521.
8. Wulff, H., P. A. Calabresi, R. Allie, S. Yun, M. Pennington, C. Beeton, and K. G. Chandy, **2003**, The voltage-gated Kv1.3 K+ channel in effector memory T cells as new target for MS, *J. Clin. Invest.*, 111: 1703-1713.
9. Beeton, C., H. Wulff, N. E. Standifer, P. Azam, K. M. Mullen, M. W. Pennington, A. Kolski-Andreaco, E. Wei, A. Grino, D. R. Counts, P. H. Wang, C. J. LeeHealey, S. A. B, A. Sankaranarayanan, D. Homerick, W. W. Roeck, J.

Tehranzadeh, K. L. Stanhope, P. Zimin, P. J. Havel, S. Griffey, H. G. Knaus, G. T. Nepom, G. A. Gutman, P. A. Calabresi, and K. G. Chandy, **2006**, Kv1.3 channels are a therapeutic target for T cell-mediated autoimmune diseases, *Proc. Natl. Acad. Sci. U. S. A.*, 103: 17414-17419.

10. Rus, H., C. A. Pardo, L. N. Hu, E. Darrah, C. Cudrici, T. Niculescu, F. Niculescu, K. M. Mullen, R. Allie, L. P. Guo, H. Wulff, C. Beeton, S. I. V. Judge, D. A. Kerr, H. G. Knaus, K. G. Chandy, and P. A. Calabresi, **2005**, The voltage-gated potassium channel Kv1.3 is highly expressed on inflammatory infiltrates in multiple sclerosis brain, *Proc. Natl. Acad. Sci. U. S. A.*, 102: 11094-11099.

11. Beeton, C., H. Wulff, J. Barbaria, O. Clot-Faybesse, M. Pennington, D. Bernard, M. D. Cahalan, K. G. Chandy, and E. Beraud, **2001**, Selective blockade of T lymphocyte K(+) channels ameliorates experimental autoimmune encephalomyelitis, a model for multiple sclerosis, *Proc. Natl. Acad. Sci. U. S. A.*, 98: 13942-13947.

12. Chandy, K. G., H. Wulff, C. Beeton, M. Pennington, G. A. Gutman, and M. D. Cahalan, **2004**, K+ channels as targets for specific immunomodulation, *Trends Pharmacol. Sci.*, 25: 280-289.

13. Cahalan, M. D., and K. G. Chandy, **1997**, Ion channels in the immune system as targets for immunosuppression, *Curr. Opin. Biotechnol.*, 8: 749-756.

14. Wulff, H., C. Beeton, and K. G. Chandy, **2003**, Potassium channels as therapeutic targets for autoimmune disorders, *Curr. Opin. Drug Discov. Devel.*, 6: 640-647.

15. Hu, L., M. Pennington, Q. Jiang, K. A. Whartenby, and P. A. Calabresi, **2007**, Characterization of the functional properties of the voltage-gated potassium channel Kv1.3 in human CD4(+) T lymphocytes, *J. Immunol.*, 179: 4563-4570.

16. Cahalan, M. D., K. G. Chandy, T. E. DeCoursey, and S. Gupta, **1985**, A voltage-gated potassium channel in human T lymphocytes, *J. Physiol.*, 358: 197-237.

17. Sakmann, B., and E. Neher, **1995**, *Single-Channel Recording*; Plenum Press: New York.

18. Chiu, D. T., and O. Orwar, **2004**, Functional cell-based high throughput drug screening, *Drug Disc. World*, 5: 45-51.

19. Fertig, N., R. H. Blick, and J. C. Behrends, **2002**, Whole cell patch clamp recording performed on a planar glass chip, *Biophys. J.*, 82: 3056-3062.

20. Schmidt, C., M. Mayer, and H. Vogel, **2000**, A Chip-Based Biosensor for the Functional Analysis of Single Ion Channels *Angew. Chem. Int. Ed. Engl.*, 39: 3137-3140.

21. Huang, C. J., A. Harootunian, M. P. Maher, C. Quan, C. D. Raj, K. McCormack, R. Numann, P. A. Negulescu, and J. E. Gonzalez, **2006**, Characterization of voltage-gated sodium-channel blockers by electrical stimulation and fluorescence detection of membrane potential, *Nat. Biotechnol.*, 24: 439-446.

22. Pihl, J., M. Karlsson, and D. T. Chiu, **2005**, Microfluidic technologies in drug discovery, *Drug Discov. Today*, 10: 1377-1383.

23. Kiss, L., P. B. Bennett, V. N. Uebele, K. S. Koblan, S. A. Kane, B. Neagle, and K. Schroeder, **2003**, High throughput ion-channel pharmacology: planar-array-based voltage clamp, *Assay Drug Dev. Technol.*, 1: 127-135.

24. Schroeder, K., B. Neagle, D. J. Trezise, and J. Worley, **2003**, IonWorks (TM) HT: A new high-throughput electrophysiology measurement platform, *J. Biomol. Screen.*, 8: 50-64.

25. Beeton, C., H. Wulff, S. Singh, S. Botsko, G. Crossley, G. A. Gutman, M. D. Cahalan, M. Pennington, and K. G. Chandy, **2003**, A novel fluorescent toxin to detect and investigate Kv1.3 channel up-regulation in chronically activated T lymphocytes, *J. Biol. Chem.*, 278: 9928-9937.

26. Guthrie, H., F. S. Livingston, U. Gubler, and R. Garippa, **2005**, A place for high-throughput electrophysiology in cardiac safety: screening hERG cell lines and novel compounds with the ion works HTTM system, *J. Biomol. Screen.*, 10: 832-840.

27. Abbas, A. K., and A. H. Lichtman, **2005**, *Cellular and Molecular Immunology*, 5th Ed. ed.; Elsevier Saunders: Philadelphia, PA.

28. Pennington, M. W., V. M. Mahnir, D. S. Krafte, I. Zaydenberg, M. E. Byrnes, I. Khaytin, K. Crowley, and W. R. Kem, **1996**, Identification of three separate binding sites on SHK toxin, a potent inhibitor of voltage-dependent potassium channels in human T-lymphocytes and rat brain, *Biochem. Biophys. Res. Commun.*, 219: 696-701.

29. Wulff, H., H. G. Knaus, M. Pennington, and K. G. Chandy, **2004**, K+ channel expression during B cell differentiation: Implications for immunomodulation and autoimmunity, *J. Immunol.*, 173: 776-786.

30. Rufer, N., A. Zippelius, P. Batard, M. J. Pittet, I. Kurth, P. Corthesy, J. C. Cerottini, S. Leyvraz, E. Roosnek, M. Nabholz, and P. Romero, **2003**, Ex vivo

characterization of human CD8(+) T subsets with distinct replicative history and partial effector functions, *Blood*, 102: 1779-1787.

31. Sallusto, F., D. Lenig, R. Forster, M. Lipp, and A. Lanzavecchia, **1999**, Two subsets of memory T lymphocytes with distinct homing potentials and effector functions, *Nature*, 401: 708-712.

32. Lee, S. C., D. E. Sabath, C. Deutsch, and M. B. Prystowsky, **1986**, Increased voltage-gated potassium conductance during interleukin 2-stimulated proliferation of a mouse helper T lymphocyte clone, *J. Cell Biol.*, 102: 1200-1208.

33. Decoursey, T. E., K. G. Chandy, S. Gupta, and M. D. Cahalan, **1987**, Mitogen induction of ion channels in murine T lymphocytes, *J. Gen. Physiol.*, 89: 405-420.

34. Deutsch, C., D. Krause, and S. C. Lee, **1986**, Voltage-gated potassium conductance in human T lymphocytes stimulated with phorbol ester, *J. Physiol.*, 372: 405-423.

35. Holmes, T. C., D. A. Fadool, and I. B. Levitan, **1996**, Tyrosine phosphorylation of the Kv1.3 potassium channel, *J. Neurosci.*, 16: 1581-1590.

36. Sharpe, A. H., and A. K. Abbas, **2006**, T-cell costimulation--biology, therapeutic potential, and challenges, *N. Engl. J. Med.*, 355: 973-975.

37. Pereira, L. E., F. Villinger, H. Wulff, A. Sankaranarayanan, G. Raman, and A. A. Ansari, **2007**, Pharmacokinetics, toxicity, and functional studies of the selective Kv1.3 channel blocker 5-(4-phenoxybutoxy)psoralen in rhesus macaques, *Exp Biol Med (Maywood)*, 232: 1338-1354.

38. Beeton, C., and K. G. Chandy, **2005**, Potassium channels, memory T cells, and multiple sclerosis, *Neuroscientist*, 11: 550-562.

39. Lafont, V., S. Loisel, J. Liautard, S. Dudal, M. Sable-Teychene, J. P. Liautard, and J. Favero, **2003**, Specific signaling pathways triggered by IL-2 in human V gamma 9V delta 2 T cells: an amalgamation of NK and alpha beta T cell signaling, *J. Immunol.*, 171: 5225-5232.

40. Hayes, S. M., and P. E. Love, **2002**, Distinct structure and signaling potential of the gamma delta TCR complex, *Immunity*, 16: 827-838.

41. Sinclair, J., J. Olofsson, J. Phil, and O. Orwar, **2003**, Stabilization of high-resistance seals in patch-clamp recordings by laminar flow, *Anal. Chem.*, 75: 6718-6722.

42. Bruggemann, A., S. Stoelzle, M. George, J. C. Behrends, and N. Fertig, **2006**, Microchip technology for automated and parallel patch-clamp recording, *Small*, 2: 840-846.

43. Uram, J. D., K. Ke, A. J. Hunt, and M. Mayer, **2006**, Label-free affinity assays by rapid detection of immune complexes in submicrometer pores, *Angew. Chem. Int. Ed. Engl.*, 45: 2281-2285.

44. Sinclair, J., J. Pihl, J. Olofsson, M. Karlsson, K. Jardemark, D. T. Chiu, and O. Orwar, **2002**, A cell-based bar code reader for high-throughput screening of ion channel-ligand interactions, *Anal. Chem.*, 74: 6133-6138.

45. Pihl, J., J. Sinclair, E. Sahlin, M. Karlsson, F. Petterson, J. Olofsson, and O. Orwar, **2005**, Microfluidic gradient-generating device for pharmacological profiling, *Anal. Chem.*, 77: 3897-3903.

CHAPTER 3

Functional Regulation of Kv1.3 Ion Channels in Human T Lymphocytes

This chapter examines the effects of immunosuppressive drugs on the activity of Kv1.3 ion channels in T cells upon stimulation. While activated T cells with high Kv1.3 activity have been implicated in the pathogenesis of several autoimmune diseases, the pathways that lead to this high Kv1.3 activity have not been explored. In this work, a recently developed, automated, high-throughput assay afforded quantification of functional levels of Kv1.3 ion channels in human $CD4^+$ T cells following mitogenic stimulation of peripheral blood mononuclear cells (PBMCs). We pre-treated PBMCs with either cyclosporin A (CsA), rapamycin, or tyrphostin AG-490 (an inhibitor of Janus kinases (Jak)-2 and Jak-3). All three drugs suppressed Kv1.3 activity after stimulation with anti-CD3 antibodies (aCD3) alone. Interestingly, only tyrphostin AG-490 fully inhibited the increase in Kv1.3 activity when recombinant interleukin (IL)-2 was present during stimulation with aCD3. In addition, both recombinant IL-2 and IL-15, but not IL-6 or IL-10, directly led to increased Kv1.3 activity in the absence of stimulation with aCD3. This work suggests that functional levels of Kv1.3 ion channels are regulated through signaling through the IL-2 receptor, mediated by Jak-3 pathways.

3.1. Introduction

Human T cells contain two major types of plasma membrane K^+ channels, the voltage gated Kv1.3 channel and the Ca^{2+}-activated KCa3.1 channel. These channels play important roles in processes involving Ca^{2+}-signaling (1-3). Kv1.3 ion channels, in particular, regulate the resting membrane potential of human T cells and allow for sustained Ca^{2+}-influx after T cell stimulation (4-6). The numbers of Kv1.3 ion channels per T cell increases after stimulation by a factor of 2-5, depending on cell phenotype and stimulation techniques (7-9). Effector memory T cells experience the largest increase in Kv1.3 activity, although the reasons for this increase are not known (8).

Recently, T cells with high numbers of Kv1.3 channels have been implicated in the pathogenesis of several autoimmune diseases (10). The Chandy and Calabresi groups found that disease-associated, autoreactive T cells isolated from patients with multiple sclerosis (MS), type-1 diabetes, and rheumatoid arthritis (RA) had elevated Kv1.3 activity after activation compared to autoreactive T cells from controls (8, 11). In addition, Rus *et al.* showed that T cells in inflammatory infiltrates in the brains of post-mortem MS patients displayed high numbers of Kv1.3 ion channels (12). Drug candidates that specifically block Kv1.3 ion channels ameliorated or delayed onset of symptoms in animal models of MS, RA, type-1 diabetes, and allergic contact dermatitis (11, 13, 14). The Kv1.3 ion channel, therefore, is a promising target for treating and studying the molecular mechanisms of autoimmune diseases (15).

Despite the disease-relevance of T cells with high levels of Kv1.3 activity, little is known about the cellular and biochemical pathways that lead to this increased activity after T cell activation. Previously, Beeton *et al.* examined the effects of

immunosuppressive drugs CsA (100 nM) and staurosporine (10 nM) on the increase of Kv1.3 activity after stimulation of a rat T cell line specific for myelin basic protein (16). Both drugs, which affect early events in T cell stimulation leading to transcription of IL-2, decreased Kv1.3 activity by ~60% (16). It is not clear, however, whether this decrease was due to the direct effects of the immunosuppressive drugs or due to the suppression of other downstream molecules that may regulate Kv1.3 activity. One likely reason for the lack of information about pathways regulating Kv1.3 activity may be due to the difficulties associated with measuring functional levels of ion channels in T cells. Previous studies have employed manual patch-clamping, which, while extremely sensitive, is serial, has low-throughput, and requires significant expertise.

Here, we use a recently-developed high-throughput assay for measuring voltage-gated ion channels in human T cells to examine pathways that lead to increased Kv1.3 activity after stimulation. This assay afforded the following characteristics: (i) automated patch clamp of 100-200 T cells in 1 h; (ii) specificity for Kv1.3 ion channels; and (iii) ability to compare different T cell populations in parallel (7, 17). Previously, this assay enabled the study of the heterogeneous, time-dependent changes in Kv1.3 activity in T cells after mitogenic stimulation (7). In the present study, we examine the effects of immunosuppressive drugs, acting at different points in the signaling cascade, on Kv1.3 activity after mitogenic stimulation (18). We also explore the effects of pro- and anti-inflammatory cytokines on Kv1.3 activity. The results presented here suggest that Kv1.3 is regulated by IL-2-dependent pathways and may provide insight towards disrupting Kv1.3 regulation for treatment of autoimmune disease.

3.2. Materials and Methods

Human subjects. We obtained peripheral venous blood from healthy subjects using protocols reviewed and approved by the Institutional Review Board at the University of Michigan. All subjects had previously exhibited a proliferative response of T cells upon stimulation with mitogenic anti-CD3 antibodies (7).

Cell culture and stimulation of T cells. We isolated peripheral blood mononuclear cells (PBMCs) from whole blood using density gradient centrifugation (Histopaque 1077 and 1119, Sigma-Aldrich, St. Louis, MO). We suspended isolated PBMCs at 1×10^6 cells mL^{-1} in culture media, defined as RPMI-1640 medium (ATCC, Manassas, VA) supplemented with 10% (v/v) fetal bovine serum (FBS, Mediatech, Herndon, VA), 100 U mL^{-1} penicillin, 100 μg mL^{-1} streptomycin (pen-strep, Invitrogen), and 55 μM 2-mercaptoethanol (Invitrogen) and then seeded PBMCs into 24-well plates (1 mL per well, BD Biosciences, San Jose, CA). For studies involving immunosuppressive drugs, we added one of the following molecules at concentrations specified in the text: cyclosporin A (CsA, Sigma-Aldrich), rapamycin (Sigma-Aldrich), or tyrphostin AG-490 (Sigma-Aldrich). Final concentrations of dimethyl sulfoxide (DMSO) were below 0.05% except in the case of 100 μM tyrphostin AG-490 (0.2% DMSO); we correspondingly added 0.2% DMSO into culture for all experiments with tyrphostin AG-490, including control experiments. Cells were incubated with drugs for 30 min at 37° C in 5% CO_2.

After pre-incubation with immunosuppressive drugs, we stimulated PBMCs by adding 150 ng mL^{-1} anti-human CD3 monoclonal antibody from mouse (aCD3, clone UCHT1, BD Biosciences), 150 ng mL^{-1} anti-human CD28 monoclonal antibody from mouse (aCD28, clone CD28.2, BD Biosciences), or 1000 U mL^{-1} recombinant human interleukin (IL)-2 (rIL-2, eBioscience, San Diego, CA), as specified in the text. For experiments with exogenous cytokines, we added the following concentrations of recombinant human cytokines (all from eBioscience): 1000 U mL^{-1} IL-15 (rIL-15), 1000 U mL^{-1} IL-6 (rIL-6), or 100 U mL^{-1} IL-10 (rIL-10). Cells were then cultured at 37° C in 5% CO_2 for ~64 h. For experiments measuring ion channel activity, we separated $CD4^+$ T cells from stimulated PBMCs using magnetic beads coated with antibodies against CD4 (Miltenyi Biotech, Auburn, CA) according to the manufacturer's instructions with minor modifications (7).

High-throughput profiling of Kv1.3 ion channels in $CD4^+$ T cells. We used an IonWorks HT high-throughput electrophysiology instrument (MDS Analytical Technologies, Sunnyvale, CA) made available via collaboration with the original developers of the technology (Essen Instruments, Ann Arbor, MI). Detailed methodology and validation of this technique for human lymphocytes can be found elsewhere (7). Briefly, we suspended isolated $CD4^+$ lymphocytes in Dulbecco's phosphate buffered saline (D-PBS) with Ca^{2+} and Mg^{2+} at a concentration of 5×10^5 to 1×10^6 cells mL^{-1} and stored the cells at room temperature for 30 min prior to electrophysiology experiments. The IonWorks HT instrument automatically dispensed the cells into a 384-well planar substrate (each well contained a single micropore to which a single T cell was attached via suction), and then gained intracellular access to the attached T cell by adding a

perforating agent (amphotericin B, 100 μg mL^{-1}, Sigma-Aldrich) in the intracellular recording solution (100 mM K^+ D-gluconic acid, 50 mM KCl, 3 mM $MgCl_2$, and 5 mM EGTA pH 7.3). A parallel array of 48 Ag/AgCl electrodes recorded the whole-cell electrical currents through the attached T cell in each well upon application of a depolarizing step pulse from −80 mV to + 40 mV for 300 ms. To render the assay specific for Kv1.3 ion channels, integrated fluidics within the IonWorks HT instrument then added a specific blocker of Kv1.3 ion channels, 6-FAM-AEEAc- *Stichodactyla helianthus* neurotoxin peptide (ShK, Bachem Biosciences, King of Prussia, PA) at a final concentration of 72 nM to each well of the patch plate (7). After 3 min incubation to block all Kv1.3 ion channels, electrical currents from the attached cells were measured again using the same voltage protocols as described above. We developed automated computer algorithms to compute the Kv1.3-specific current, which we defined as the difference between the pre-compound (pre-ShK) and post-compound (post-ShK) currents in cells that maintained stable seals resistances > 75 MΩ (7). Typically, we examined four different $CD4^+$ T cell conditions (e.g. different concentrations of drugs in culture) per 384-well plate, obtaining successful Kv1.3 measurements in 25-60 $CD4^+$ T cells for each condition.

Flow cytometry assays for measuring T cell activation markers. We measured expression of T cell activation markers using a four-color flow cytometer (FACScalibur, Becton Dickinson, Franklin Lakes, NJ). PBMCs cultured in flat-bottom 96-well plates (treated exactly as PBMCs for Kv1.3 measurements) were stained with anti-human CD4 antibodies conjugated to allophycocyanin (APC) plus antibodies conjugated with phycoerythrin (PE) against one of the following three human antigens: CD69, CD25, or

CD26 (all antibodies from BD Biosciences). All staining, incubation (30 min), and wash procedures occurred at 4° C using D-PBS (without Ca^{2+} or Mg^{2+}) supplemented with 2% FBS. We typically quantified mean fluorescence intensity (MFI) of PE-labeled antibodies for at least 10,000 cells gated as live cells on the basis of forward- and side-scatter and also gated for high expression of CD4 (Weasel analysis software, The Walter and Eliza Hall Institute, Parkville, Australia).

Quantitative real-time RT-PCR for measurements of Kv1.3 mRNA. We used two-step quantitative real-time RT-PCR (qRT-PCR) to quantify expression of Kv1.3 mRNA. We separated ~1×10^6 $CD4^+$ T cells from PBMCs stimulated for either 24 or 48 h, as described above and extracted total mRNA using a commercially available kit (RNeasy Mini, Qiagen, Valencia, CA). Absorbance readings confirmed A260/A280 ratios between 1.6 and 2.0 for all samples. We reverse transcribed 250 ng mRNA for each sample (QuantiTect reverse transcription kit, Qiagen) and immediately diluted the resulting cDNA by a factor of two. For qRT-PCR reactions (25 μL reaction volumes in 96-well plates using an Applied Biosystems ABI7500 thermal cycler), we used SYBR green (QuantiTect SYBR green PCR kit, Qiagen) as a reporter dye for double stranded DNA synthesized from primer pairs to the following human genes: KCNA3, IL-2, GAPDH, or RPLP0 (using pre-designed QuantiTect primers from Qiagen). After 40 thermal cycles, we determined the cycle threshold (C_T) values and calculated expression levels using comparative C_T methods. We quantified expression levels of IL-2 and KCNA3 relative to either GAPDH or RPLP0 and normalized them to the expression levels of $CD4^+$ T cells cultured without added stimulation.

Statistical analyses. We used the Kolmogorov-Smirnov test to compare distributions of Kv1.3 currents in $CD4^+$ T cells which were stimulated under different conditions (R Project for Statistical Computing). All *p* values and significance levels are specified in the text. To represent distributions of Kv1.3 currents in the figures throughout the text, we used box plots with the following characteristics: whiskers represent the 10^{th} and 90^{th} percentile of Kv1.3 values in the distributions; the large box represents the values between the 25^{th} and 75^{th} percentile; the solid line within the box represents the median value; and the dark square depicts the mean value.

To obtain IC_{50} values of half-maximal suppression of Kv1.3 activity after stimulation with various concentrations of immunosuppressive drugs, we fit normalized data to the logistic equation.

3.3. CsA attenuates the increase in Kv1.3 activity after stimulation except with strong CD28 co-stimulation

To test the role of early signaling events after stimulation through the TCR-CD3 complex on regulating Kv1.3 activity, we measured the effects of cyclosporin A (CsA), a commonly used immunosuppressive drug. CsA inhibits calcineurin and blocks expression of IL-2 and other cytokines when T cells are stimulated via the TCR-CD3 complex (19). We examined $CD4^+$ T cells isolated from human PBMCs that were pre-treated with CsA and stimulated with mitogenic antibodies for ~64 h. In a previous study, human T cells reached maximum Kv1.3 activity between 48 and 72 h after stimulation, depending on the subject (7).

CsA inhibited the increase of Kv1.3 activity after stimulation with anti-human CD3 monoclonal antibodies (aCD3) in a dose-dependent manner (IC_{50} = 75 nM, Fig. 3.1*A*). $CD4^+$ T cells treated with 400 nM and 1000 nM CsA showed no significant differences in Kv1.3 activity compared to T cells cultured without any stimulation (p=0.99 for both concentrations, Fig. 3.1*D*). A comparison of Kv1.3 activity to other T cell activation markers showed that CsA inhibited expression of CD26 (Fig. 3.1*B*), expansion of cell volume (Fig. 3.1*C*), and T cell proliferation after stimulation with aCD3 alone.

When we stimulated PBMCs in the presence of co-stimulatory anti-human CD28 monoclonal antibodies (aCD28) in addition to aCD3, however, CsA no longer inhibited the increase in Kv1.3 activity (Fig. 3.1*A*). Kv1.3 activity was significantly higher (p<0.01) with added aCD28 at every CsA concentration tested above 10 nM (Fig. 3.1D). Addition of aCD28 alone had no affect on Kv1.3 activity. Examining other activation markers, CsA did not inhibit expression of CD26 or expansion of cell volume after stimulation with aCD28 plus aCD3 (Fig. 3.1*B*,*C*). Previous studies found that strong CD28 co-stimulation led to expression of cytokines including IL-2 in the presence of high concentrations of CsA, (18, 20) by activating pathways separate from calcineurin-signaling (21). Interestingly, stimulation with aCD3 plus aCD28 of cells treated with 100 nM CsA led to significantly higher Kv1.3 activity than that found in cells stimulated without CsA (p<0.01, Fig. 3.1*D*). Expression of CD25 and CD26 also exhibited peak levels at 100 nM CsA. These results suggest that calcineurin-dependent signaling may negatively-regulate Kv1.3 activity and that the suppression of Kv1.3 activity by CsA after

stimulation with aCD3 alone was due to inhibition of molecules and pathways distinct from calcineurin.

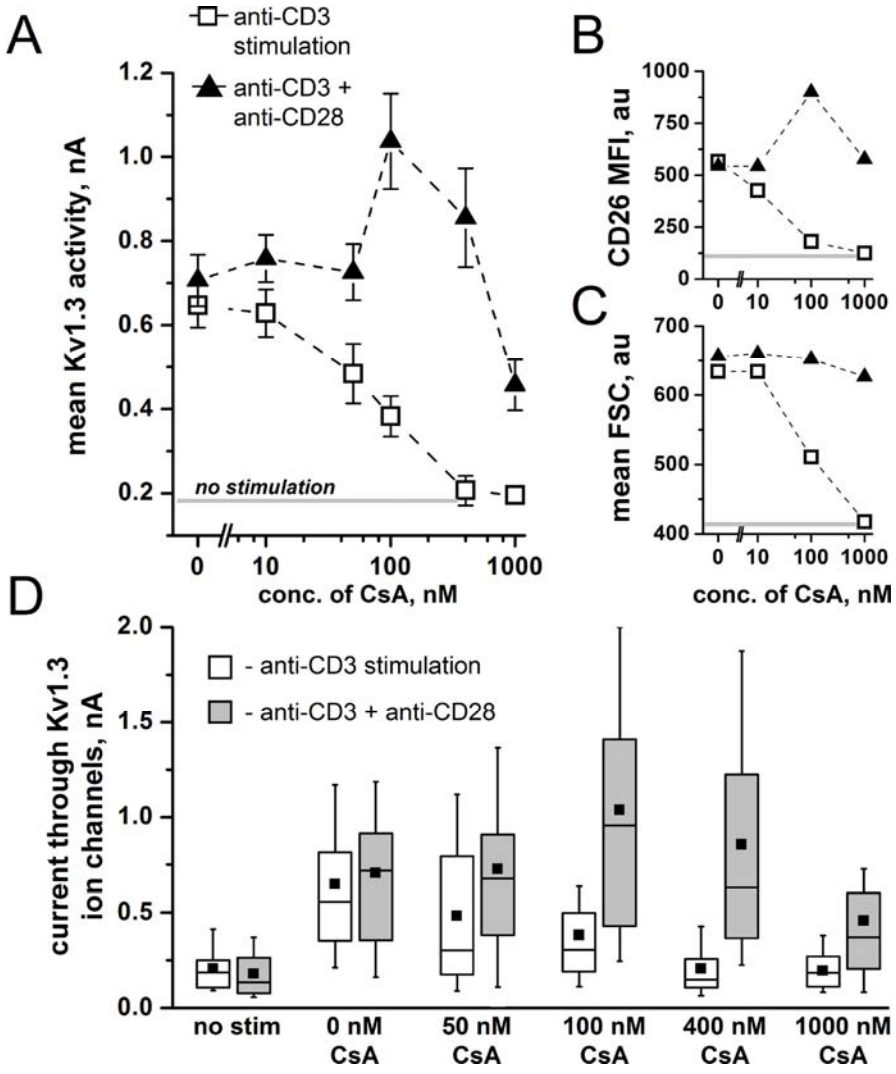

Figure 3.1 | Effects of cyclosporin A (CsA) on Kv1.3 ion channel activity in CD4$^+$ T cells after mitogenic stimulation. (A) Mean Kv1.3 activity ± standard error in CD4$^+$ T cells (N = 20-65 cells per point) isolated from PBMCs that were pre-incubated with the specified concentrations of CsA and stimulated for ~64 h with either anti-CD3 antibodies (□) or anti-CD28 plus anti-CD3 antibodies (▲). **(B)** Flow cytometric analysis of mean CD26 expression in gated CD4$^+$ T cells selected from PBMCs treated as described in (A). **(C)** Flow cytometric analysis of mean forward scatter (FSC) in gated CD4$^+$ T cells. The solid grey lines in panels (A-C) represent values from T cells cultured for ~64 h without mitogenic stimulation and without CsA. **(D)** Box plots indicating the distributions of current through Kv1.3 ion channels in the CD4$^+$ T cells described in (A). Large boxes depict the range of the 25th and 75th percentile of Kv1.3 currents, whiskers represent the 10th and 90th percentile of currents, and the median Kv1.3 current is depicted by the solid line, the mean Kv1.3 current by the black square (■) within the boxes. All measurements are from PBMCs isolated from the same human subject but were repeated and validated using a second subject.

3.4. Rapamycin inhibits the increase of Kv1.3 activity after mitogenic stimulation

While CsA affects IL-2 expression and the early stages of T cell activation, we used rapamycin to examine the role of late-stage events in the pathways leading to Kv1.3 up-regulation. Rapamycin, another commonly used immunosuppressive drug, inhibits the mammalian target of rapamycin (mTOR) complex (22). The mTOR complex is a serine-threonine kinase that regulates cellular growth and proliferation (23), generally after signaling of IL-2 through the IL-2 receptor (24). A major motivation for examining the effects of rapamycin on Kv1.3 activity was that we previously found that the increase in Kv1.3 activity correlated strongly with the increase in cell size after stimulation (7).

As shown in Figure 3.2, rapamycin inhibited, in a dose-dependent manner, the increase in Kv1.3 in $CD4^+$ T cells after stimulation with aCD3 alone (IC_{50} = 5 nM). Examining the distributions of Kv1.3 currents in cells treated with high concentrations of rapamycin (100 nM and 1000 nM), the median and mean currents showed little difference from cells cultured without stimulation (p>0.2, Fig. 3.2*D*). At these concentrations of rapamycin, however, 10-15% of $CD4^+$ T cells still exhibited high Kv1.3 activity (>0.6 nA), suggesting that Kv1.3 activity is not affected strongly by rapamycin in this subpopulation of cells. Comparing Kv1.3 activity to other activation markers, rapamycin inhibited proliferation, partially inhibited (~50%) expansion of cell volume, and only slightly affected expression of CD25 and CD26 surface markers (Fig. 3.2*B,C*).

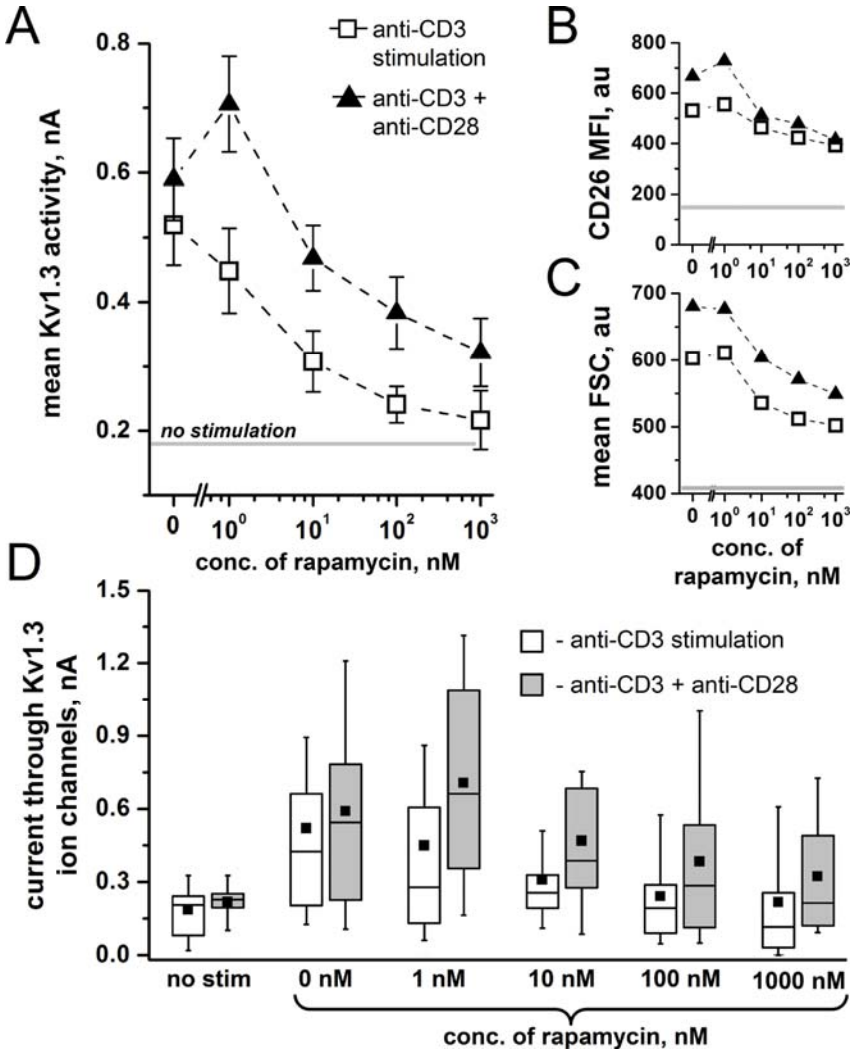

Figure 3.2 | Effects of rapamycin on Kv1.3 ion channel activity in CD4$^+$ T cells after mitogenic stimulation. (A) Mean Kv1.3 activity ± standard error in CD4$^+$ T cells (N = 23-53 cells per point) isolated from PBMCs that were pre-incubated with the specified concentrations of rapamycin and stimulated for ~64 h with either anti-CD3 antibodies (□) or anti-CD28 plus anti-CD3 antibodies (▲). **(B)** Flow cytometry analysis of mean CD26 expression in gated CD4$^+$ T cells selected from PBMCs treated as described in (A). The solid grey lines in panels (A-C) represent values from T cells cultured without mitogenic stimulation and without rapamycin. **(C)** Flow cytometric analysis of mean forward scatter (FSC) in gated CD4$^+$ T cells. **(D)** Box plots indicating the distributions of current through Kv1.3 ion channels in the CD4$^+$ T cells described in (A). Measurements are from PBMCs isolated from the same human subject but were repeated and validated using a second subject.

Upon adding aCD28 to stimulation with aCD3, rapamycin still decreased Kv1.3 activity in a dose-dependent manner. The addition of aCD28, however, led to ~50%

higher mean Kv1.3 activity at rapamycin concentrations between 1 and 1000 nM. Mean cell volume showed similar expansion upon stimulation with aCD3 and aCD28. These results suggest that while rapamycin inhibits the increase of Kv1.3 activity after stimulation, additional pathways can also increase Kv1.3 activity through mTOR-independent pathways.

3.5. Recombinant IL-2 increases Kv1.3 activity following stimulation of T cells

The addition of aCD28 to stimulation with aCD3 led to increased Kv1.3 activity in cells treated with either rapamycin or CsA. It was not clear, however, whether this increase was directly due to CD28 co-stimulatory pathways or to signaling induced by increased expression of cytokines such as IL-2. To answer this question, we measured the effects of high levels of recombinant IL-2 (rIL-2) on Kv1.3 activity in $CD4^+$ T cells isolated from three separate human subjects.

In each of the four conditions tested (aCD3 with no drugs, aCD3 with 400 nM CsA, aCD3 with 100 nM rapamycin, and no aCD3 with no drugs), the addition of rIL-2 led to a significant increase in Kv1.3 activity after ~64 h culture ($p<0.01$, Fig. 3.3). We observed the largest average Kv1.3 currents upon stimulation with rIL-2 and aCD3 in the presence of CsA, again suggesting a possible role of calcineurin-dependent pathways in negatively regulating Kv1.3 activity. In addition, even without added anti-CD3 stimulation, rIL-2 increased mean Kv1.3 activity by a factor of ~2 compared to cells without added rIL-2. Distributions of Kv1.3 currents in cells stimulated with rIL-2 alone showed no significant differences compared to cells stimulated with aCD3 alone

(p=0.10). Previously, Lee *et al.* found that the mouse T lymphocyte line, L2, exhibited similar increases in Kv1.3 activity upon treatment with rIL-2 (25), although mice T cells exhibit marked differences in K^+-channel behavior compared to human T cells (10, 26). Signaling through the TCR-CD3 complex, therefore, is not necessary for obtaining cells with high levels of Kv1.3 activity in human $CD4^+$ T cells.

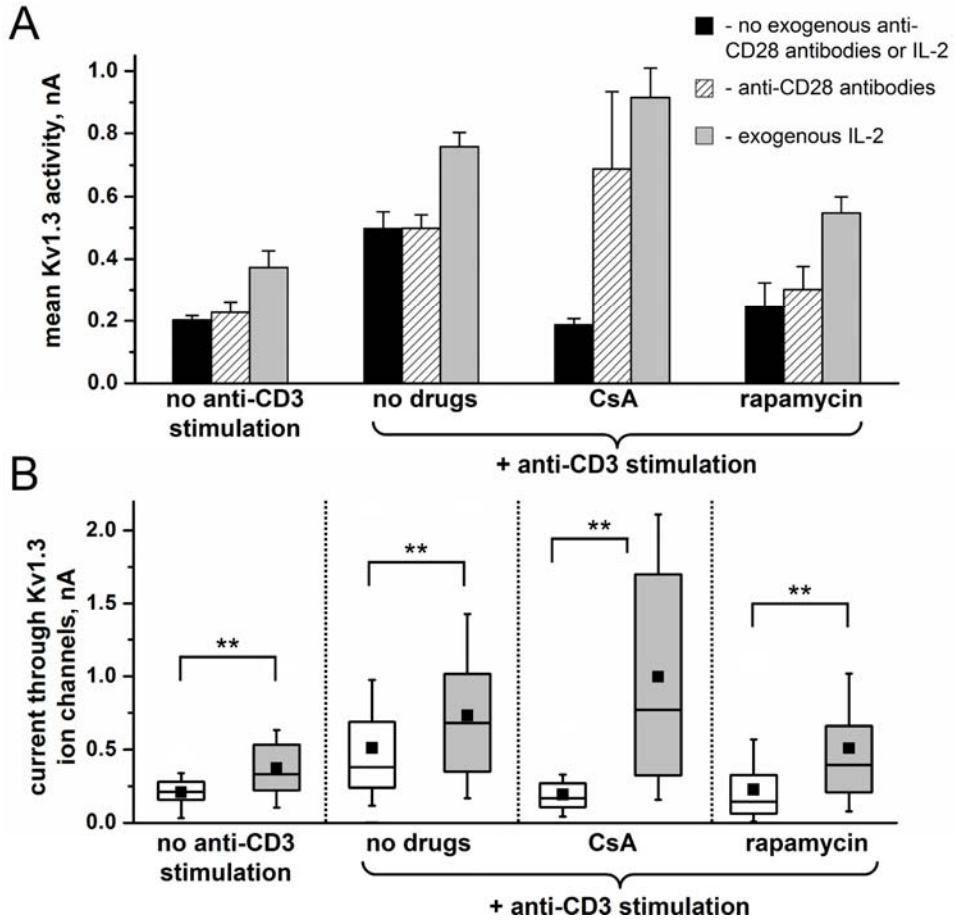

Figure 3.3 | Increase of Kv1.3 ion channel activity after culture with exogenous IL-2. (A) Mean Kv1.3 activity in $CD4^+$ T cells isolated from PBMCs cultured for 60 hours with either anti-CD3 antibodies (black bars), anti-CD28 plus anti-CD3 antibodies (striped bars), or recombinant IL-2 plus anti-CD3 antibodies (gray bars). Before stimulation, PBMCs were pre-incubated with either 400 nM CsA, 100 nM rapamycin, or no drugs, as indicated. All values represent the average and standard error of mean Kv1.3 measurements using three human subjects. **(B)** Box plots showing the distributions of current through Kv1.3 ion channels in the $CD4^+$ T cells described in (A), with the grey boxes representing cells cultured with IL-2 and the white boxes representing cells without IL-2 and without anti-CD28 antibodies. Distributions were constructed by combining the individual Kv1.3 currents from all three human subjects (N = 47-128 cells per specified condition). Significant differences between distributions were determined using the Kolmogorov-Smirnov test and are depicted with ** ($p < 0.01$).

We observed four additional interesting effects of rIL-2 on Kv1.3 activity. First, treating cells with rapamycin led to a significant decrease in Kv1.3 activity in cells stimulated with aCD3 and rIL-2 ($p<0.01$), again suggesting a partial role of mTOR pathways in regulating Kv1.3 activity. Second, flow cytometry studies of activation markers revealed that treating cells with rIL-2 in addition to aCD3 led to greatly increased CD25 and CD26 expression. In particular, the increased expression of CD25, which is part of the complex comprising the IL-2 receptor, especially may help explain increased Kv1.3 activity in cells treated with aCD3 and rIL-2 compared to cells treated with aCD3 alone. Treatment with rIL-2 in the absence of aCD3 stimulation did not lead to increased CD25 expression. Third, using quantitative RT-PCR, increased Kv1.3 activity after stimulation did not correlate with increased expression of Kv1.3 mRNA (Fig. 3.4). And fourth, stimulating cells with aCD3 plus aCD28 plus rIL-2 showed no differences in Kv1.3 activity compared to cells stimulated with aCD3 plus rIL-2 (e.g. no aCD28), suggesting that aCD28 pathways do not have direct effects on Kv1.3 activity. Together, these results indicate that Kv1.3 activity is regulated by pathways induced by IL-2 induced signaling but not at the transcriptional level.

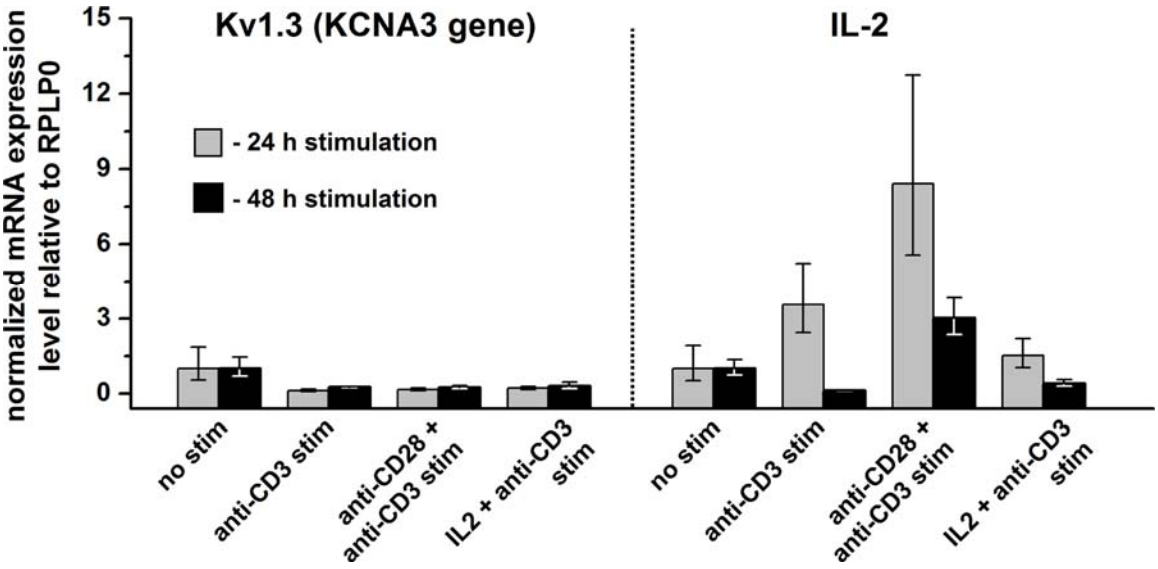

Figure 3.4 | Quantitative RT-PCR measurements of KCNA (Kv1.3) and IL-2 mRNA expression after mitogenic stimulation. mRNA was extracted from $CD4^+$ T cells isolated from PBMCs cultured for either 24 h (black bars) or 48 h (grey bars) with either anti-CD3 antibodies, anti-CD28 antibodies plus anti-CD3 antibodies, recombinant IL-2 plus anti-CD3 antibodies, or no added mitogenic antibodies,. RPLP0 was used as a normalizer gene, and expression levels of KCNA (left) and IL-2 (right) are expressed relative to the condition of no added mitogen stimulation (e.g. "no stim"). Values represent average ± standard deviation of triplicate quantitative RT-PCR measurements and are representative of two independent experiments from two human subjects.

3.6. IL-15 and IL-2 increase Kv1.3 activity in the absence of CD3-signaling

While exogenous IL-2 increased Kv1.3 activity in $CD4^+$ T cells, it was not clear through which mechanisms this increase might occur. The heterotrimeric receptor for IL-2 (IL-2R) initiates downstream signaling through its IL-2Rβ and γ_c subunits, which activate Janus kinases (Jak)-1 and Jak-3 (27). These kinases in turn stimulate signaling transducers and activators of transcription (Stat)-3 and Stat5, as well as additional pathways (28). To ascertain which specific Jak/Stat pathways might be involved in regulating Kv1.3 activity, we measured the effects of the following recombinant human cytokines: IL-15, which activates Jak-1 and Jak-3 through its receptor which includes the IL-2Rβ and γ_c subunits (28); IL-6, which primarily activates Stat-1 and Stat-3 pathways

through Jak-1 and Jak-2 (29); and IL-10, which in T cells primarily activates Stat-3, as well as Stat-1 and Stat-5, through Jak-1 and tyrosine kinase-2 (Tyk-2) (30).

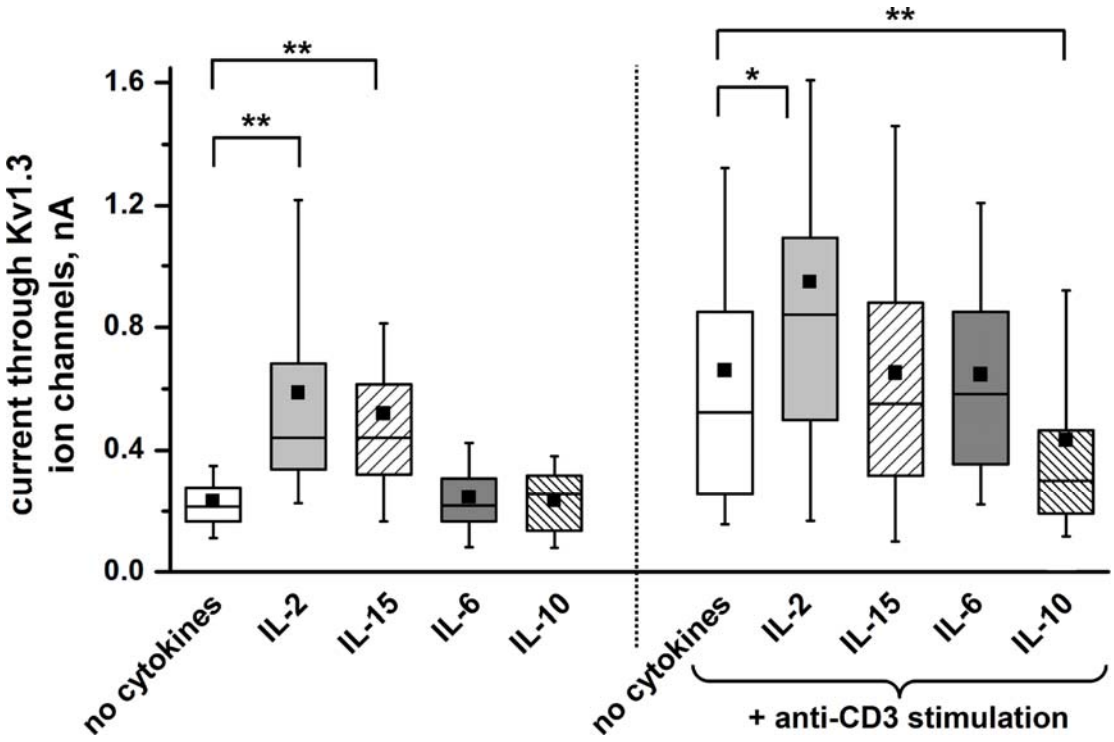

Figure 3.5 | Effects of exogenous cytokines on Kv1.3 activity. Box plots represent distributions of currents through Kv1.3 ion channels in $CD4^+$ T cells isolated from PBMCs cultured for ~64 h with either IL-2, IL-15, IL-6, IL-10, or no exogenous cytokines (N = 20-60 cells per condition). Distributions on the left were from cells cultured only with the specified exogenous cytokine, while the distributions on the right were measured in cells cultured with anti-CD3 antibodies in addition to the indicated cytokine. Significant differences between specified distributions were determined using the Kolmogorov-Smirnov test and are depicted by * ($p < 0.05$) or ** ($p < 0.01$).

In the absence of stimulation with aCD3, both rIL-2 and recombinant IL-15 (rIL-15) led to significantly increased Kv1.3 activity in $CD4^+$ T cells compared to cells with no added cytokines (p<0.01, Fig. 3.5). Treating cells with recombinant IL-6 (rIL-6) or recombinant IL-10 (rIL-10) had no effect on Kv1.3 activity (Fig. 3.5). In cells stimulated with aCD3, only rIL-2 led to increased Kv1.3 activity compared to cells stimulated with

aCD3 but without cytokines ($p<0.05$). The cytokines rIL-6 and rIL-15 had no significant effects on Kv1.3 activity. The absence of an effect of rIL-15 on cells stimulated with aCD3 may be due to competition with expressed IL-2 for receptor activity (31). Finally, rIL-10 led to decreased Kv1.3 activity in cells stimulated with aCD3 compared to cells stimulated without cytokines ($p<0.01$), although this decrease may be due to decreased expression of IL-2 in cells treated with rIL-10 (32). Together these results highlight the importance of Jak-3 in regulating Kv1.3 activity through Stat-3 independent pathways.

3.7. Tyrphostin AG-490 inhibits increase in Kv1.3 activity after stimulation

To confirm the role of Jak-3 in regulating Kv1.3 activity, we measured the effects of tyrphostin AG-490 on Kv1.3 activity in $CD4^+$ T cells. Tyrphostin AG-490 is a potent inhibitor of Jak-2 and Jak-3 kinases (IC_{50} = ~25 μM) that inhibits proliferation of T cells (33, 34). Importantly, tyrphostin AG-490 does not affect Jak-1, Tyk-2, early activation kinases such as Lck and Syk, or expression of CD25 (34, 35).

As shown in Figure 3.6, treating cells with 100 μM tyrphostin AG-490 inhibited increases in Kv1.3 activity after stimulation. In all three stimulation conditions tested (aCD3 alone, aCD3 plus aCD28, and aCD3 plus rIL-2), Kv1.3 activity in cells treated with 100 μM tyrphostin AG-490 showed no significant differences compared to cells cultured without stimulation. Treating cells with a lower concentration of tyrphostin AG-490 (10 μM) did not significantly reduce the increase of Kv1.3 activity upon stimulation (Fig. 3.6). This concentration was below the effective concentration for inhibiting Jak-3 activity (34) but above the concentration reported for inhibiting Jak-2 (35). Tyrphostin AG-490 had no effects on upregulation of CD25 or CD26 except with stimulation by

aCD3 plus rIL-2, in which case expression was reduced to levels of aCD3 stimulation without rIL-2. These results, combined with the result that Jak-2 activation through IL-6 had no effects on Kv1.3 activity, suggest that increases in Kv1.3 activity primarily occur through Jak-3-dependent pathways.

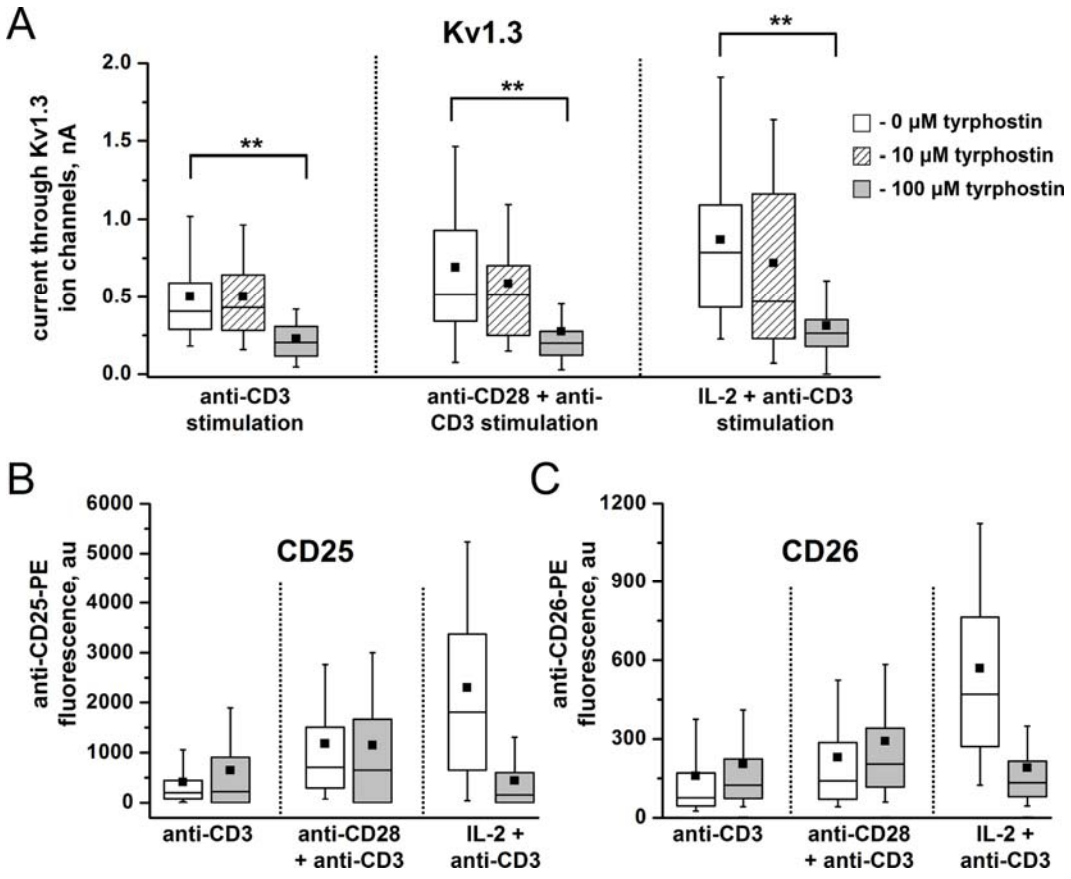

Figure 3.6 | Tyrphostin AG-490-induced inhibition of the increase of Kv1.3 activity after stimulation. (A) Box plots representing $CD4^+$ T cells isolated from PBMCs cultured for ~64 h with either anti-CD3 antibodies, anti-CD28 plus anti-CD3 antibodies, or recombinant IL-2 plus anti-CD3 stimulation. Before stimulation, PBMCs were pre-incubated with either no tyrphostin (white boxes), 10 µM tyrphostin (striped boxes), or 100 µM tyrphostin (grey boxes). Significant differences between specified distributions were determined using the Kolmogorov-Smirnov test and are depicted by ** ($p < 0.01$). **(B)** Box plots representing flow cytometric distributions of CD25 expression in gated $CD4^+$ lymphocytes selected from PBMCs described in (A), with white boxes depicting cells cultured with 0 µM tyrphostin and grey boxes depicting cells cultured with 100 µM tyrphostin. **(C)** Box plots representing flow cytometric distributions of CD26 expression in gated $CD4^+$ lymphocytes as described in (A). Measurements of Kv1.3 activity (*N*=19-45 cells per condition) and activation markers are representative of experiments with PBMCs from two human subjects.

3.8. Discussion

Potassium ion channels in T cells are emerging targets for the treatment of human autoimmune diseases (36, 37). Compounds that block Kv1.3 ion channel activity, in particular, are of interest because they potently suppress the effector memory phenotype of T cells (T_{em}) while having minimal effects on naïve or central memory phenotypes (38). The efficacy of blockers of Kv1.3 activity in animal models of MS, RA, and type 1 diabetes presumably arises from this preferential suppression of T_{em} cells relevant to disease pathogenesis (8, 11, 13). While considerable efforts have focused on developing drug compounds to block Kv1.3 activity (15, 39, 40), the approach of altering Kv1.3 activity by affecting its regulation has not been explored. In this study, we used high-throughput profiling of Kv1.3 ion channels in $CD4^+$ T cells to elucidate which pathways regulate Kv1.3 activity after stimulation.

The results presented here indicate that IL-2R pathways play a critical role in increasing Kv1.3 activity after stimulation of human T cells. Four findings support this conclusion: (i) rIL-2 and rIL-15, which both signal through the IL-2Rβ and γ_c subunits of the IL2-R, increased Kv1.3 activity in the absence of mitogenic stimulation (Fig. 3.5); (ii) adding rIL-2 to mitogenic stimulation increased Kv1.3 activity compared to mitogenic stimulation alone, presumably through increased levels of both IL-2 and IL-2R (Fig. 3.3); (iii) rapamycin, which inhibits cell cycle progression in T cells (41), suppressed Kv1.3 activity after stimulation (Fig. 3.2); and (iv) CsA exhibited no inhibitory effects on Kv1.3 activity when stimulation occurred in the presence of rIL-2 or aCD28, which can bypass CsA leading to expression of IL-2 (Fig. 3.1). Interestingly, calcineurin-dependent pathways activated by signaling through the TCR-CD3 complex may negatively regulate

Kv1.3 activity, as treating cells with CsA actually increased mean Kv1.3 activity after mitogenic stimulation in the presence of rIL-2 or aCD28 antibodies (Fig. 3.1).

In terms of which IL-2R pathways play roles in regulating Kv1.3 activity, we found that Jak-3-dependent pathways are critical for increasing Kv1.3 activity. Signaling through the IL-2Rβ and γ_c subunits of the IL-2R (by rIL-2 and rIL-15), which activate Jak-1 and Jak-3, led to increased Kv1.3 activity (Fig. 3.5). Signaling through Jak-1, Jak-2, and Tyk-2 pathways (using rIL-6 or rIL-10) had no effects on Kv1.3 activity (Fig. 3.5). Lack of effects of rIL-6 also suggests that Stat3-activation does not regulate Kv1.3 activity. Finally, tyrphostin AG-490, which selectively inhibits Jak-2 and Jak-3, suppressed the increase in Kv1.3 activity after mitogenic stimulation only at a concentration that completely inhibited Jak-3 (Fig. 3.6).

We found that mTOR-associated pathways regulate Kv1.3 activity, as rapamycin partially inhibited increase of Kv1.3 activity depending on stimulation conditions. The mTOR complex is a downstream target of Jak-3 (42), although it can also be activated by CD28-pathways through protein kinase B (Akt) signaling pathways (21, 43) or phosphatidylinositol-3-OH kinase (PI(3)K) pathways (44, 45). Two pieces of evidence suggest that CD28-activated pathways do not strongly regulate Kv1.3 activity. First, we observed only slight increases in Kv1.3 activity upon adding aCD28 to stimulation with aCD3 (Fig. 3.3). Second, tyrphostin AG-490 suppressed Kv1.3 activity in cells stimulated with aCD28 and aCD3 (Fig. 3.5), highlighting the importance of Jak-3 in regulating Kv1.3 activity even in presence of CD28-costimulation.

In addition to mTOR-pathways, other Jak-3 pathways independent of rapamycin contributed to regulation of Kv1.3 activity (Fig. 3.2). One such pathway likely to regulate

Kv1.3 activity is Stat-5, which can regulate rapamycin-independent cellular growth and survival through activation of Pim kinases (46). Other potential Jak-3 activated pathways that may play roles in regulating Kv1.3 activity are the Akt, PI(3)K, and mitogen-activated protein kinases, although these pathways are not specific to Jak-3 activation (24).

Understanding the pathways involved in upregulating Kv1.3 activity in T cells has several implications for the roles and functions of Kv1.3 ion channels. First, as mentioned previously, T cells with high Kv1.3 activity have been found in inflammatory infiltrates from patients with MS (12). The fact that IL-2 and IL-15 can increase Kv1.3 activity independent of TCR-CD3 signaling (Fig. 3.6) suggests that these cells may acquire high Kv1.3 activity because of the cytokine environment in the infiltrates in addition to stimulation through the TCR. Second, the fact that T cell pathways associated with cellular growth also regulate Kv1.3 activity highlights the role of Kv1.3 ion channels in regulating T cell volume. Third, it is interesting that Kv1.3 ion channels are regulated by different mechanisms and pathways than the other major K^+ channel in T cells, KCa3.1, which is regulated transcriptionally by protein kinase C (47). These differences may suggest molecular mechanisms by which different phenotypes of T cells acquire certain distributions of K^+ ion channels, favoring either Kv1.3 or KCa3.1, after stimulation (8).

A major question regarding the regulation of Kv1.3 activity in T cells is the mechanism by which this regulation occurs. Previous reports have determined that the increased Kv1.3 activity correlates with increased number of active channels in the plasma membrane. We demonstrated, however, that increases in Kv1.3 activity did not correlate with increased expression of Kv1.3 mRNA (Fig. 3.4), a finding that agrees with

several previous studies (48, 49). The gene for Kv1.3 ion channels, interestingly, may even be an effective housekeeping gene in human T cells, as it demonstrated remarkable stability compared to GADPH and RPLP0 in quantitative RT-PCR studies. While not regulated at the transcriptional level, Kv1.3 activity may be increased through translation, through activation (50), or by insertion of pre-synthesized Kv1.3 channels into the plasma membrane from intracellular stores (4). The model of translational regulation seems promising given the role of mTOR and Stat-5 pathways in increasing translation which precedes cell growth and survival (51, 52).

A second question is whether affecting regulation of Kv1.3 ion channels may offer benefits similar to drug compounds that directly block Kv1.3 activity. The effects of rapamycin on Kv1.3 activity after stimulation are interesting given the potency of rapamycin as a clinical immunosuppressant. A recent study indicated that rapamycin altered lymphocyte trafficking by affecting down-regulation of chemokine receptor 7 (CCR7) and CD62L in activated T cells (53). As activated T_{em} have low expression of CCR7 and CD62L, but elevated levels of Kv1.3 activity (8), it would be interesting if altered Kv1.3 activity in these cell types contributed to the effects of rapamycin.

Finally, this study highlights the potential of using high-throughput methods of measuring Kv1.3 activity for performing immunological studies of T cell activation. The high-throughput method used here allowed automated and direct comparison of cells treated under different stimulation conditions or drug-treatments. In addition, the total number of $CD4^+$ T cells measured for Kv1.3 activity in this study (>5000 cells) would be virtually impossible using traditional, manual techniques for measuring functional Kv1.3 activity. Despite these enabling characteristics, current high-throughput

electrophysiology methods do have several drawbacks, including high cost, inability to measure ligand-gated ion channels, and lower throughput than true high-throughput methods such as flow cytometry; however, advances in microfluidics and microfabrication may address some of these limitations in the near future (54, 55). High-throughput electrophysiology, therefore, offers a useful and accessible tool to study ion channel activity in T cells, and more importantly, as demonstrated in this study, may reveal insight into the functional roles of ion channels in immune responses and human disease.

Chapter 3 References

1. DeCoursey, T. E., K. G. Chandy, S. Gupta, and M. D. Cahalan, **1984**, Voltage-gated K+ channels in human T lymphocytes: a role in mitogenesis?, *Nature*, 307: 465-468.
2. Grissmer, S., R. S. Lewis, and M. D. Cahalan, **1992**, Ca(2+)-activated K+ channels in human leukemic T cells, *J. Gen. Physiol.*, 99: 63-84.
3. Lewis, R. S., **2001**, Calcium signaling mechanisms in T lymphocytes, *Annu. Rev. Immunol.*, 19: 497-521.
4. Lewis, R. S., and M. D. Cahalan, **1995**, Potassium and calcium channels in lymphocytes, *Annu. Rev. Immunol.*, 13: 623-653.
5. Freedman, B. D., M. A. Price, and C. J. Deutsch, **1992**, Evidence for voltage modulation of IL-2 production in mitogen-stimulated human peripheral blood lymphocytes, *J. Immunol.*, 149: 3784-3794.

6. Cahalan, M. D., H. Wulff, and K. G. Chandy, **2001**, Molecular properties and physiological roles of ion channels in the immune system, *J. Clin. Immunol.*, 21: 235-252.

7. Estes, D. J., S. Memarsadeghi, S. K. Lundy, F. Marti, D. D. Mikol, D. A. Fox, and M. Mayer, **2008**, High-throughput profiling of ion channel activity in primary human lymphocytes, *Anal. Chem.*, 80: 3728-3735.

8. Wulff, H., P. A. Calabresi, R. Allie, S. Yun, M. Pennington, C. Beeton, and K. G. Chandy, **2003**, The voltage-gated Kv1.3 K+ channel in effector memory T cells as new target for MS, *J. Clin. Invest.*, 111: 1703-1713.

9. Matteson, D. R., and C. Deutsch, **1984**, K channels in T lymphocytes: a patch clamp study using monoclonal antibody adhesion, *Nature*, 307: 468-471.

10. Chandy, G., H. Wulff, C. Beeton, P. Calabresi, G. A. Gutman, and M. Pennington, **2006**, The Kv1.3 potassium channel: physiology, pharmacology, and therapeutic indications, In: *Voltage-Gated Ion Channels as Drug Targets*; Triggle, D. J., M. Gopalakrishnan, D. Rampe, and W. Zheng, Eds.; Wiley-VCH: Weinheim, Germany, pp 214-252.

11. Beeton, C., H. Wulff, N. E. Standifer, P. Azam, K. M. Mullen, M. W. Pennington, A. Kolski-Andreaco, E. Wei, A. Grino, D. R. Counts, P. H. Wang, C. J. LeeHealey, S. A. B, A. Sankaranarayanan, D. Homerick, W. W. Roeck, J. Tehranzadeh, K. L. Stanhope, P. Zimin, P. J. Havel, S. Griffey, H. G. Knaus, G. T. Nepom, G. A. Gutman, P. A. Calabresi, and K. G. Chandy, **2006**, Kv1.3 channels are a therapeutic target for T cell-mediated autoimmune diseases, *Proc. Natl. Acad. Sci. U. S. A.*, 103: 17414-17419.

12. Rus, H., C. A. Pardo, L. N. Hu, E. Darrah, C. Cudrici, T. Niculescu, F. Niculescu, K. M. Mullen, R. Allie, L. P. Guo, H. Wulff, C. Beeton, S. I. V. Judge, D. A. Kerr, H. G. Knaus, K. G. Chandy, and P. A. Calabresi, **2005**, The voltage-gated potassium channel Kv1.3 is highly expressed on inflammatory infiltrates in multiple sclerosis brain, *Proc. Natl. Acad. Sci. U. S. A.*, 102: 11094-11099.

13. Azam, P., A. Sankaranarayanan, D. Homerick, S. Griffey, and H. Wulff, **2007**, Targeting effector memory T cells with the small molecule Kv1.3 blocker PAP-1 suppresses allergic contact dermatitis, *J. Invest. Dermatol.*, 127: 1419-1429.

14. Beeton, C., H. Wulff, J. Barbaria, O. Clot-Faybesse, M. Pennington, D. Bernard, M. D. Cahalan, K. G. Chandy, and E. Beraud, **2001**, Selective blockade of T lymphocyte K(+) channels ameliorates experimental autoimmune encephalomyelitis, a model for multiple sclerosis, *Proc. Natl. Acad. Sci. U. S. A.*, 98: 13942-13947.

15. Chandy, K. G., H. Wulff, C. Beeton, M. Pennington, G. A. Gutman, and M. D. Cahalan, **2004**, K+ channels as targets for specific immunomodulation, *Trends Pharmacol. Sci.*, 25: 280-289.

16. Beeton, C., H. Wulff, S. Singh, S. Botsko, G. Crossley, G. A. Gutman, M. D. Cahalan, M. Pennington, and K. G. Chandy, **2003**, A novel fluorescent toxin to detect and investigate Kv1.3 channel up-regulation in chronically activated T lymphocytes, *J. Biol. Chem.*, 278: 9928-9937.

17. Schroeder, K., B. Neagle, D. J. Trezise, and J. Worley, **2003**, IonWorks (TM) HT: A new high-throughput electrophysiology measurement platform, *J. Biomol. Screen.*, 8: 50-64.

18. Sigal, N. H., and F. J. Dumont, **1992**, Cyclosporin A, FK-506, and rapamycin: pharmacologic probes of lymphocyte signal transduction, *Annu. Rev. Immunol.*, 10: 519-560.

19. Liu, J., J. D. Farmer, Jr., W. S. Lane, J. Friedman, I. Weissman, and S. L. Schreiber, **1991**, Calcineurin is a common target of cyclophilin-cyclosporin A and FKBP-FK506 complexes, *Cell*, 66: 807-815.

20. June, C. H., J. A. Ledbetter, M. M. Gillespie, T. Lindsten, and C. B. Thompson, **1987**, T-cell proliferation involving the CD28 pathway is associated with cyclosporine-resistant interleukin 2 gene expression, *Mol. Cell. Biol.*, 7: 4472-4481.

21. Kane, L. P., P. G. Andres, K. C. Howland, A. K. Abbas, and A. Weiss, **2001**, Akt provides the CD28 costimulatory signal for up-regulation of IL-2 and IFN-gamma but not TH2 cytokines, *Nat. Immunol.*, 2: 37-44.

22. Abraham, R. T., and G. J. Wiederrecht, **1996**, Immunopharmacology of rapamycin, *Annu. Rev. Immunol.*, 14: 483-510.

23. Fingar, D. C., and J. Blenis, **2004**, Target of rapamycin (TOR): an integrator of nutrient and growth factor signals and coordinator of cell growth and cell cycle progression, *Oncogene*, 23: 3151-3171.

24. Abbas, A. K., and A. H. Lichtman, **2005**, *Cellular and Molecular Immunology*, 5th Ed. ed.; Elsevier Saunders: Philadelphia, PA.

25. Lee, S. C., D. E. Sabath, C. Deutsch, and M. B. Prystowsky, **1986**, Increased voltage-gated potassium conductance during interleukin 2-stimulated proliferation of a mouse helper T lymphocyte clone, *J. Cell Biol.*, 102: 1200-1208.

26. Decoursey, T. E., K. G. Chandy, S. Gupta, and M. D. Cahalan, **1987**, Mitogen induction of ion channels in murine T lymphocytes, *J. Gen. Physiol.*, 89: 405-420.

27. Malek, T. R., **2008**, The biology of interleukin-2, *Annu. Rev. Immunol.*, 26: 453-479.

28. Ma, A., R. Koka, and P. Burkett, **2006**, Diverse functions of IL-2, IL-15, and IL-7 in lymphoid homeostasis, *Annu. Rev. Immunol.*, 24: 657-679.

29. Schindler, C., and J. E. Darnell, Jr., **1995**, Transcriptional responses to polypeptide ligands: the JAK-STAT pathway, *Annu. Rev. Biochem.*, 64: 621-651.

30. Moore, K. W., R. de Waal Malefyt, R. L. Coffman, and A. O'Garra, **2001**, Interleukin-10 and the interleukin-10 receptor, *Annu. Rev. Immunol.*, 19: 683-765.

31. Zhang, X., S. Sun, I. Hwang, D. F. Tough, and J. Sprent, **1998**, Potent and selective stimulation of memory-phenotype CD8+ T cells in vivo by IL-15, *Immunity*, 8: 591-599.

32. de Waal Malefyt, R., H. Yssel, and J. E. de Vries, **1993**, Direct effects of IL-10 on subsets of human CD4+ T cell clones and resting T cells. Specific inhibition of IL-2 production and proliferation, *J. Immunol.*, 150: 4754-4765.

33. Kirken, R. A., R. A. Erwin, D. Taub, W. J. Murphy, F. Behbod, L. Wang, F. Pericle, and W. L. Farrar, **1999**, Tyrphostin AG-490 inhibits cytokine-mediated JAK3/STAT5a/b signal transduction and cellular proliferation of antigen-activated human T cells, *J. Leukoc. Biol.*, 65: 891-899.

34. Wang, L. H., R. A. Kirken, R. A. Erwin, C. R. Yu, and W. L. Farrar, **1999**, JAK3, STAT, and MAPK signaling pathways as novel molecular targets for the

tyrphostin AG-490 regulation of IL-2-mediated T cell response, *J. Immunol.*, 162: 3897-3904.

35. Meydan, N., T. Grunberger, H. Dadi, M. Shahar, E. Arpaia, Z. Lapidot, J. S. Leeder, M. Freedman, A. Cohen, A. Gazit, A. Levitzki, and C. M. Roifman, **1996**, Inhibition of acute lymphoblastic leukaemia by a Jak-2 inhibitor, *Nature*, 379: 645-648.

36. Koo, G. C., J. T. Blake, A. Talento, M. Nguyen, S. Lin, A. Sirotina, K. Shah, K. Mulvany, D. Hora, Jr., P. Cunningham, D. L. Wunderler, O. B. McManus, R. Slaughter, R. Bugianesi, J. Felix, M. Garcia, J. Williamson, G. Kaczorowski, N. H. Sigal, M. S. Springer, and W. Feeney, **1997**, Blockade of the voltage-gated potassium channel Kv1.3 inhibits immune responses in vivo, *J. Immunol.*, 158: 5120-5128.

37. Beeton, C., and K. G. Chandy, **2005**, Potassium channels, memory T cells, and multiple sclerosis, *Neuroscientist*, 11: 550-562.

38. Beeton, C., M. W. Pennington, H. Wulff, S. Singh, D. Nugent, G. Crossley, I. Khaytin, P. A. Calabresi, C. Y. Chen, G. A. Gutman, and K. G. Chandy, **2005**, Targeting effector memory T cells with a selective peptide inhibitor of Kv1.3 channels for therapy of autoimmune diseases, *Mol. Pharmacol.*, 67: 1369-1381.

39. Pennington, M. W., V. M. Mahnir, D. S. Krafte, I. Zaydenberg, M. E. Byrnes, I. Khaytin, K. Crowley, and W. R. Kem, **1996**, Identification of three separate binding sites on SHK toxin, a potent inhibitor of voltage-dependent potassium channels in human T-lymphocytes and rat brain, *Biochem. Biophys. Res. Commun.*, 219: 696-701.

40. Schmitz, A., A. Sankaranarayanan, P. Azam, K. Schmidt-Lassen, D. Homerick, W. Hansel, and H. Wulff, **2005**, Design of PAP-1, a selective small molecule Kv1.3 blocker, for the suppression of effector memory T cells in autoimmune diseases, *Mol. Pharmacol.*, 68: 1254-1270.

41. Schmelzle, T., and M. N. Hall, **2000**, TOR, a central controller of cell growth, *Cell*, 103: 253-262.

42. Stepkowski, S. M., R. A. Erwin-Cohen, F. Behbod, M. E. Wang, X. Qu, N. Tejpal, Z. S. Nagy, B. D. Kahan, and R. A. Kirken, **2002**, Selective inhibitor of Janus tyrosine kinase 3, PNU156804, prolongs allograft survival and acts synergistically with cyclosporine but additively with rapamycin, *Blood*, 99: 680-689.

43. Song, J., S. Salek-Ardakani, T. So, and M. Croft, **2007**, The kinases aurora B and mTOR regulate the G1-S cell cycle progression of T lymphocytes, *Nat. Immunol.*, 8: 64-73.

44. Bromley, S. K., W. R. Burack, K. G. Johnson, K. Somersalo, T. N. Sims, C. Sumen, M. M. Davis, A. S. Shaw, P. M. Allen, and M. L. Dustin, **2001**, The immunological synapse, *Annu. Rev. Immunol.*, 19: 375-396.

45. Mondino, A., and D. L. Mueller, **2007**, mTOR at the crossroads of T cell proliferation and tolerance, *Semin. Immunol.*, 19: 162-172.

46. Fox, C. J., P. S. Hammerman, and C. B. Thompson, **2005**, The Pim kinases control rapamycin-resistant T cell survival and activation, *J. Exp. Med.*, 201: 259-266.

47. Ghanshani, S., H. Wulff, M. J. Miller, H. Rohm, A. Neben, G. A. Gutman, M. D. Cahalan, and K. G. Chandy, **2000**, Up-regulation of the IKCa1 potassium channel during T-cell activation. Molecular mechanism and functional consequences, *J. Biol. Chem.*, 275: 37137-37149.

48. Cai, Y. C., P. B. Osborne, R. A. North, D. C. Dooley, and J. Douglass, **1992**, Characterization and functional expression of genomic DNA encoding the human lymphocyte type n potassium channel, *DNA Cell Biol.*, 11: 163-172.

49. Attali, B., G. Romey, E. Honore, A. Schmid-Alliana, M. G. Mattei, F. Lesage, P. Ricard, J. Barhanin, and M. Lazdunski, **1992**, Cloning, functional expression, and regulation of two K+ channels in human T lymphocytes, *J. Biol. Chem.*, 267: 8650-8657.

50. Payet, M. D., and G. Dupuis, **1992**, Dual regulation of the n type K+ channel in Jurkat T lymphocytes by protein kinases A and C, *J. Biol. Chem.*, 267: 18270-18273.

51. Brown, E. J., and S. L. Schreiber, **1996**, A signaling pathway to translational control, *Cell*, 86: 517-520.

52. Lockyer, H. M., E. Tran, and B. H. Nelson, **2007**, STAT5 is essential for Akt/p70S6 kinase activity during IL-2-induced lymphocyte proliferation, *J. Immunol.*, 179: 5301-5308.

53. Sinclair, L. V., D. Finlay, C. Feijoo, G. H. Cornish, A. Gray, A. Ager, K. Okkenhaug, T. J. Hagenbeek, H. Spits, and D. A. Cantrell, **2008**, Phosphatidylinositol-3-OH kinase and nutrient-sensing mTOR pathways control T lymphocyte trafficking, *Nat. Immunol.*, 9: 513-521.

54. Sinclair, J., J. Pihl, J. Olofsson, M. Karlsson, K. Jardemark, D. T. Chiu, and O. Orwar, **2002**, A cell-based bar code reader for high-throughput screening of ion channel-ligand interactions, *Anal. Chem.*, 74: 6133-6138.

55. Bruggemann, A., S. Stoelzle, M. George, J. C. Behrends, and N. Fertig, **2006**, Microchip technology for automated and parallel patch-clamp recording, *Small*, 2: 840-846.

CHAPTER 4

Quantifying Disease Activity in Patients with Multiple Sclerosis and Rheumatoid Arthritis Based on Kv1.3 Ion Channel Activity in T Cells

This chapter examines using Kv1.3 activity in human T cells isolated from peripheral blood as a marker for the activity of autoimmune disease. We used a recently developed high-throughput assay to profile Kv1.3 activity in $CD4^+$ and $CD8^+$ T cells from patients with multiple sclerosis (MS) and rheumatoid arthritis (RA). Patients with a chronic progressive (CP) form of MS exhibited significantly higher Kv1.3 activity compared to healthy controls or MS patients in remission. Developing metrics to quantify the percentage of T cells with "high" Kv1.3 activity made it possible to distinguish between CP-MS patients and controls with 100% sensitivity and 94% specificity. Controls with acute inflammatory disorders, however, also exhibited high Kv1.3 activity, suggesting that Kv1.3 activity is a general marker for active inflammation. We explored this hypothesis by examining a second autoimmune disease, RA. Patients with an active form of RA exhibited significantly higher Kv1.3 activity than patients with inactive RA, and Kv1.3 activity correlated with erythrocyte sedimentation rate. High-throughput profiling of Kv1.3 ion channels in T cells introduces

a promising new strategy for quantifying activity of immune-mediated inflammation and may have clinical applications for diagnosis and therapeutic monitoring of autoimmune disease.

4.1. Introduction

Kv1.3 ion channels in the plasma membrane of human T cells are emerging targets for the treatment of human autoimmune disease (1). Drug compounds that inhibit Kv1.3 selectively suppress activation of effector memory T (T_{em}) cells (2), which are implicated in the pathogenesis of several autoimmune diseases (3, 4). The Kv1.3 ion channel may also serve as a marker of autoimmune disease, as T cells increase the number of functional Kv1.3 ion channels in their plasma membrane after activation (5-7). T_{em} cells, including autoreactive T cells from peripheral blood of patients with MS and the synovial fluid of RA patients, experience an especially large increase (~5-fold) upon stimulation (7, 8). A recent report found these T cells with high Kv1.3 activity in inflammatory infiltrates in the brains of post-mortem MS patients, highlighting the importance of cells with high Kv1.3 activity for the pathogenesis of human disease (9).

While many previous studies have examined changes in various surface- and activation-markers in T cells from peripheral blood in the context of autoimmune disease (10-12), Kv1.3 ion channels have not been profiled in T cells from peripheral blood. A major reason may be that traditional techniques to quantify Kv1.3 channels (e.g. patch-clamping) are low-throughput, labor-intensive, and not amenable to profiling Kv1.3 activity in heterogeneous cell populations such as peripheral blood T cells (13). Recently, we developed a high-throughput method for measuring Kv1.3 activity in T cells (14).

This assay is automated, specific, and able to measure Kv1.3 activity in ~150 T cells within 1 h (14). Here, we use this assay to profile Kv1.3 activity in T cells isolated from the peripheral blood of patients with MS and patients with RA. The results presented in this work indicate that MS and RA patients with active disease have elevated Kv1.3 activity in their T cells compared to healthy controls or patients with inactive disease. Such quantitative measurements of disease activity may have clinical use for diagnosing and therapeutic monitoring of human autoimmune disease.

4.2. Materials and Methods

We obtained peripheral, venous blood from control subjects and patients with MS or RA (Table 1 and Supporting Table 4-App.1). Patient history and a neurological exam allowed determination of whether MS patients had relapsing-remitting (RR-) or chronic progressive (CP-, either secondary-progressive, or primary-progressive) forms of MS. Similarly, RA patients were classified as having "active" (moderate-to-severe symptoms) or "inactive" (minimal or no symptoms) disease based on findings during a rheumatologic exam including number of inflamed joints and the necessity for changes in treatment regimen. All subjects provided written informed consent, and protocols were approved by the Institutional Review Board at the University of Michigan.

From freshly isolated blood from each patient, we isolated $CD4^+$ and $CD8^+$ T cells from PBMCs using commercially available magnetic bead separation techniques (Miltenyi Biotech, Auburn, CA). In these isolated T cells (examining $CD4^+$ and $CD8^+$ T cells for each patient in parallel), we measured electrical currents through Kv1.3 ion channels using a high-throughput electrophysiology device (IonWorks HT, MS

Analytical Technologies, Sunnyvale, CA) with protocols described elsewhere (14). Measurements of Kv1.3 activity occurred 3.9 ± 0.7 h (mean ± standard deviation) after the blood draw, with the exact same protocols (and similar time-lapses) used for all patients.

Table 4.1. Characteristics of MS patients and control subjects at time of blood draw

Variable	Healthy Controls (*N*=17)	MS Patients		
		Total (*N*=21)	Relapsing-Remitting (*N*=15)	Chronic Progressive (*N*=6) [a]
Age (yr)	42.1 ± 11.2	43.0 ± 11.0	38.9 ± 9.1	53.5 ± 8.0 *
Female gender (%)	60	71	80	50
Ethnicity (%)				
Caucasian (%)	94	90	87	100
African American (%)	6	10	13	0
CBC values				
RBC ($\times 10^6$ / mm^3)	4.6 ± 0.5	4.6 ± 0.4	4.5 ± 0.4	4.6 ± 0.5
WBC ($\times 10^3$ / mm^3)	6.3 ± 1.5	6.7 ± 1.9	6.3 ± 1.7	7.6 ± 2.2
Lymphocytes (%)	30.5 ± 9.8	26.5 ± 6.7	27.2 ± 5.1	24.9 ± 9.7
Flow cytometry measurements [b]				
CD4:CD8 ratio	1.7 ± 1.3	1.5 ± 1.3	1.1 ± 0.8	1.9 ± 1.7
$CD4^+$ T_{em} (%) [c]	11.1 ± 3.5	14.6 ± 3.9 *	14.5 ± 3.3	14.8 ± 5.0
$CD8^+$ T_{em} (%) [c]	17.7 ± 7.1	21.3 ± 4.6	21.0 ± 5.5	21.6 ± 4.0
Kv1.3 measurements, number of cells measured per sample from each patient				
$CD4^+$ T cells (*N*)	80 ± 16	71.7 ± 20.3	71 ± 21	75 ± 19
$CD8^+$ T cells (*N*)	62 ± 16	56.8 ± 19.1	56 ± 19	59 ± 21

Values are expressed as mean ± standard deviation. Significant differences between the indicated population and healthy controls are indicated by * ($p<0.05$).

[a] Clinically diagnosed primary (*N*=3) or secondary progressive (*N*=3) MS

[b] Flow cytometry performed using randomly-selected subsets of overall population, with 6 relapsing-remitting MS patients, 5 secondary/primary progressive MS patients, and 12 control subjects

[c] Percentage of $CD4^+$ or $CD8^+$ T cells gated as $CD62L^-$ $CD45RA^-$ using custom-defined regions for each patient (Supporting Information)

To obtain additional information about patient blood samples, we carried out complete blood counts (CBCs, University of Michigan Clinical Laboratory) from whole blood; for RA patients, we additionally determined levels of C reactive protein (CRP) and erythrocyte sedimentation rate (ESR). We also performed flow cytometric analysis using PBMCs and isolated $CD4^+$ and $CD8^+$ T cells (stored at 4° C prior to cytometry). Flow cytometry (FACScalibur, Becton Dickinson, Franklin Lakes, NJ) confirmed purity of isolated T cells (>95% for both $CD4^+$ and $CD8^+$ T cells), allowed determination of effector and memory subsets (using anti-CD62L-FITC and anti-CD45RA-APC), and provided quantification of activation markers (using anti-CD45RO-PE, anti-CD25-PE, and anti-CD26-PE, all antibodies monoclonal were anti-human antibodies from mouse, purchased from BD Biosciences, San Jose, CA).

To determine significant differences between patient populations, we used the non-parametric Mann-Whitney *U* test, and indicated the resulting *p* values throughout the text. For determination of correlation between variables, we used Pearson's correlation coefficient (*r*) and computed statistical significance of the correlation using Student's two-tailed *t* test (with $p<0.05$ indicating significant correlation).

4.3. Results and discussion

We used a high-throughput assay to quantify Kv1.3 activity in T cells from peripheral blood of patients with MS (*N*=21) and healthy controls (*N*=17) (14). This assay afforded measurements of Kv1.3 activity in ~75 $CD4^+$ T cells and ~60 $CD8^+$ T cells per MS patient or control subject. For analysis, we classified MS patients (none of whom were on active treatment) as either relapsing-remitting (RR) or chronic-progressive

(CP) MS patients (Table 4.1). Importantly, none of the RR-MS patients had experienced active MS attacks in the 2 months prior to measuring Kv1.3 activity.

Patients with CP-MS exhibited significantly higher mean values of Kv1.3 activity in both $CD4^+$ (25% higher, p=0.004) and $CD8^+$ (40%, p=0.04) T cells compared to healthy controls (Fig. 4.1*A*). These differences were not due to the increased ages of CP-MS patients compared to healthy controls; comparing Kv1.3 activity in CP-MS patients to a subset of healthy controls with ages that matched CP-MS patients (N=10 controls) again yielded significantly higher Kv1.3 in both $CD4^+$ (20% higher p=0.03) and $CD8^+$ subsets (37% higher, p=0.04) from CP-MS patients. In contrast to CP-MS patients, Kv1.3 levels from patients with RR-MS displayed no differences compared to healthy controls in either $CD4^+$ or $CD8^+$ T cells.

While mean values afforded significant differences between CP-MS patients and healthy controls, this analysis did not utilize a major advantage of the high-throughput assay used in this work which results from obtaining distributions of Kv1.3 activity in individual T cells. In order to benefit from the information in these distributions of Kv1.3 activity, we employed a technique commonly used in flow cytometry, quantifying the percentage of cells in a distribution with values above a defined threshold (Fig. 4.1*B*). To define this threshold, we constructed cumulative fraction plots to determine at which current values the distributions of Kv1.3 activity in $CD4^+$ T cells from healthy controls and from CP-MS patients exhibited differences (Fig. 4-App.1). Interestingly, distributions of Kv1.3 activity from patients with CP-MS exhibited a general "shift" towards higher current values compared to distributions from healthy controls. The

current value that provided the maximal difference between current distributions from CP-MS patients and healthy controls was 0.32 nA (Fig. 4-App.1).

Using this optimized threshold, we analyzed the percentage of T cells from each healthy control and MS patient with "high" Kv1.3 activity above this threshold value (Fig. 4.1*B,C*). In $CD4^+$ T cells, CP-MS patients exhibited a 2-fold higher average percentage of T cells with high Kv1.3 activity compared to controls ($p<0.0001$). In addition, this metric made it possible to distinguish between CP-MS patients and healthy controls with 100% sensitivity and 94% selectivity (Fig. 4.1*C* and Fig. 4-App.2). In $CD8^+$ T cells, CP-MS patients also exhibited a significantly higher (~2-fold, $p=0.03$) percentage of T cells with high Kv1.3 activity compared to healthy controls, although individual values overlapped between the two populations (Fig. 4.1*D*). Similarly to the analysis of mean values of Kv1.3 activity, these differences were not due to age differences between CP-MS patients and healthy controls (Fig. 4.1*C*). Also, as in the case with mean values, patients with RR-MS did not exhibit differences in either $CD4^+$ or $CD8^+$ T cells using threshold metrics. These results indicate that CP-MS patients, with active symptoms of MS, have an increased percentage of T cells (especially in the $CD4^+$ subset) in peripheral blood with high Kv1.3 activity compared to healthy controls or patients in a relapsing form of MS.

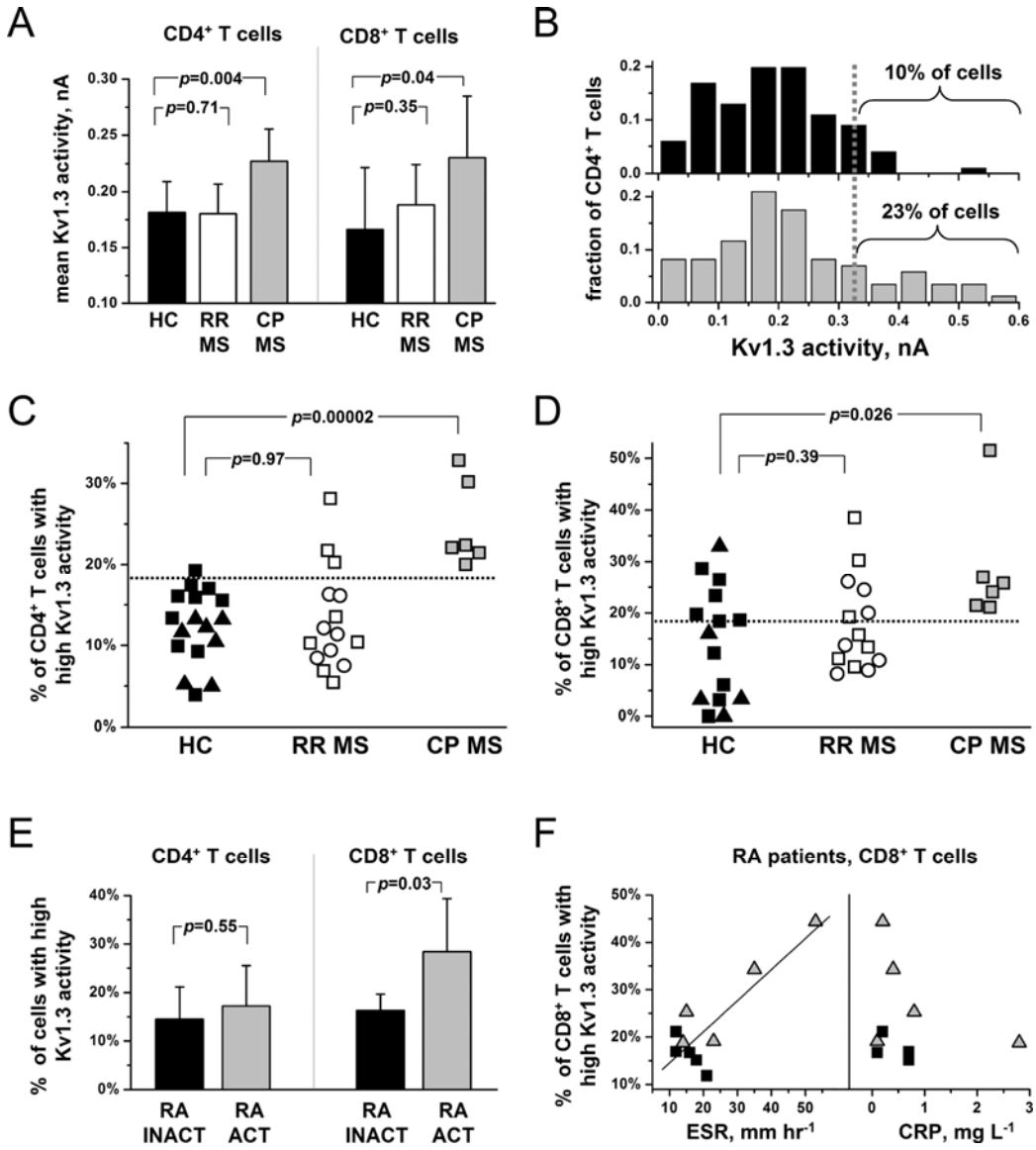

Figure 4.1 | Kv1.3 ion channel activity in T cells isolated from peripheral blood of patients with MS or RA compared to activity from controls. (A) Mean Kv1.3 activity in T cells from healthy controls (HC), relapsing-remitting MS patients (RR-MS), and chronic-progressive MS (CP-MS) patients. (B) Representative histograms of Kv1.3 activity in $CD4^+$ T cells from a healthy control (top) and from a patient with CP-MS (bottom). The dashed line indicates the threshold for classifying T cells as having "high" levels of Kv1.3 activity. (C) Percentage of $CD4^+$ T cells with high Kv1.3 activity for each HC, RR-MS, and CP-MS patient studied. Square symbols represent patients or controls between the ages of 40 and 65. (D) Percentage of $CD8^+$ T cells with high Kv1.3 activity for each control subject or MS patient. (E) Average percentage of T cells with high Kv1.3 activity from RA patients with active (RA-ACT) and inactive (RA-INACT) disease. (F) Percentage of $CD8^+$ T cells with high Kv1.3 activity as a function of either erythrocyte sedimentation rate (ESR, left) or levels of C reactive protein levels (CRP), measured from patients with active (gray triangles) and inactive (black squares) RA. Columns with error bars depict average ± standard deviation. Significant differences between specified control and MS populations were determined using the Mann-Whitney *U* test. Resulting *p* values are indicated above the columns that are compared.

In addition to healthy controls, we also measured Kv1.3 activity in T cells from three "diseased" controls displaying active symptoms of an inflammatory disorder (diverticulitis, urinary tract infection (UTI), or recent myocardial infarction combined with type 2 diabetes) at the time of blood draw (Fig. 4-App.4). The $CD4^+$ subset of T cells from all three subjects contained a significant percentage of cells with high Kv1.3 activity, similar to patients with CP-MS (Fig. 4-App.4). Subjects with active IBD or UTI exhibited an especially high percentage of $CD4^+$ T cells with high Kv1.3 (~35%). These results suggest that high Kv1.3 in T cells as a marker of disease is not specific to patients with MS, but may be indicative of general inflammatory disorders.

To test this hypothesis, we measured Kv1.3 activity in T cells from peripheral blood of patients with a second autoimmune disease, RA (N=10). All of the RA patients were on active therapy, but only half of the patients exhibited "active" symptoms of RA (moderate-to-severe) at the time of blood draw (4-App.Table). Using the same threshold metrics defined for MS patients, we found that patients with active RA had a significantly higher average percentage (80% higher) of cells with high Kv1.3 activity in $CD8^+$ T cells compared to patients with inactive RA (p=0.03) or healthy controls (p=0.04) (Fig. 4.1E). Interestingly, we found no significant differences in Kv1.3 activity in $CD4^+$ T cells from patients with active RA compared to patients with inactive RA (Fig. 4.1E).

Comparing Kv1.3 activity in each RA patient to CRP and ESR values, which are commonly used clinical markers for inflammation, we found that the percentage of $CD8^+$ T cells with high Kv1.3 activity correlated significantly with ESR (p<0.05, Fig. 4.1F). Interestingly, ESR values themselves were not significantly different (p=0.20) in the active and inactive RA populations examined. Kv1.3 activity in $CD4^+$ T cells did not

correlate with ESR, and CRP did not correlate with Kv1.3 activity in either $CD4^+$ or $CD8^+$ T cells (Fig. 4.1*F*). These results suggest that Kv1.3 activity in $CD8^+$ T cells of RA patients is a marker of immune-mediated inflammation that correlates more strongly with disease activity than do general inflammation markers such as CRP and ESR.

A major question that arises from this work is what factors lead to increased Kv1.3 activity in T cells in peripheral blood in vivo. To address this question, we performed flow cytometric analyses of activation and differentiation markers from patients with CP-MS and healthy controls to correlate with Kv1.3 activity. The percentages of $CD4^+$ T cells that were central memory (T_{cm}) or naïve (T_{naive}) exhibited no correlations to Kv1.3 activity (Fig. 4-App.6). Interestingly, the percentages of $CD4^+$ T cells that were of the effector memory (T_{em}) phenotype did correlate weakly (p=0.08) to Kv1.3 activity, although this correlation was negative. This finding is surprising given that T_{em} cells strongly upregulate Kv1.3 activity upon activation (7).

Examining mean fluorescence intensity (MFI) of known activation markers in the entire population of $CD4^+$ T cells, we found that neither CD25, CD26, nor CD45RO exhibited significant differences between CP-MS patients and healthy control subjects, in contrast to mean Kv1.3 activity (Fig. 4.1, Fig. 4-App.7). Interestingly, mean Kv1.3 activity did correlate significantly to CD26 expression specifically in the T_{naive} subset (p<0.04), examining individual patients or subjects (there were no other significant correlations). This correlation is interesting because elevated expression of CD26 in peripheral blood T cells has been reported for RR-MS patients with active clinical symptoms (11, 15). Kv1.3 activity and CD26 expression, therefore, may exhibit similar levels that are altered to similar extents in patients with different forms of MS; Kv1.3

activity, however, is a superior marker (also compared to CD25 or CD45RO) for distinguishing between CP-MS patients and healthy control subjects.

The flow cytometry analysis of T cell activation markers did highlight one major advantage of using Kv1.3 activity as a marker of T cell activation. Expression of CD25, CD26, and CD45RO depended heavily on whether the T cell was of the T_{em}, T_{cm}, or T_{naive} phenotype. In general, memory T cells (either T_{cm} or T_{em}) exhibited greater than 2-fold expression of activation markers compared to T_{naive} cells (Fig. 4-App.7). As a result, changes in MFI in the total $CD4^+$ population of these activation markers may be a result of either activation of cells or altered percentages of T_{naive} or memory cells. Kv1.3 activity, in contrast, exhibited 2 to 5-fold lower coefficients of variations than these activation markers, indicating significantly decreased differences in activity among various phenotypes of T cells. This low variation makes Kv1.3 activity a sensitive marker for detecting differences in T cells from peripheral blood between various populations of human subjects or patients.

Several other factors lead to elevated Kv1.3 activity in T cells. Inflammatory cytokines, such as interleukin (IL)-2 and IL-15, can increase Kv1.3 activity in T cells, even in the absence of antigenic stimulation (6, 16). Another recent study found that a decreased glutamate level (which is associated with several autoimmune disorders) increased functional activity of Kv1.3 ion channels in T cells (17). In addition, T cell activation can also lead to increased Kv1.3 activity in T cells (14, 18). High Kv1.3 activity in T cells, therefore, may represent the integrated effect of three stimuli: (i) inflammatory serum conditions; (ii) cytokines; and (iii) T cell stimulation.

There are several potential clinical applications of measuring Kv1.3 activity in peripheral blood T cells. One promising use is for aid in diagnosing patients with primary-progressive MS, as Kv1.3 activity in $CD4^+$ T cells afforded a 97% accuracy in distinguishing between CP-MS and healthy controls (Fig. 4.1*C* and Fig. 4-App.2). Another application of Kv1.3 activity may be to determine progression of patients with RR-MS to CP-MS, which is especially important given the fact that CP-MS patients are generally resistant to traditional MS therapies (19, 20). As a third clinical application, Kv1.3 activity in $CD8^+$ T cells may also be useful as a marker of therapeutic monitoring of inflammation in patients with RA. High-throughput electrophysiology to measure Kv1.3 activity in T cells, therefore, offers a promising new strategy to quantify activity of immune-mediated inflammation for diagnosing and therapeutic monitoring of human autoimmune disease.

4-App.Table. Characteristics of RA patients at the time of blood draw

Patient ID	Age (yr)	Gender (M/F)	RA Medications	$CD4^+$ T cells with high Kv1.3 (%)	$CD8^+$ T cells with high Kv1.3 (%)
Patients with active RA					
1	55	F	azathioprine, prednisone, infliximab	15	44
2	59	F	sulfasalazine, prednisone, hydroxychloroquine	22	34
3	53	F	adalimumab	25	25
4	41	F	prednisone, hydroxychloroquine	4	19
5	53	F	methotrexate, sulfasalazine, prednisone, rituximab	20	19
Avg ± Stdev	**52 ± 7**			**17 ± 8**	**28 ± 11**
Patients with inactive RA					
6	36	F	methotrexate	16	21
7	46	F	leflunomide, prednisone, hydroxychloroquine	19	17
8	57	F	methotrexate, prednisone, hydroxychloroquine, adalimumab	6	17
9	46	M	methotrexate, sulfasalazine, prednisone, hydroxychloroquine, adalimumab	10	15
10	69	F	hydroxychloroquine	20	12
Avg ± Stdev	**51 ± 13**			**14 ± 7**	**16 ± 3**

All patients were Caucasian.

4-App.1. Optimizing thresholds for determining T cells with high Kv1.3 activity

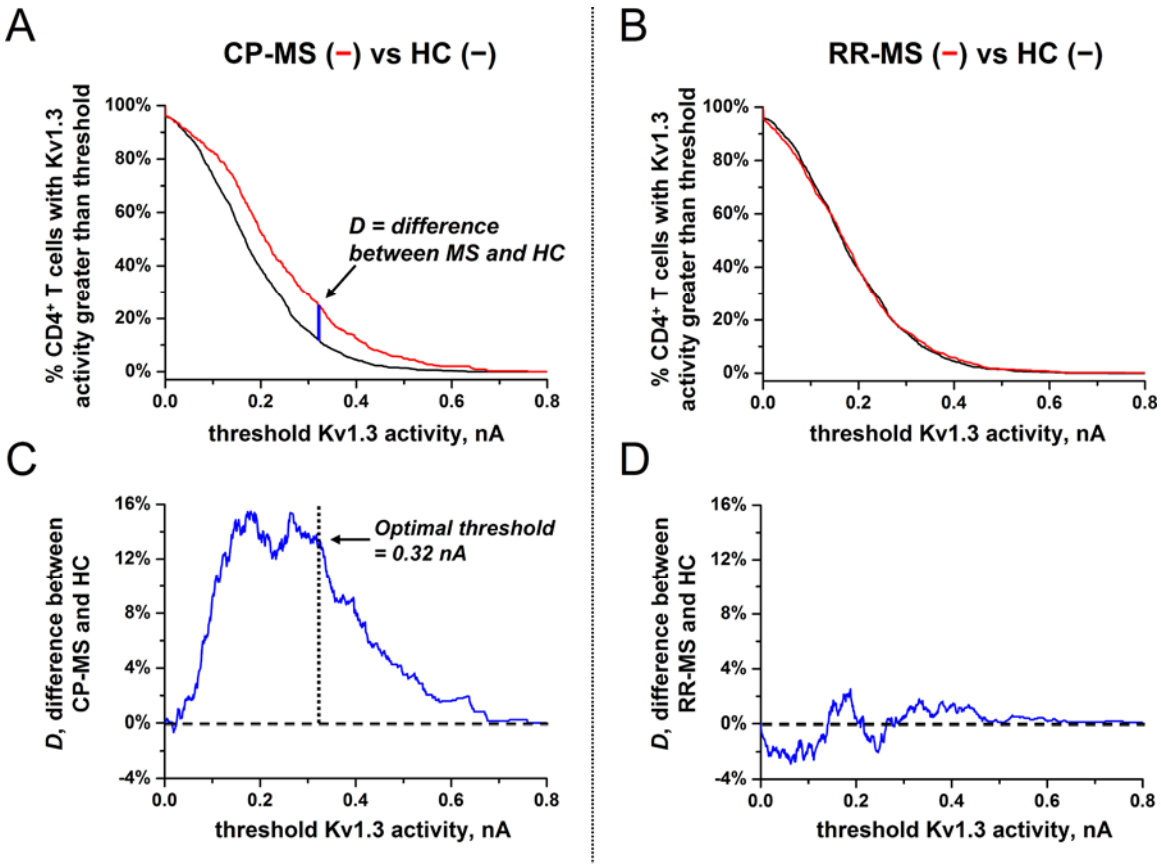

Figure 4-App.1 | Optimizing thresholds for determining T cells with high Kv1.3 activity. **(A)** Cumulative fraction plot depicting percentage of $CD4^+$ T cells from chronic progressive MS patients (CP-MS, −) and healthy controls (HC, −) with Kv1.3 currents greater than the threshold current value indicated by the x-axis. Plots indicate the combined Kv1.3 currents from 6 CP-MS patients (448 cells total) and 17 HC-MS patients (1427 cells total). **(B)** Cumulative fraction plots as described in (A) with relapsing-remitting MS patients (RR-MS, −, 1058 cells total) instead of CP-MS patients. **(C)** Difference, *D*, between cumulative fractions of CP-MS patients and HC subjects as a function of current threshold. The optimal threshold was defined as the largest current value that provided a *D*>13%. **(D)** Difference, *D*, between cumulative fraction plots of RR-MS paitents and HC subjects.

4-App.2. Receiver operating characteristic (ROC) curve depicting sensitivity versus (1-sensitivity) for determining between chronic progressive MS patients and healthy controls

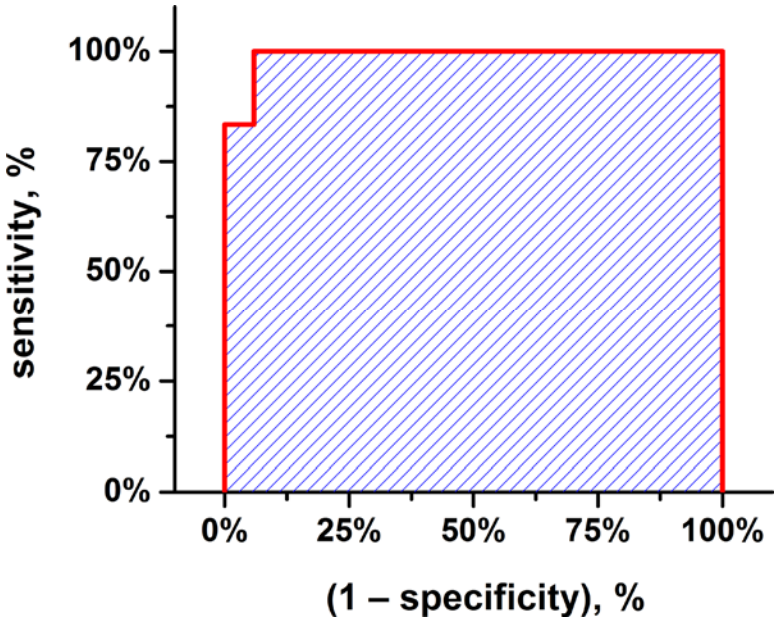

Figure 4-App.2 | Receiver operating characteristic (ROC) curve depicting sensitivity versus (1-specificity) for determining between chronic progressive MS patients (CP-MS) and healthy controls. ROC curves represent a useful statistical tool to evaluate diagnostic tests. For a list of all possible "threshold" values to separate two patient populations (here examining the percentage of $CD4^+$ T cells with high Kv1.3 activity in CP-MS patients and control subjects), sensitivity and specificity are calculated. Sensitivity is then plotted as a function of (1-specificity), and the resulting area under the curve is known as the "ROC" value. An ROC value of 100% represents a diagnostic test that affords 100% sensitivity and 100% specificity. In the figure above, examining the percentage of $CD4^+$ T cells with high Kv1.3 activity afforded an ROC of 99%, indicating that the metric is effective at determining between CP-MS patients and healthy controls.

4-App.3. Correlation between Kv1.3 activity and age in healthy control subjects

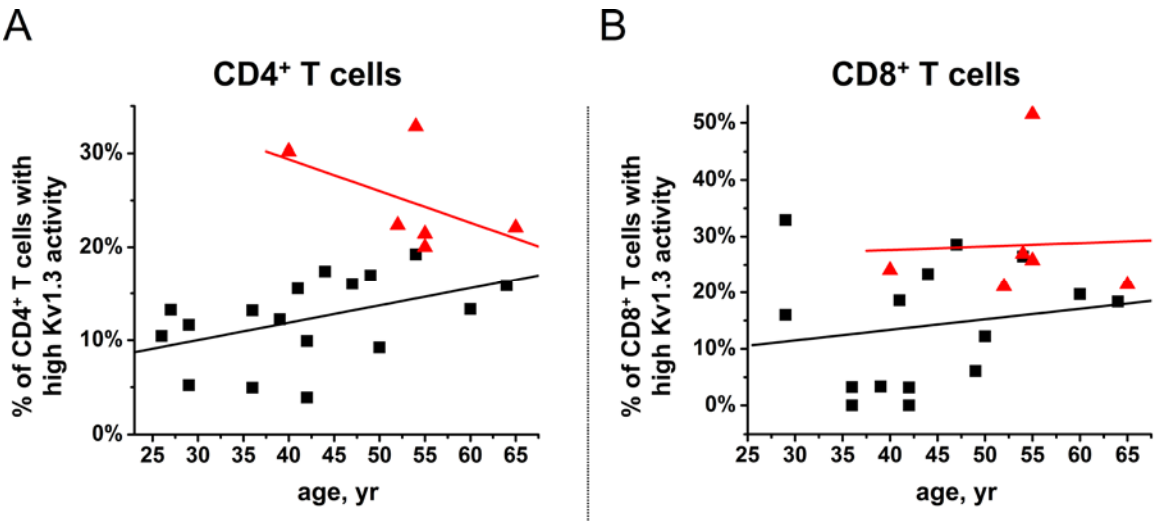

Parameters for linear fit of % CD4⁺ T cells with high Kv1.3 activity versus age			
Population	Slope (%/yr)	*r*	*p* value
Healthy Controls (■)	0.19	0.45	0.07
Chronic Progressive MS (▲)	-0.34	-0.51	0.31

Parameters for linear fit of % CD8⁺ T cells with high Kv1.3 activity versus age			
Population	Slope (%/yr)	*r*	*p* value
Healthy Controls (■)	0.19	0.17	0.54
Chronic Progressive MS (▲)	0.01	0.04	0.93

Figure 4-App.3 | Correlation between Kv1.3 activity and age in healthy control subjects and chronic progressive MS patients. (A) Percentage of $CD4^+$ T cells with high Kv1.3 activity as a function of age, with each point representing values from a single healthy control (■) or chronic progressive MS patient (▲). Solid lines represent linear best fits to the data, with the red line fitting data from chronic progressive MS patients, and the black line fitting data from healthy controls. Parameters detailing the quality of the fit are in the table below the panel. **(B)** Percentage of $CD8^+$ T cells with high Kv1.3 activity as a function of age, with the same conditions as panel (A) except with $CD8^+$ T cells. Correlations were computed using Pearson's correlation coefficient (r) with significance of the correlation computed using Student's t test ($p<0.05$ indicates significance).

4-App.4. Kv1.3 activity in CD4$^+$ T cells from control subjects exhibiting active symptoms of disease at time of blood draw

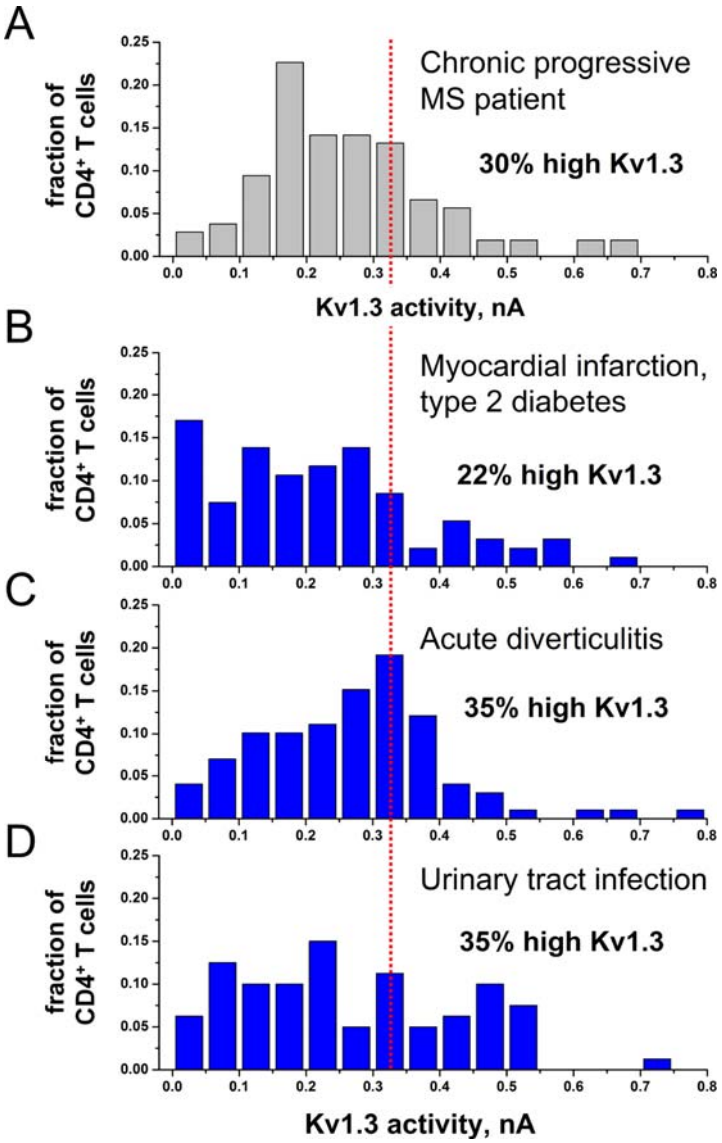

Figure 4-App.4 | Kv1.3 activity in CD4$^+$ T cells from control subjects exhibiting active disease at the time of blood draw. (A) Histogram of Kv1.3 activity in CD4$^+$ T cells from an individual chronic progressive MS patient (*N*=106 cells). This histogram serves as a reference for histograms from diseased controls. The percentage listed above the histogram represents the percentage of CD4$^+$ T cells with high Kv1.3 activity above the threshold used throughout this work. **(B)** Histogram of Kv1.3 activity in CD4$^+$ T cells from a control subject with type 2 diabetes and a recent myocardial infarction (*N*= 94 cells). **(C)** Same as panel (B) for a control subject with acute diverticulitis (*N*=99 cells). **(D)** Same as panels (A,B) for a control subject with a urinary tract infection (*N*=80 cells).

4-App.5. Correlation between Kv1.3 activity and subsets of CD4$^+$ T cells

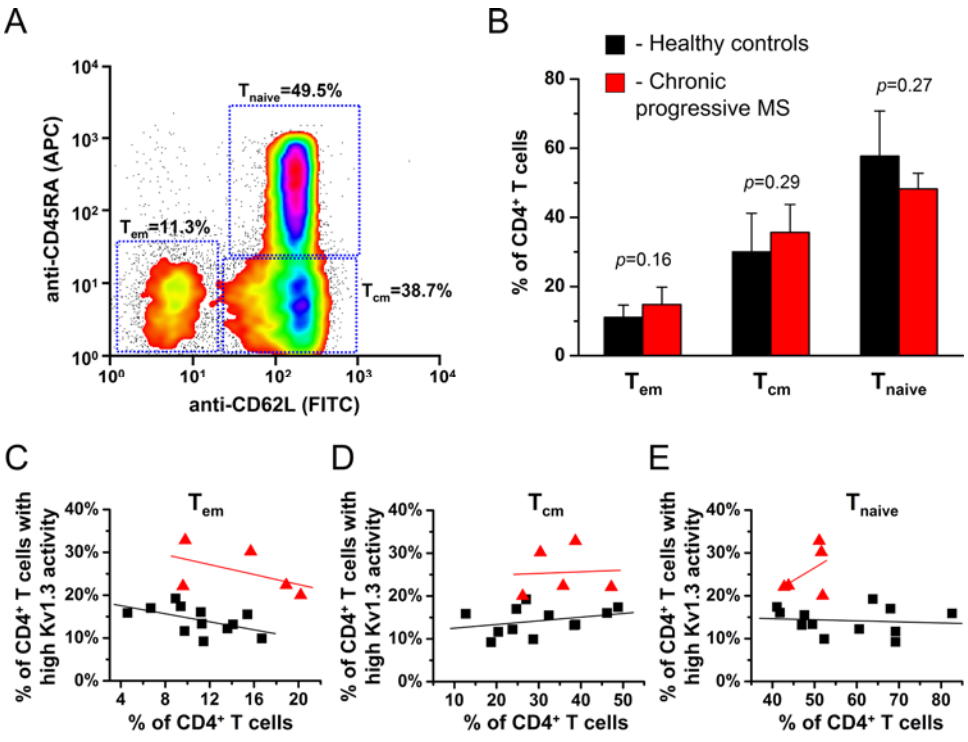

Fit parameters for linear fit of % of CD4$^+$ T cells with high Kv1.3 activity versus % of CD4$^+$ T cells with Tem, Tcm, or Tnaive cell surface markers.				
Phenotype	**Subject / patient population**	**Slope (% Kv1.3 high/% cell phenotype)**	***r***	***p* value**
T_{em} cells	Healthy control	-0.47	-0.53	0.08
	Chronic progressive MS	-0.50	-0.51	0.38
T_{cm} cells	Healthy control	0.09	0.31	0.33
	Chronic progressive MS	0.04	0.05	0.93
T_{naive} cells	Healthy control	-0.02	-0.10	0.75
	Chronic progressive MS	0.50	0.48	0.41

Figure 4-App.5 | Correlation between Kv1.3 activity and percentage of effector and memory subsets in CD4$^+$ T cells. (A) Representative flow cytometric plot of markers (CD62L and CD45RA) used to define effector memory (T_{em}), central memory (T_{cm}), and naïve (T_{naive}) subsets within CD4$^+$ T cells. Note that "gating" regions were adjusted for each subject or patient, using density plots to define boundaries between subsets. **(B)** Average percentage of CD4$^+$ T cells that were T_{em}, T_{cm}, or T_{naive}, respectively, from healthy controls and chronic progressive MS patients. Columns represent average ± standard deviation, with *p* values determined using the Mann-Whitney *U* test. **(C)** Percentage of CD4$^+$ T cells with high Kv1.3 activity plotted as a function of the percentage of CD4$^+$ T cells that were T_{em} for each individual healthy control (■) or chronic progressive MS patient (▲). Solid lines represent linear fits to the data, with the red line fitting data from chronic progressive MS patients, and the black line fitting data from healthy controls. Parameters detailing the quality of the fit are in the table below the panel. **(D)** Same as panel (C) examining T_{cm} cells instead of T_{em} cells. **(E)** Same as panels (C,D) examining T_{naive} cells instead of T_{em} or T_{cm} cells. Correlations were computed using Pearson's correlation coefficient (*r*) with significance of the correlation computed using Student's *t* test ($p<0.05$ indicates significance).

4-App.6. Correlation between Kv1.3 activity and subsets of CD8$^+$ T cells

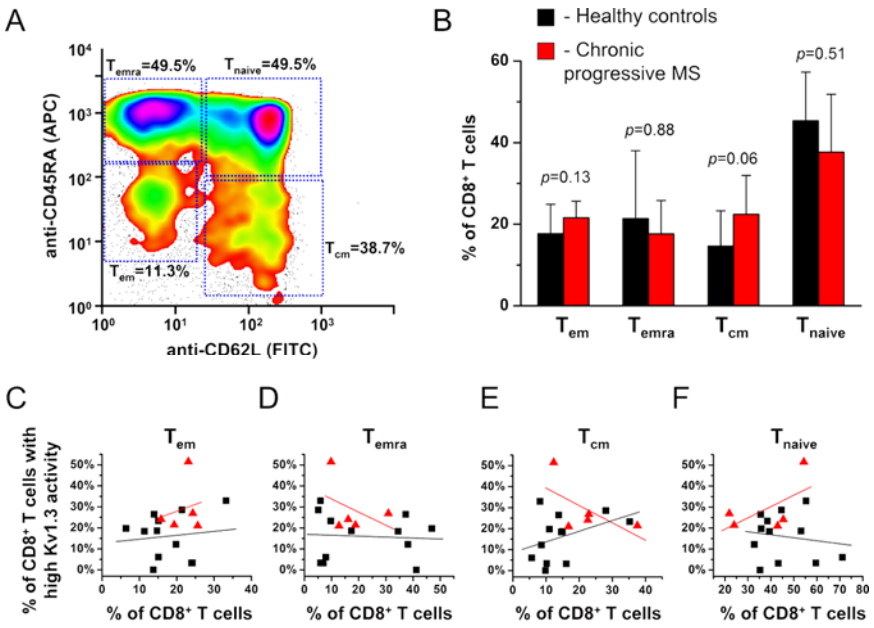

Fit parameters for linear fit of % of CD4⁺ T cells with high Kv1.3 activity versus % of CD4⁺ T cells with Tem, Tcm, or Tnaive cell surface markers.				
Phenotype	**Subject / patient population**	**Slope (% Kv1.3 high/% cell phenotype)**	***r***	***p* value**
T_{em} cells	Healthy control	0.19	0.12	0.70
	Chronic progressive MS	0.66	0.21	0.74
T_{emra} cells	Healthy control	-0.05	-0.07	0.83
	Chronic progressive MS	-0.63	-0.40	0.51
T_{cm} cells	Healthy control	0.50	0.40	0.20
	Chronic progressive MS	-0.8	-0.61	0.27
T_{naive} cells	Healthy control	-0.14	-0.16	0.62
	Chronic progressive MS	0.54	0.60	0.29

Figure 4-App.6 | Correlation between Kv1.3 activity and percentage of effector and memory subsets in CD8$^+$ T cells. **(A)** Sample flow cytometric plot of markers (CD62L and CD45RA) used to define effector memory (T_{em}), central memory (T_{cm}), naïve (T_{naive}), and T_{emra} subsets within CD8$^+$ T cells. Note that "gating" regions were adjusted for each subject or patient, using density plots to define boundaries between subsets. **(B)** Average percentage of CD8$^+$ T cells that were T_{em}, T_{cm}, T_{naive}, or T_{emra} respectively, from healthy controls and chronic progressive MS patients. Columns represent average ± standard deviation, with significant differences between MS and control populations determined using the Mann-Whitney *U* test. **(C)** Percentage of CD8$^+$ T cells with high Kv1.3 activity plotted as a function of the percentage of CD8$^+$ T cells that were T_{em} for each individual healthy control (■) or chronic progressive MS patient (▲). Solid lines represent linear fits to the data, with the red line fitting data from chronic progressive MS patients, and the black line fitting data from healthy controls. Parameters detailing the quality of the fit are in the table below the panel. **(D)** Same as panel (C) examining T_{emra} cells instead of T_{em} cells. **(E)** Same as panels (C,D) examining T_{cm} cells instead of T_{em} or T_{emra} cells. **(F)** Same as panels (C,D,E) examining T_{naive} cells instead of T_{em},T_{cm}, or T_{emra} cells. Correlations were computed using Pearson's correlation coefficient (*r*) with significance of the correlation computed using Student's *t* test ($p<0.05$ indicates significance).

4-App.7. Comparison of Kv1.3 activity to other T cell activation markers in CD4$^+$ T cells from peripheral blood of patients with chronic progressive MS or healthy controls.

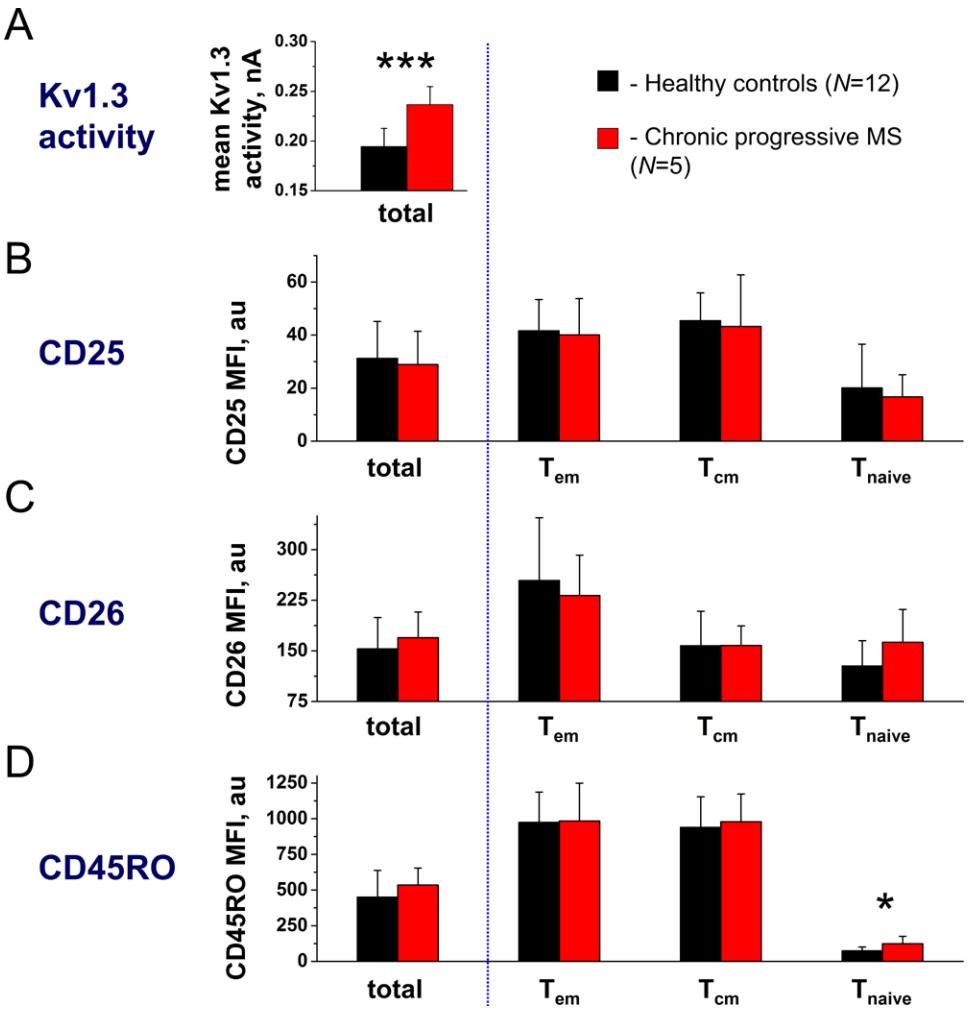

Figure 4-App.7 | Comparison of Kv1.3 activity to other T cell activation markers in CD4$^+$ T cells from peripheral blood of patients with chronic progressive MS or healthy controls. **(A)** Mean Kv1.3 activity in CD4$^+$ T cells, with columns depicting average ± standard deviation from healthy controls (*N*=12) or patients with chronic progressive MS (*N*=5). **(B)** Mean fluorescence intensity (MFI) of anti-CD25-PE in all CD4$^+$ T cells (total) or in effector memory (T_{em}), central memory (T_{cm}), or naïve (T_{naive}) subsets as defined in Figure 4-App.5. **(C)** MFI of anti-CD26-PE in all CD4$^+$ T cells (total) or in T_{em}, T_{cm}, or T_{naive} subsets. **(D)** MFI of anti-CD45RO-PE in all CD4$^+$ T cells (total) or in T_{em}, T_{cm}, or T_{naive} subsets. Differences between MS patients and control subjects were determined using the Mann-Whitney *U* test, with significance indicated as *** (p<0.01), ** (p<0.05), or * (p<0.10).

4-App.8. Comparison of Kv1.3 activity to other T cell activation markers in CD8+ T cells from peripheral blood of patients with chronic progressive MS or healthy controls.

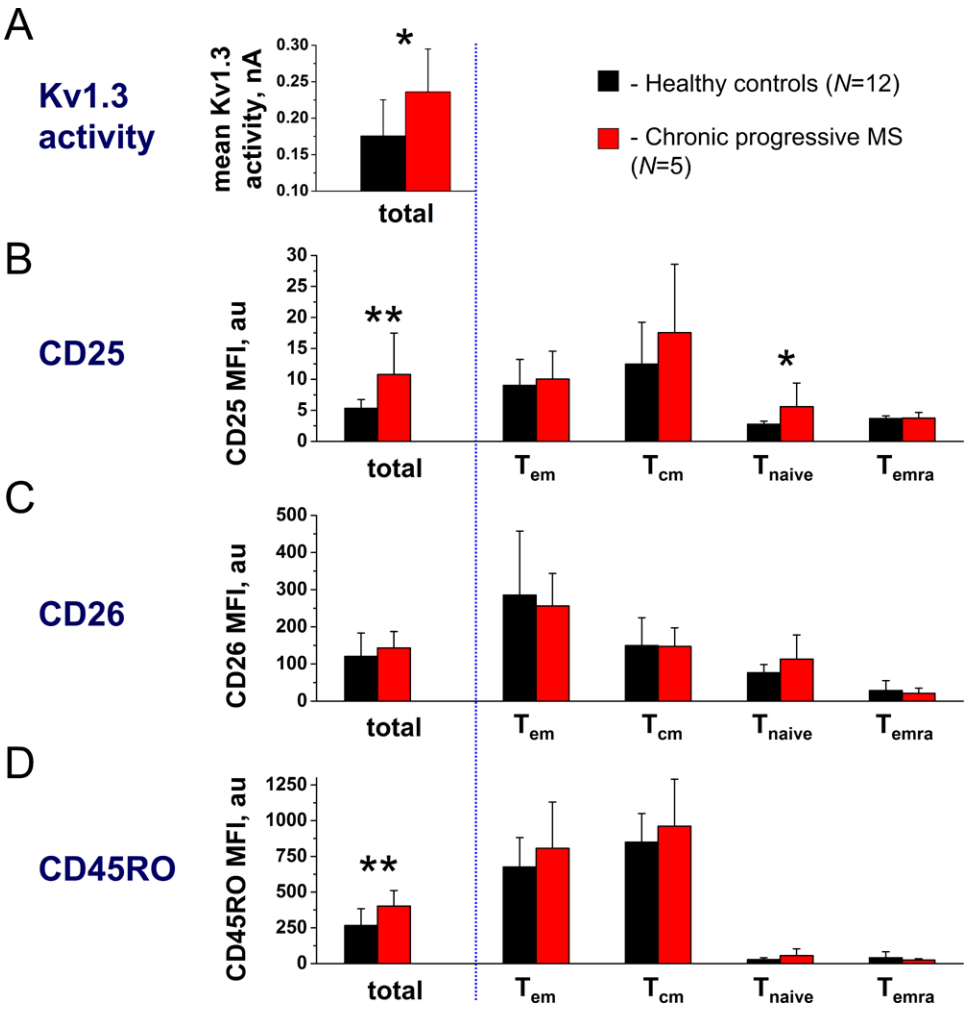

Figure 4-App.8 | Comparison of Kv1.3 activity to other T cell activation markers in CD8$^+$ T cells from peripheral blood of patients with chronic progressive MS or healthy controls. **(A)** Mean Kv1.3 activity in CD8$^+$ T cells, with columns depicting average ± standard deviation from healthy controls (*N*=12) or patients with chronic progressive MS (*N*=5). **(B)** Mean fluorescence intensity (MFI) of anti-CD25-PE in all CD8$^+$ T cells (total) or in effector memory (T_{em}), central memory (T_{cm}), naïve (T_{naive}), or T_{emra} subsets as defined in Figure 4-App.6. **(C)** MFI of anti-CD26-PE in all CD8$^+$ T cells (total) or in T_{em}, T_{cm}, T_{naive}, or T_{emra} subsets. **(D)** MFI of anti-CD45RO-PE in all CD8$^+$ T cells (total) or in T_{em}, T_{cm}, T_{naive}, or T_{emra} subsets. Differences between MS patients and control subjects were determined using the Mann-Whitney *U* test, with significance indicated as *** (p<0.01), ** (p<0.05), or * (p<0.10).

Chapter 4 References

1. Chandy, K. G., H. Wulff, C. Beeton, M. Pennington, G. A. Gutman, and M. D. Cahalan, **2004**, K+ channels as targets for specific immunomodulation, *Trends Pharmacol. Sci.*, 25: 280-289.
2. Beeton, C., M. W. Pennington, H. Wulff, S. Singh, D. Nugent, G. Crossley, I. Khaytin, P. A. Calabresi, C. Y. Chen, G. A. Gutman, and K. G. Chandy, **2005**, Targeting effector memory T cells with a selective peptide inhibitor of Kv1.3 channels for therapy of autoimmune diseases, *Mol. Pharmacol.*, 67: 1369-1381.
3. Beeton, C., and K. G. Chandy, **2005**, Potassium channels, memory T cells, and multiple sclerosis, *Neuroscientist*, 11: 550-562.
4. Scholz, C., K. T. Patton, D. E. Anderson, G. J. Freeman, and D. A. Hafler, **1998**, Expansion of autoreactive T cells in multiple sclerosis is independent of exogenous B7 costimulation, *J. Immunol.*, 160: 1532-1538.
5. Decoursey, T. E., K. G. Chandy, S. Gupta, and M. D. Cahalan, **1987**, Mitogen induction of ion channels in murine T lymphocytes, *J. Gen. Physiol.*, 89: 405-420.
6. Lee, S. C., D. E. Sabath, C. Deutsch, and M. B. Prystowsky, **1986**, Increased voltage-gated potassium conductance during interleukin 2-stimulated proliferation of a mouse helper T lymphocyte clone, *J. Cell Biol.*, 102: 1200-1208.
7. Wulff, H., P. A. Calabresi, R. Allie, S. Yun, M. Pennington, C. Beeton, and K. G. Chandy, **2003**, The voltage-gated Kv1.3 K+ channel in effector memory T cells as new target for MS, *J. Clin. Invest.*, 111: 1703-1713.

8. Beeton, C., H. Wulff, N. E. Standifer, P. Azam, K. M. Mullen, M. W. Pennington, A. Kolski-Andreaco, E. Wei, A. Grino, D. R. Counts, P. H. Wang, C. J. LeeHealey, S. A. B, A. Sankaranarayanan, D. Homerick, W. W. Roeck, J. Tehranzadeh, K. L. Stanhope, P. Zimin, P. J. Havel, S. Griffey, H. G. Knaus, G. T. Nepom, G. A. Gutman, P. A. Calabresi, and K. G. Chandy, **2006**, Kv1.3 channels are a therapeutic target for T cell-mediated autoimmune diseases, *Proc. Natl. Acad. Sci. U. S. A.*, 103: 17414-17419.

9. Rus, H., C. A. Pardo, L. N. Hu, E. Darrah, C. Cudrici, T. Niculescu, F. Niculescu, K. M. Mullen, R. Allie, L. P. Guo, H. Wulff, C. Beeton, S. I. V. Judge, D. A. Kerr, H. G. Knaus, K. G. Chandy, and P. A. Calabresi, **2005**, The voltage-gated potassium channel Kv1.3 is highly expressed on inflammatory infiltrates in multiple sclerosis brain, *Proc. Natl. Acad. Sci. U. S. A.*, 102: 11094-11099.

10. Hafler, D. A., D. A. Fox, M. E. Manning, S. F. Schlossman, E. L. Reinherz, and H. L. Weiner, **1985**, In vivo activated T lymphocytes in the peripheral blood and cerebrospinal fluid of patients with multiple sclerosis, *N. Engl. J. Med.*, 312: 1405-1411.

11. Khoury, S. J., C. R. Guttmann, E. J. Orav, R. Kikinis, F. A. Jolesz, and H. L. Weiner, **2000**, Changes in activated T cells in the blood correlate with disease activity in multiple sclerosis, *Arch. Neurol.*, 57: 1183-1189.

12. Estess, P., H. C. DeGrendele, V. Pascual, and M. H. Siegelman, **1998**, Functional activation of lymphocyte CD44 in peripheral blood is a marker of autoimmune disease activity, *J. Clin. Invest.*, 102: 1173-1182.

13. Chiu, D. T., and O. Orwar, **2004**, Functional cell-based high throughput drug screening, *Drug Disc. World*, 5: 45-51.

14. Estes, D. J., S. Memarsadeghi, S. K. Lundy, F. Marti, D. D. Mikol, D. A. Fox, and M. Mayer, **2008**, High-throughput profiling of ion channel activity in primary human lymphocytes, *Anal. Chem.*, 80: 3728-3735.

15. Jensen, J., A. R. Langkilde, C. Fenst, M. S. Nicolaisen, H. G. Roed, M. Christiansen, and F. Sellebjerg, **2004**, CD4 T cell activation and disease activity at onset of multiple sclerosis, *J. Neuroimmunol.*, 149: 202-209.

16. Estes, D. J., S. K. Lundy, F. Marti, D. A. Fox, and M. Mayer, **2008**, Functional regulation of Kv1.3 ion channels in human T lymphocytes, *In preparation*.

17. Poulopoulou, C., Z. Papadopoulou-Daifoti, A. Hatzimanolis, K. Fragiadaki, A. Polissidis, E. Anderzanova, P. Davaki, C. G. Katsiari, and P. P. Sfikakis, **2008**, Glutamate levels and activity of the T cell voltage-gated potassium Kv1.3 channel in patients with systemic lupus erythematosus, *Arthritis Rheum.*, 58: 1445-1450.

18. Beeton, C., H. Wulff, S. Singh, S. Botsko, G. Crossley, G. A. Gutman, M. D. Cahalan, M. Pennington, and K. G. Chandy, **2003**, A novel fluorescent toxin to detect and investigate Kv1.3 channel up-regulation in chronically activated T lymphocytes, *J. Biol. Chem.*, 278: 9928-9937.

19. Wolinsky, J. S., P. A. Narayana, P. O'Connor, P. K. Coyle, C. Ford, K. Johnson, A. Miller, L. Pardo, S. Kadosh, and D. Ladkani, **2007**, Glatiramer acetate in primary progressive multiple sclerosis: results of a multinational, multicenter, double-blind, placebo-controlled trial, *Ann. Neurol.*, 61: 14-24.

20. Frohman, E. M., M. K. Racke, and C. S. Raine, **2006**, Multiple sclerosis--the plaque and its pathogenesis, *N. Engl. J. Med.*, 354: 942-955.

CHAPTER 5

Conclusions and Future Applications

5.1. Evaluation and potential impact of high-throughput screening of ion channels for clinical and immunological applications

In this thesis, we developed a high-throughput assay for measuring ion channel activity in human T cells, and we applied this assay to address relevant clinical and immunological questions. There are several areas in which this work may have impact.

The assay developed in this work is the first application of high-throughput electrophysiology to a primary cell type. While we focused on measuring Kv1.3 currents in different subsets of lymphocytes, the methodology may be general to a range of primary cell types and ion channel species. Compared to traditional patch clamping, high-throughput devices offer several advantages including high-degree of automation, a more than 20-fold higher throughput, and the ability to compare cells in parallel under well-defined conditions. In addition, the high-throughput approach afforded distributions of ion channel activity in single cells, which is important for analyzing heterogeneous populations of cells such as lymphocytes. The advantages afforded by this assay make the study of ion channels in primary cells accessible to a host of immunologists and

clinicians who currently lack the expertise, equipment, and initiative to perform manual patch clamp.

In terms of clinical applications, this work provides a new approach to quantifying activity of human autoimmune diseases. Measuring Kv1.3 activity afforded 97% accuracy in distinguishing between healthy controls and patients with chronic progressive MS, and thus offers a promising approach for diagnosing primary progressive MS. Currently, diagnosing primary progressive MS can present significant clinical challenges; one of the patients examined in this study exhibited unexplained MS-like symptoms for 18 years before clinical diagnosis of primary-progressive MS. This patient displayed a large percentage of $CD4^+$ T cells with high Kv1.3 activity. Measuring Kv1.3 activity may make it possible to diagnose MS at an early stage in such difficult cases.

Another potential clinical application of measuring Kv1.3 activity is to determine progression of relapsing-remitting MS to chronic progressive MS. Patients who progress to chronic progressive MS become resistant to several treatments that are beneficial for relapsing-remitting MS patients (1, 2). Measuring Kv1.3 activity may allow for optimizing effective therapeutic options for these progressive patients. A third potential clinical application of Kv1.3 activity, i.e. therapeutic monitoring of patients with RA, is discussed in detail later in this chapter as a promising future application of this work.

In terms of immunological implications, this work provides new insights into the changes in Kv1.3 activity in T cells upon activation. The high-throughput assay for measuring Kv1.3 activity enabled detailed time-courses of Kv1.3 activity upon stimulation, as well as the ability to profile the varied and heterogeneous responses of control subjects in upregulation of Kv1.3 activity after stimulation. We also explored T

cell pathways that regulate Kv1.3 activity. Many of these immunological experiments would be impractical or impossible using traditional patch clamp techniques. In addition, understanding the regulation of Kv1.3 activity offers insight into novel therapeutic approaches to disrupt Kv1.3 ion channel activity for altering Ca^{2+}-signaling, migration, or proliferation of T cells. Such approaches may be useful in treatment of autoimmune diseases, similar to approaches currently being explored using drug compounds to block Kv1.3 activity.

Despite the advantages and potential clinical applications of the high-throughput assay presented in this work, there are several drawbacks that may limit the use of Kv1.3 activity in clinical settings. First, high-throughput electrophysiology devices are typically very expensive and only found in pharmaceutical companies. Even after acquiring the instrument, individual experiments remain expensive (due to the costs of the disposable patch plate substrate) compared to standard clinical tests. Second, these electrophysiology devices are not currently produced for clinical applications, and variations in different devices, patch plates, and protocols may not allow elucidation of the differences in Kv1.3 activity between patient populations (especially when compared between different clinical facilities). And third, while we demonstrated significant differences in Kv1.3 activity between patient populations, studies with a larger numbers of patients will be needed to establish Kv1.3 activity as a quantitative measurement that affords clinically relevant and practical advantages over currently used clinical markers and techniques.

Despite these challenges, high-throughput profiling of ion channels enables a range of clinical and immunological studies that would not be possible using traditional

patch clamp. The remainder of this chapter discusses some of the potential future applications of this promising technology.

5.2. High-throughput screening of Kv1.3 ion channels for therapeutic monitoring of RA

The most promising future application of the work presented in this thesis is to use high throughput screening of ion channels in T cells to quantify disease activity for therapeutic monitoring in patients with RA. In our preliminary study of Kv1.3 ion channels in patients with RA, Kv1.3 activity in $CD8^+$ T cells correlated with disease activity. This correlation was stronger than the correlation between disease activity and either erythrocyte sedimentation rate (ESR) or C reactive protein (CRP) levels. These last two markers are commonly used by rheumatologists and are general for inflammation (3); these markers, however, are not specific to a certain cell type or inflammation mechanism. Therefore, Kv1.3 activity might provide an improved clinical measurement for quantifying disease activity, and in addition might determine which subset of lymphocytes is stimulated during this active disease. Another motivation for using RA as a model disease is the diverse different treatment options for RA, with several drugs exhibiting different mechanisms of action to suppress RA (4, 5). Knowing the activity of certain subsets of lymphocytes (assessed by Kv1.3 measurements) may provide additional clinical insight to aid the rheumatologist in selecting and monitoring a treatment regimen. A prospective study would be the following:

- Recruitment of patients with RA who are on active treatment. A sample patient population might consist of patients on adalimumab (a TNF-α inhibitor), patients on

rituximab, which depletes B cells (6), patients on methotraxate (affects purine metabolism and inhibits T cell activation) and patients on prednisone (an orally delivered steroid).

- At regular intervals (3 months), patients would donate ~10-20 mL of their peripheral blood for measurement of Kv1.3 activity in both $CD4^+$ and $CD8^+$ T cells. Patients would also provide blood in the case of an adverse event, such as a flare of symptoms associated with RA. It might also be interesting to quantify Kv1.3 activity in B cells; a recent report highlighted the role of memory B cells in relapses of RA patients treated with rituxan (7), and these B cells have been reported to exhibit high levels of Kv1.3 activity (8).
- In addition to Kv1.3 measurements the following standard clinical measurements would be taken: complete blood count (CBC), ESR, CRP, number of inflamed joints, and a disease activity index for RA.
- We would also measure serum levels of glutamate and selected cytokines using ELISA. Recently, Poulopoulou et al. found that patients with active systemic lupus erythematosus (SLE) had lower serum levels of glutamate than healthy controls or patients with inactive SLE (9). They also found that in vitro, low levels of glutamate led to increased Kv1.3 activity in T cells compared to control levels of glutamate. In addition, we found that exogenous cytokines increased Kv1.3 activity in the absence of TCR stimulation. Therefore, it would be clinically and scientifically interesting to correlate Kv1.3 activity to these serum markers in order to understand the physiological relevance of T cells with high Kv1.3 activity in peripheral blood.

The above tests would determine the extent to which Kv1.3 activity is a useful clinical marker of disease activity, and it would also provide general information about the correlation of serum glutamate levels and cytokines with Kv1.3 activity in the context of RA.

5.3. High-throughput screening of Kv1.3 ion channels for diagnosis of MS

The original goal of the work presented in this thesis was to develop a new tool to aid in the diagnosis of MS. Despite advances in understanding the pathogenesis of MS, clinical diagnosis of MS remains a significant challenge (10). The criteria for diagnosis (MacDonald criteria) require clinical evidence of lesions in the brain (typically using MRI) disseminated in time and space (11). As a result, diagnosis typically occurs well after damage to the brain has already occurred, typically several years after presentation of initial symptoms (12, 13). An ideal clinical test would afford definitive diagnosis of MS at the first presentation of clinical symptoms.

In profiling of Kv1.3 activity in patients with MS, we found that patients with progressive forms of MS had significantly higher Kv1.3 activity in their $CD4^+$ T cells compared to healthy controls. While measurements of Kv1.3 activity have potential clinical applications for diagnosing patients with primary progressive MS, patients with relapsing-remitting (RR-) MS (all of whom were in remission) did not exhibit differences in Kv1.3 activity compared to controls. To be able to distinguish between healthy controls and RR-MS patients, we attempted to detect differences in Kv1.3 activity in T cells from controls and RR-MS patients upon specific stimulation of PBMCs using MS-relevant myelin antigens (14). These antigens consisted of myelin basic protein (MBP),

as well as selected peptides from MBP, proteolipid protein, and myelin oligodendrocyte glycoprotein (14). Stimulation protocols involved adding antigen to PBMCs at various concentrations, and testing either Kv1.3 activity or activation markers using flow cytometry at times after stimulation ranging from 3 d to 2 weeks.

Unfortunately, these stimulation protocols never resulted in differences between PBMCs stimulated with antigen and PBMCs cultured without stimulation. Within 2 weeks, most naïve and central memory T cells died, leaving enriched populations of effector memory T (T_{em}) cells. These populations, however, were nearly identical (both before and after mitogenic stimulation) whether PBMCs were cultured with or without antigen, suggesting that disease-reactive T cells did not proliferate sufficiently to be detected above the background population of T_{em} cells (Fig. 5.1). Interestingly, these T cells cultured for 7 d without stimulation exhibited very high levels of Kv1.3 activity upon stimulation, which is indicative of T_{em} cells.

In the works from the Chandy group in which disease-specific autoreactive T cell lines were generated from the blood of MS and control patients (Fig. 1.3), stimulation proceeded over the course of 6 weeks and usually involved multiple blood draws to replenish antigen presenting cells (15, 16). Such long stimulation times are needed for non-specific cells to die, leaving only proliferating disease reactive cells. These protocols are not conducive, however, to a diagnostic assay. Profiling of Kv1.3 activity after stimulation with MS-specific antigens, therefore, provides significant challenges for detecting differences between MS patients and controls in a short time-period.

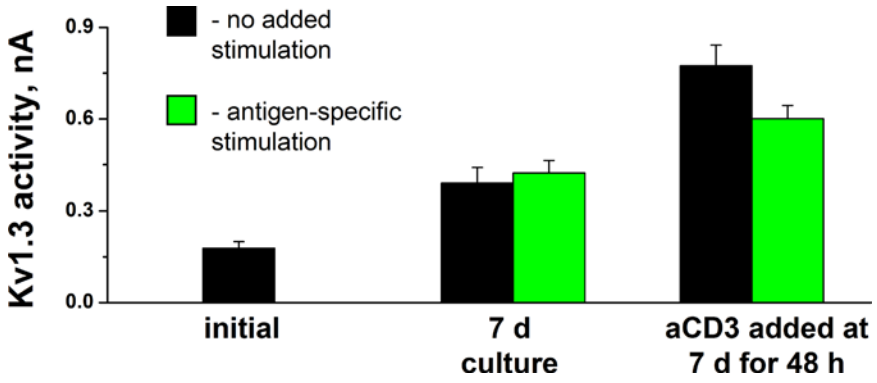

Figure 5.1 | Kv1.3 activity in T cells upon antigen-specific stimulation. Using a healthy control subject, Kv1.3 activity was initially measured from $CD4^+$ T cells isolated from freshly drawn blood (left). PBMCs from this control were then cultured either with 1× tetanus toxoid (green) or without added stimulation (black) for 7 d prior to Kv1.3 measurements in isolated $CD4^+$ T cells (middle). After 7 d culture, PBMCs from these two conditions were suspended in fresh media and stimulated with anti-CD3 antibodies (aCD3) for 48 h prior to measurements of Kv1.3 activity in $CD4^+$ T cells (right). There were no significant differences between cells with or without specific stimulation in any condition. These findings were also representative of specific stimulation of PBMCs from MS patients with myelin-specific antigens.

Despite the problems associated with antigen-specific stimulation, profiling Kv1.3 activity from peripheral blood might still have applicability for diagnosing RR-MS. In particular, correlating neurological symptoms, an MRI-detected lesion, and high activity of T cells in peripheral blood (using Kv1.3 levels as a marker for T cell activity) at the presentation of first symptoms might provide a method to diagnose MS. The limitations of such experiments are difficulties in accessing such patient populations (before treatment with immunosuppressive drugs) and the long time scale (~3 years) needed to obtain definitive clinical diagnosis for correlation with initial Kv1.3 activity (17).

5.4. Technological enhancements to improve throughput of automated electrophysiology devices

In the experiments throughput this thesis, the IonWorks HT technology afforded measurements of Kv1.3 activity in 100-200 T cells per experimental run (~1 h). While this throughput is significantly higher than traditional manual patch-clamp, it is still several orders of magnitude lower than a true high-throughput technology (e.g. flow cytometry). Higher throughput would enable the quantification of Kv1.3 activity in additional lymphocyte subsets (or treatments with different immunosuppressive drugs) in parallel, and it would also provide a more accurate profiling of ion channel activity in cell types with heterogeneous expression of ion channels. We found that the throughput of the assay presented in this work depended strongly on subset (with B cells having less than a 25% success rate for measurements) (Fig. 5.2). The reasons for the different throughputs of various subsets of lymphocytes are not clear but may provide insights into improving throughput of the IonWorks HT for experiments with primary lymphocytes (Fig. 5.2).

The first strategy for improving throughput is to modify the surface properties of the "patch plate" for performing planar patch-clamp using the IonWorks HT platform. Currently, the "patch plate" is composed of plastic (polyimide) which results in low seal resistances between the attached cell and substrate (compared to traditional patch clamp using glass substrates (18)). These low seal resistances lead to instability of the cell on the substrate, especially after application of drug (Fig. 5.2), as well as a large "leak" current that can mask small currents. Coating the patch plate with poly-L-lysine or with a thin-film of a glass-like polymer might improve the seals and throughput obtained by the IonWorks HT system. These coatings would improve seals by promoting cell adhesion,

and also by "smoothing" sub-micron irregularities in the microfabricated surface of the patch plate. Additionally, coating the surface with antibodies to the cell type of interest (e.g. $CD4^+$ T cells) might improve seal resistances.

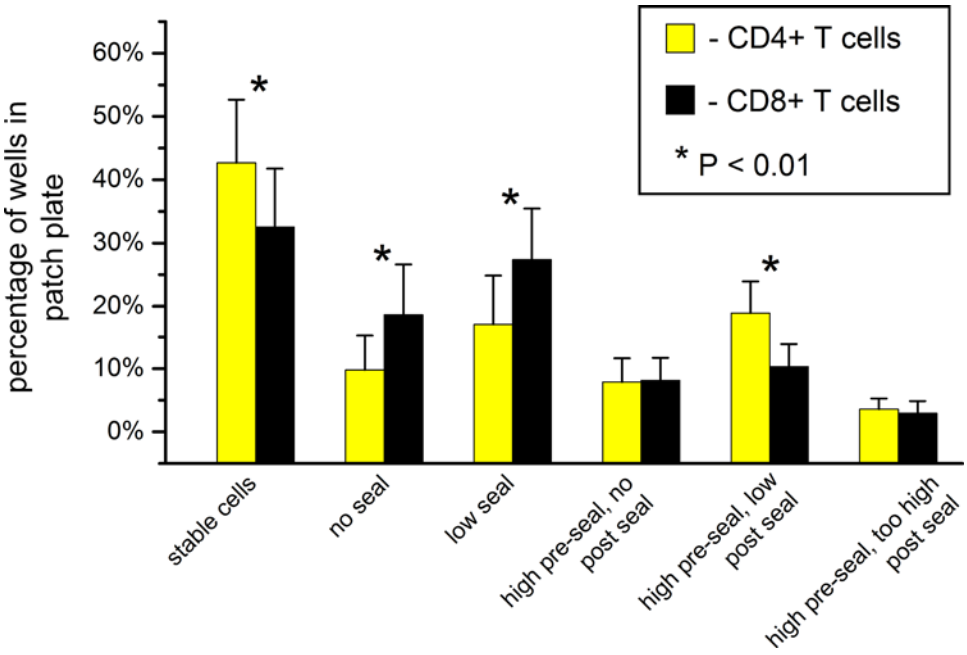

Figure 5.2 | Analysis of throughput of $CD4^+$ and $CD8^+$ T cells using IonWorks HT technology. For 31 experiments with MS and control patients, each of the 11904 wells of the "patch plate" was assessed an outcome of whether the well resulted in a successful Kv1.3 measurement (stable cells) or an unsuccessful measurement. The reasons for unsuccessful measurements were the following: (i) no initial sealing of a cell to the micropore in the well (no seal); (ii) establishment of a seal resistance below 75 MΩ (low seal); or (iii) variation of pre- to post-compound seal resistances greater than 25%. Columns depict averages and standard deviation of the 31 experiments, with $CD4^+$ (yellow) and $CD8^+$ T cells (black) each comprising half of the patch plate. *P* values were computed using Welch's *t* test and represent differences between $CD4^+$ and $CD8^+$ T cells for the indicated metric.

The second strategy to improve throughput would be to produce patch plates with smaller diameters of micropores. We found that the throughput of the IonWorks HT system for lymphocytes depended strongly on the batch of "patch plates" used for measurements, as micropore diameters and geometries varied between batches. Generally, patch plates with small micropores (<1.8 μm diameter) yielded the highest

percentage of successful measurements. In addition, we found that within each patch plate, the smallest micropores produced the highest percentage of successful measurements of Kv1.3 activity (Fig. 5.3). The IonWorks HT system was designed primarily for large cell lines (>20 μm diameter), and these cells are relatively insensitive to the size of micropores (19). Lymphocytes (~7 μm), however, are much closer to the size of the micropores, which can lead to low seal resistances and instability of T cells on the micropores. Two obstacles for reducing micropore size are technological difficulties associated with forming repeatable and consistent pores with small diameters (20), and the fact that current "patch plates" are manufactured commercially using proprietary techniques.

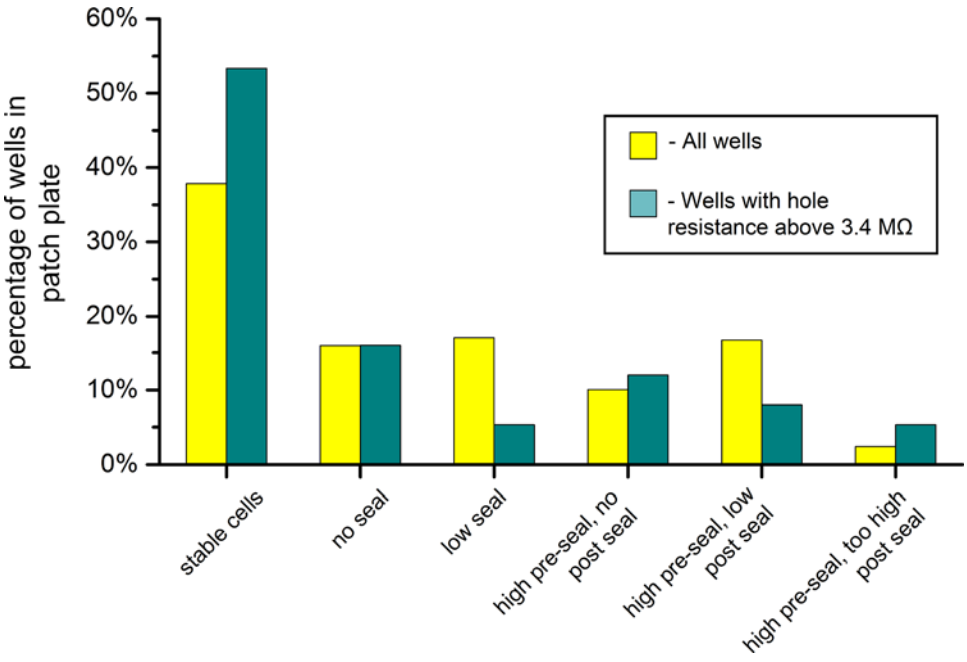

Figure 5.3 | Comparison of throughput of CD4$^+$ T cells in specific wells of the patch plate with micropores having "small" diameters to the throughput of the entire patch plate. Wells with "small diameter" micropores were defined as having an open hole resistance greater than 3.4 MΩ. Measurements of throughput were from three independent experiments (comprising 574 wells, 75 of which had "small diameter" micropores) using patch plates from the same processing batch.

The final strategy for improving throughput would include the development of new devices offering a "patch plate" with more than 384 independent wells. Currently, MDS Technologies produces the IonWorks Quattro, which is similar to the IonWorks HT system except that each well of the "patch plate" contains 64 micropores instead of one single micropore (21). Each well, therefore, provides an average of the whole-cell currents through less than 64 cells attached to each micropore. Such a system is not amenable to measurements with lymphocytes, as fewer than 40% of lymphocytes establish seals with micropores. However, the technology of machining 64 micropores in each of the 384 wells would be of great applicability if each of the wells were able to be individually addressed by electrodes and the fluidics system.

In addition to increasing throughput, it would also be useful to be able to monitor cellular capacitances of T cells using the IonWorks HT device. Capacitance values, which are readily measured in manual patch clamp experiments, are proportional to membrane surface area (22), thus allowing computation of Kv1.3 current densities in the membranes of attached cells. Measurements of current density would answer the question of whether the T cells in patients with MS and RA had high Kv1.3 activity simply because they had enlarged T cells or because of increased surface-density of Kv1.3 ion channels. The IonWorks HT device currently does not measure capacitances, although perhaps the creative design of voltage protocols (involving triangle voltage pulses) may afford these measurements.

5.5. Profiling of drug compounds that block Kv1.3 ion channels using activated human T cells

Suppressing Kv1.3 ion channel activity in T cells is a promising approach for treating human autoimmune diseases mediated by T_{em} cells (23). As such, several research groups and pharmaceutical companies are actively working to develop human-suitable drug compounds to block Kv1.3 ion channels (24-26). To test the efficacy of such compounds, researchers typically quantify the percentage inhibition of Kv1.3 ion channels recombinantly over-expressed in cell lines (27). These cells, while expressing high levels of Kv1.3 activity, provide different membrane composition of lipids and proteins than human T cells in blood (28). Ideally, promising drug compounds for blocking Kv1.3 activity could be screened on human T cells from various subjects (including those with disease), in addition to cell lines, to confirm the efficacy of the drug.

We tested the capability of the high-throughput assay presented in this thesis to profile the effects of drug compounds on Kv1.3 activity in human T cells. The IonWorks HT system provides several useful features for compound profiling of drugs that block ion channels, most notably the ability to add different concentrations to different wells across the patch plate. Using cell lines, the IonWorks HT technology allows characterization of an entire dose-response curve of a particular drug compound (generating an IC_{50}) in a single run (29).

T cells, however, provide several complications in using the IonWorks HT technology for compound profiling. First, we typically achieved successful Kv1.3 measurements in ~40% of the wells of the patch plate using T cells (30). This lower

throughput (compared to cell lines which have a success rate of >75%) reduces the number of measurements of inhibition by a given concentration of drug per experiment. Second, T cells isolated directly from blood have low Kv1.3 activity (~0.18 nA average), barely above the average leak current caused by the low seal resistance of the IonWorks HT system. This low Kv1.3 activity makes it difficult to quantify the percentage of inhibition by drug compounds, because the "baseline" current cannot be separated from the leak current.

To solve the problem of leak current, we used activated human T cells to profile drug compounds that block Kv1.3 ion channels. We stimulated freshly isolated human T cells for 64 h using 150 ng mL^{-1} anti-CD3 and anti-CD28 antibodies. After stimulation, we isolated $CD8^+$ T cells using magnetic bead separation techniques, and then used these isolated cells for IonWorks HT experiments. We previously found that activated T cells expressed high levels of Kv1.3 activity, with >75% of cells having Kv1.3 activity greater than 0.5 nA before addition of compound (31); we used this threshold of 0.5 nA to discard measurements of percentage drug-inhibition that may be affected by leak currents. Another advantage of using activated T cells is that these cells afford a higher percentage of successful measurements than T cells freshly isolated from human blood (30).

Using these activated $CD8^+$ T cells, we obtained dose-response curves of the inhibition of Kv1.3 ion channels by the drugs margatoxin (IC_{50} = 110 pM), psora-4 (IC_{50} = 3 nM), nifedipine (IC_{50} = 5 μM), and TRAM-34 (IC_{50} = 3 μM) (Fig. 5.4). For each drug, we performed at least three separate IonWorks HT experiments, with two of the experiments being from the same subject and with the second experiment performed

immediately following the first (i.e. "back-to-back") (Table 5.1). To quantify IC_{50} values, we normalized values of percentage inhibition, using the percentage of current block by 72 nM ShK as the "maximal" value and the percentage of current block by D-PBS as the "minimal" value.

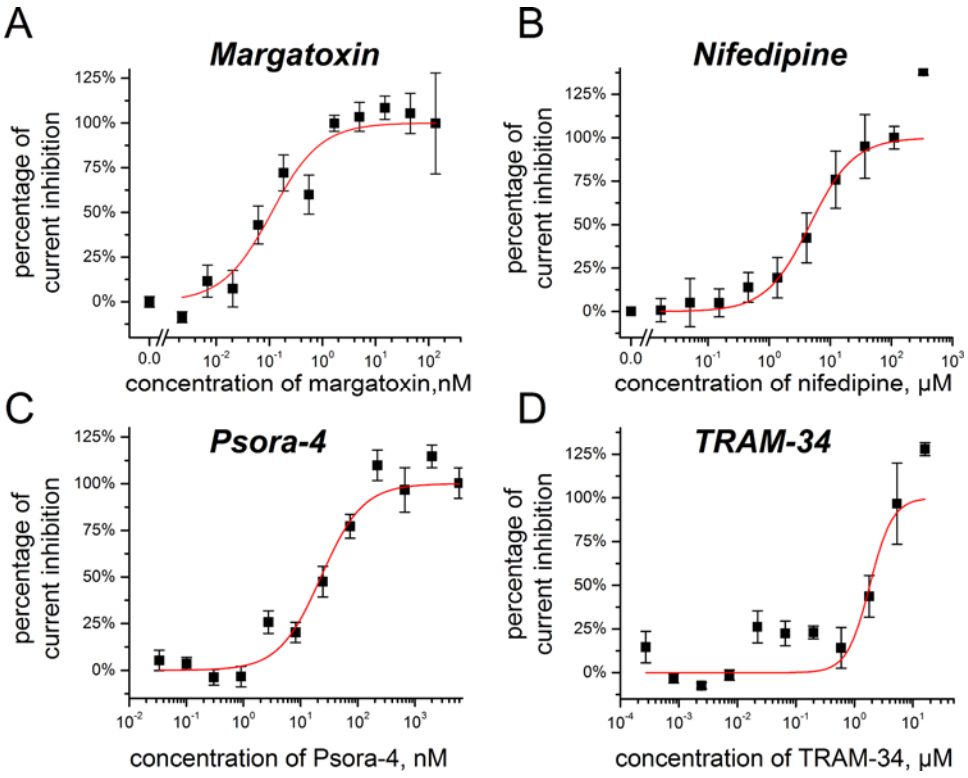

Figure 5.4 | Compound-profiling of drug compounds that block Kv1.3 ion channels using activated human $CD8^+$ T cells. (A) Effects of margatoxin on inhibition of Kv1.3 activity. Results are combined from two consecutive experiments from the same human subject. The red line indicates a logistic fit to the dose-dependent inhibition of Kv1.3 activity by margatoxin. **(B)** Same as panel (A), but profiling the effects of nifedipine instead of margatoxin. **(C)** Same as panel (A), except profiling the effects of psora-4. **(D)** Same as panel (A) except profiling the effects of TRAM-34. Note, TRAM-34 was insoluble above 15 µM. Percentage inhibition was normalized for each drug compound, using 72 nM ShK to determine "maximal inhibition" and using D-PBS to determine "minimal inhibition".

Using each of the four drugs, we were able to produce representative dose-response curves depicting the percentage current block as a function of concentration of drug compound (Fig. 5.4). The curve for TRAM-34 did not exhibit a plateau at maximal

inhibition of Kv1.3 activity because of drug insolubility above 15 μM. When combining "back-to-back" experiments, we obtained IC_{50} values for margatoxin, nifedipine, and TRAM-34 that were within 10% of the listed value for inhibition of Kv1.3 currents (Table 5.1). In contrast, values from single experiments varied in IC_{50} values, even between consecutive experiments with the same subject (Table 5.1). These results suggest that single experiments using the IonWorks HT technology using T cells are not sufficient to obtain IC_{50} values drug compounds that block Kv1.3 activity, presumably due to the low numbers of successful measurements of percentage block for a given concentration of drug.

Interestingly, experiments with psora-4 using T cells on the IonWorks HT instrument produced IC_{50} values that were 5- to 7-fold higher than reported in literature (Table 5.1). These elevated IC_{50} values were observed using two separate human subjects and combining consecutive experiments (Table 5.1). A primary reason for these elevated IC_{50} values may be interactions between psora-4 and exposed surfaces in the fluidics and patch-plate wells of the IonWorks HT instrument. Non-specific binding to these surfaces would result in an elevated IC_{50} value, and such effects have been reported for other compounds using automated high-throughput electrophysiology (29).

This work, therefore, demonstrates that automated high-throughput electrophysiology technology can provide a platform for obtaining IC_{50} values for drug compounds that block Kv1.3 ion channels using human lymphocytes. While two consecutive experiments were needed to obtain representative IC_{50} values on activated human T cells, several factors may improve the accuracy of the assay using single experiments. First, we recently found that stimulating T cells with IL-2 in addition to

anti-CD3 antibodies provided 1.5- to 2-fold higher average Kv1.3 current than in T cells stimulated with anti-CD28 and anti-CD3 antibodies. Such elevated Kv1.3 currents would enable higher throughput (more cells with pre-compound current greater than 0.5 nA) and improved accuracy of percentage inhibition especially at concentrations near the IC_{50} value. A second enhancement might include modifications to the "patch plate" surface (discussed above) to improve seal resistances and throughput of T cells on the IonWorks device. Even without enhancements, the methodology presented here provides an enabling tool that affords rapid compound profiling of drug compounds that block Kv1.3 activity using primary human T cells, which are ultimately the target of the these compounds (24).

5.6. Simultaneous measurement of Kv1.3 and KCa3.1 channels using high-throughput electrophysiology

The assay presented in this thesis measures, specifically, Kv1.3 activity in human T cells. An ideal assay for quantifying K^+ ion channel activity in T cells, however, would also measure activity of the other major K^+ ion channel in T cells, KCa3.1. Wulff *et al.* showed that T cells selectively upregulate either Kv1.3 or KCa3.1 ion channels after stimulation, depending on phenotype (15). These findings, however, were obtained using manual patch clamp using a limited number of cells (15). Since both channels regulate Ca^{2+}-signaling upon activation, a high-throughput approach to profile Kv1.3 and KCa3.1 activity in the same cell might reveal interesting and unknown K^+ channel distributions, especially in the context of human disease. In addition, profiling both channels at the same time would allow rapid characterization of ion channel distribution in a range of

immune cell types, such as regulatory T cells, Th-1, Th-2, or Th-17 cells (all $CD4^+$), in which K^+ channel distributions have not yet been reported.

Table 5.1. Summary of compound profiling of drugs that block Kv1.3 ion channels using activated human T cells

Experiment	Measured IC_{50}	Hill slope (*p*)	Pearson's correlation coefficient (*r*)
Margatoxin (IC_{50} = 110 pM)			
Control #1, Exp. #1	59.6 ± 257 pM	15.5	0.92
Control #1, Exp. #2	322 ± 121 pM	0.65 ± 0.14	0.92
Control #1, Avg	**110 ± 30 pM**	**0.94 ± 0.21**	**0.95**
Control #2	264 ± 68 pM	2.9 ± 1.5	0.90
Nifedipine (IC_{50} = 5 µM)			
Control #3, Exp. #1	4.9 ± 2.9 µM	0.7 ± 0.3	0.83
Control #3, Exp. #2	4.4 ± 1.2 µM	1.4 ± 0.5	0.94
Control #3, Avg	**4.7 ± 1.6 µM**	**1.2 ± 0.4**	**0.92**
Control #4	3.6 ± 1.1 µM	2.2 ± 1.4	0.86
TRAM-34 (IC_{50} = 3 µM) *			
Control #5, Exp #1	1.8 ± 0.5 µM	2.2 ± 1.5	0.84
Psora-4 (IC_{50} = 3 nM)			
Control #6, Exp #1	22.6 ± 6.8 nM	2.1 ± 1.2	0.92
Control #6, Exp #2	20.5 ± 7.4 nM	0.7 ± 0.2	0.92
Control #6, Avg	**22.7 ± 5.2 nM**	**1.2 ± 0.3**	**0.96**
Control #7, Exp #1	19.8 ± 12.6 nM	0.7 ± 0.3	0.80
Control #7, Exp #2	14.1 ± 12.3 nM	1.2 ± 1.1	0.50
Control #7, Avg	**17.1 ± 6.4 nM**	**0.8 ± 0.2**	**0.91**

There are two major problems with measuring KCa3.1 channels in T cells using the IonWorks HT technology. First, T cells freshly isolated from blood express low numbers of KCa3.1 channels (10-20 channels per cell) (32). These low numbers, coupled with a single channel conductance of ~12 pS (33), may make it impossible to distinguish KCa3.1 from the leak current in freshly isolated T cells (due to the low seal resistance of T cells on the IonWorks HT device). Activated T cells, however, express 20-fold more KCa3.1 channels than resting T cells (15), making possible the measurement of KCa3.1 channels above the background leak current.

A second problem is that the IonWorks HT system does not permit perfusion of the intracellular recording solution. Since KCa3.1 channels open in response to increases in intracellular Ca^{2+} levels (which is typically accomplished by perfusion of a Ca^{2+}_{high} intracellular solution using traditional patch clamp (34)), this increase in Ca^{2+} must come from the extracellular solution in the IonWorks HT system. One strategy is to deliver compounds that open plasma membrane CRAC channels in the T cell attached to the micropore in each well to increase $[Ca^{2+}]_i$ from the extracellular solution (Fig. 5.5). Either thapsigargin (which opens intracellular stores of Ca^{2+} to activate plasma membrane CRAC channels) or ionomycin (a Ca^{2+} ionophore) might be able to elevate the intracellular concentration of Ca^{2+} to activate KCa3.1 channels (35).

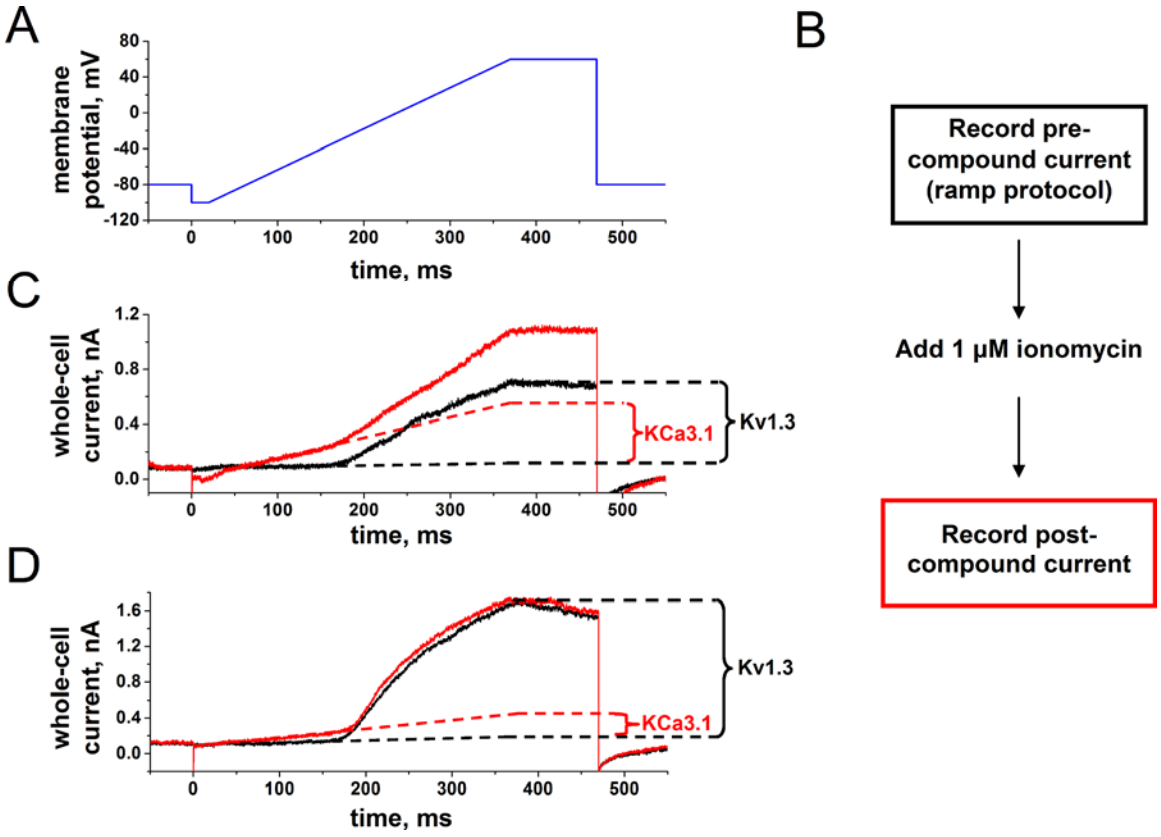

Figure 5.5 | Strategy for measuring Kv1.3 and KCa3.1 channels simultaneously in T cells using IonWorks HT technology. (A) Voltage-protocol for measuring Kv1.3 and KCa3.1 ion channels in the same experiment. A ramp protocol affords elucidation of ligand-gated KCa3.1 channels at hyperpolarizations and small depolarizations, while voltage-gated channels open sharply upon depolarization above an activating threshold. **(B)** General strategy used in this experiment. First, whole-cell electrical current was recorded using the voltage-ramp in (A), with only Kv1.3 channels opening upon depolarization. Then, 1 µM ionomycin was added (5 min incubation time) to the attached T cells to increase $[Ca^{2+}]_i$ and open KCa3.1 channels. Whole-cell current was recorded a second time, with both KCa3.1 and Kv1.3 channels contributing to the recorded current. (C) Sample measurement with a cell that exhibited a stable seal resistance upon compound addition, with pre-compound current represented in black and post-compound current in red. The dashed lines depict a strategy to quantify, respectively, KCa3.1 and Kv1.3 channel contributions to the overall current. (D) A second sample measurement of Kv1.3 and KCa3.1 currents in the same cell.

We performed a proof-of-principle experiment to measure Kv1.3 and KCa3.1 channels in parallel in mitogen activated $CD4^+$ T cells using the IonWorks HT device. In this experiment, we first measured whole-cell electrical current using a voltage ramp, with Kv1.3 ion channels opening upon depolarization, and then added ionomycin (1 µM),

using the automated fluidics of the IonWorks HT device to each well of patch plate (Fig. 5.5). After incubation, we re-measured the whole cell electrical current, which was now composed of both Kv1.3 and KCa3.1 activity. While this experiment did seem to permit elucidation of both Kv1.3 and KCa3.1 channels in the same cells (Fig. 5.5), the apparent KCa3.1 activity (Fig. 5.5) may be due to increases of the leak current after addition of ionomycin. Optimization of protocols (e.g. concentration and incubation times of thapsigargin or ionomycin) using manual patch-clamp or automated single-cell planar patch-clamp technologies (Nanion, Munich, Germany (36)) will be an important next step before trying again to measure KCa3.1 channels using the IonWorks HT device.

5.7. Determining the molecular mechanisms of increased Kv1.3 activity after stimulation of T cells

In Chapter 3, we profiled the effects of immunosuppressive drugs on regulating Kv1.3 activity upon stimulation of T cells. Several questions, however, remain about the mechanisms by which Kv1.3 activity increases after stimulation: (i) is the increase the result of increased translation of new Kv1.3 proteins?; (ii) is the increase the result of insertion of vesicles containing Kv1.3 proteins into the plasma membrane?; and (iii) which additional pathways might be involved in affecting Kv1.3 regulation?

An approach to determine whether increased Kv1.3 activity correlates to increase Kv1.3 protein levels involves using Western blot techniques to analyze Kv1.3 protein levels in $CD4^+$ T cells isolated after stimulation. Useful experiments would involve analysis of Kv1.3 protein levels in $CD4^+$ T pre-treated with immunosuppressive drugs using different stimulation conditions, as well as time-course studies of the changes in

protein levels following stimulation. Three difficulties associated with these studies are: (i) difficulties associated with quantifying protein levels in Western blot studies; (ii) selection of a reference protein with levels that do not change upon stimulation (e.g. GAPDH may not be sufficient); and (iii) selection of a polyclonal antibody to Kv1.3 proteins, as commercial sources may not be specific to Kv1.3 ion channels (personal communication with Prof. Christine Beeton).

In addition to Western blot studies, there are several additional immunosuppressive drugs that may provide useful insights into the regulation of Kv1.3 activity. It would especially be interesting to examine a more selective and potent inhibitor of Jak-3 than tyrphostin AG-490 (for example the recently-developed CP-690550 compound, Pfizer (37)) to verify the specific effects of Jak-3 inhibitors on Kv1.3 activity. In addition, inhibitors of PI(3)K (LY294002 (Sigma-Aldrich) or wortmannin (Sigma-Aldrich)), MAP kinase (U0126 (Sigma-Aldrich)), and AKT (Triciribine, EMD Biosciences) might provide insight on the pathways that regulate Kv1.3 activity. One problem associated with studying these drugs may be that their effects on IL-2 and IL-2R expression make it difficult to isolate effects on Kv1.3 activity. In addition, LY294002 has been reported to block Kv ion channels (38).

5.8. siRNA studies to assess the role of increased Kv1.3 activity in activated human T cells

To further study the immunological relevance of Kv1.3 regulation in T cells, it would be interesting to use small interfering RNA strands (siRNA) to inhibit translation of Kv1.3 ion channels in T cells. Such an approach would answer four central questions

related to the regulation of ion channels in T cells: (i) whether Kv1.3 activity regulated at the transcriptional level; (ii) whether inhibiting the upregulation of Kv1.3 activity affects Ca^{2+}-signaling, cytokine secretion, and proliferation of T cells; (iii) whether some cell phenotypes (e.g. T_{em}) are affected by disrupting Kv1.3 regulation more than other subsets; and (iv) whether inhibiting the increase in Kv1.3 activity after stimulation can provide therapeutic benefit in animal models of autoimmune disease.

While siRNA technology offers a specific tool to disrupt regulation of Kv1.3 activity, there are significant challenges associated with delivering siRNA to primary lymphocytes. Typically, lymphocytes are resistant to transfection by conventional reagents including cationic lipids and polymers (39). Electroporation experiments succeed in delivering siRNA to lymphocytes in vitro, although this technique may lead to significant cell death (40). Promising new methods for delivering siRNA to lymphocytes include viral vectors (41) and antibody fragment-protamine fusion proteins (mixed with siRNA) to target siRNA to particular T cells (42).

5.9. Modeling the roles of Kv1.3 and KCa3.1 ion channels in regulating T cell activation

In addition to using high-throughput screening to measure Kv1.3 ion channels in T cells, we also used inhibitors of Kv1.3 and KCa3.1 ion channels to explore the roles of these ion channels in T cells (Fig. 5.6). Five interesting findings arose from these studies. (i) Blocking KCa3.1 ion channels (with TRAM-34) alone had no effect on expression of activation markers (CD25, CD26) or proliferation of $CD4^+$ T cells after stimulation (Fig. 5.6*A*,*B*). (ii) Blocking KCa3.1, in combination with blocking Kv1.3, had profound effects

on reducing proliferation and expression of activation markers in T cells activated by anti-CD3 antibodies (Fig. 5.6*A,C*). The effects of the inhibition of both Kv1.3 and KCa3.1 were significantly greater than blocking either channel alone. (iii) When stimulation protocols employed either anti-CD28 antibodies or recombinant IL-2 (in addition to anti-CD3 antibodies), K^+ channel blockers had no effects on either CD25 expression or T cell proliferation. (Fig. 5.6*A,C*). (iv) Expression of CD26 in $CD4^+$ T cells after activation was especially sensitive to drug compounds that block Kv1.3 channels. These compounds significantly CD26 expression even when anti-CD28 antibodies were added to stimulation (Fig. 5.6*B*). And (v), inhibiting either Kv1.3 or KCa3.1 ion channels reduced Ca^{2+} influx in freshly isolated T cells after stimulation. The combination of blocking both channels, however, produced the largest reduction in Ca^{2+} influx (Fig. 5.6*D*). It is interesting that blocking KCa3.1 ion channels had a similar effect in reducing influx of Ca^{2+} compared to blocking Kv1.3 channels; inhibiting KCa3.1 channels, however, had no measurable effects on downstream events such as proliferation and expression of activation markers (Fig. 5.6, green columns).

One approach that may elucidate the roles of Kv1.3 and KCa3.1 ion channels in regulating Ca^{2+}-signaling in T cells would be to use confocal microscopy to monitor Ca^{2+} signaling in single T cells. While a microscopic-based approach has been used since the 1980's to measure $[Ca^{2+}]_i$ in individual T cells (43), the effects of selective blockers of Kv1.3 and KCa3.1 ion channels on single-cell Ca^{2+}-signaling have not been elucidated using human T cells (34). These experiments would provide insights into the roles of KCa3.1 and Kv1.3 ion channels in generating different types of Ca^{2+}-signals (e.g. oscillations) (44, 45). In addition, these experiments would allow examination of single-

cell Ca^{2+}-signaling in different phenotypes of T cells (e.g. T_{em} cells) to probe the effects of K^+-channels in regulating Ca^{2+}-signaling in different phenotypes of cells.

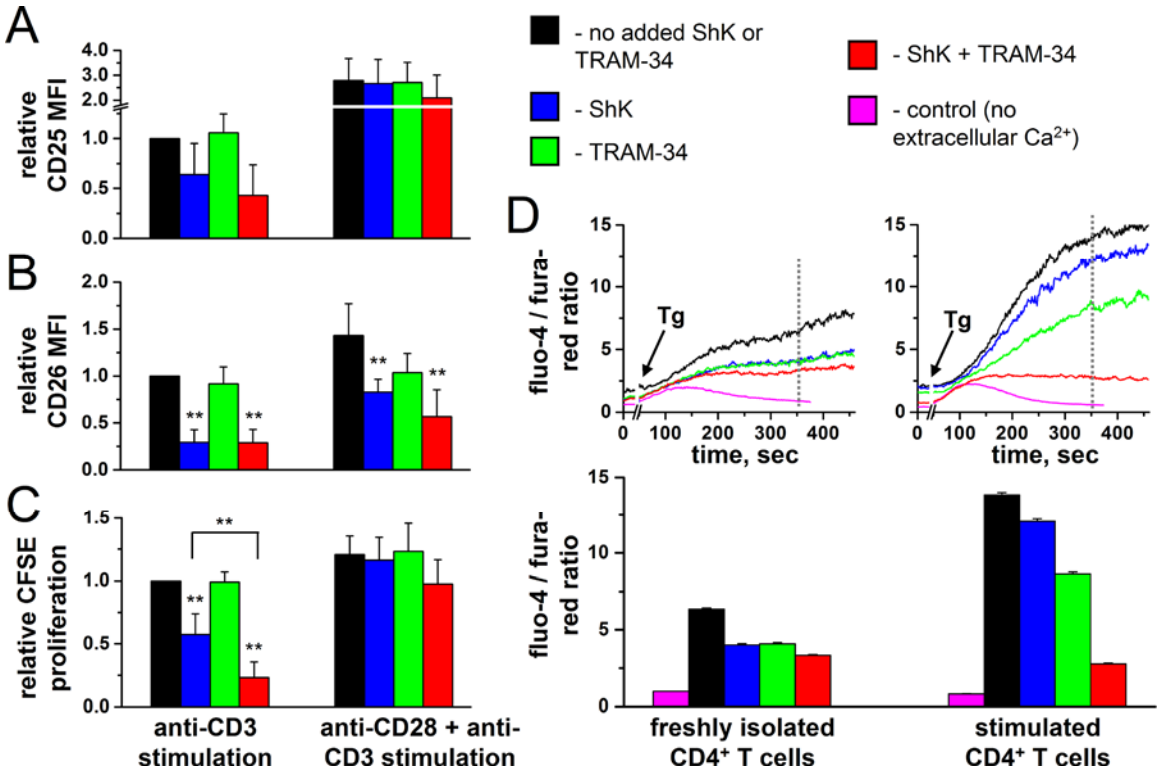

Figure 5.6 | Flow cytometric analysis of the effects of K^+-channel blockers on expression of activation markers, proliferation, and Ca^{2+}-signaling in $CD4^+$ T cells. (A) Expression of CD25 in gated $CD4^+$ T cells selected from PBMCs cultured with either anti-CD3 antibodies (four columns on left) or anti-CD28 plus anti-CD3 antibodies (right) for ~64 h. PBMCs were pre-incubated with either 100 nM ShK to block Kv1.3 channels, 1000 nM TRAM-34 to block KCa3.1 channels, 100 nM ShK plus 1000 nM TRAM-34, or with no added ion channel blockers. Expression levels are expressed as the average and standard deviation of relative mean fluorescence intensity (MFI) from four human subjects. Expression was normalized for each subject using the MFI of cells cultured with anti-CD3 antibodies as the "maximum" value, and MFI of cells cultured without any mitogenic antibodies as the "minimum" value. **(B)** Expression of CD26 in gated $CD4^+$ T cells selected from PBMCs described in *(A)*. **(C)** Proliferation of $CD4^+$ T cells selected from PBMCs initially loaded with 0.25 μM CFSE dye and cultured as described in *(A)* for 96 h. Asterisks (**) represent statistical significance (p<0.01 using Welch's t test) compared to the condition of no added ion channel blockers. **(D)** Calcium signaling, measured using flow cytometry to measure the ratio of two Ca^{2+} sensitive dyes, in $CD4^+$ T cells from freshly drawn blood (left) or after stimulation of PBMCs for 64 h with anti-CD3 plus anti-CD28 antibodies (right). PBMCs were pre-incubated with the indicated K^+-channel blocker for 30 min prior to flow cytometric analysis. Thapsigargin (Tg, 1 μM) was added to cells after 30 seconds of analysis to initiate Ca^{2+}-signaling. The bar graphs (bottom panel) represent the average intracellular Ca^{2+} levels at the 350 s time-point (represented by the dashed line). Ca^{2+}-measurements are representative of experiments with two different human subjects.

In addition to quantifying the effects of K^+-channel blockers on Ca^{2+}-signaling in single cells, it would also be useful to construct mathematical and computer models of Ca^{2+}-signaling in T cells. There are several factors leading to increases of $[Ca^{2+}]_i$, with the main sources being the release of Ca^{2+} from intracellular stores as well as the opening of plasma membrane Ca^{2+}-channels to allow influx of Ca^{2+} from outside the cell (46). There are also several "sinks" leading to decreased $[Ca^{2+}]_i$, including: (i) sarco-endoplasmic reticulum Ca^{2+}-ATPases (SERCA) pumps that pump Ca^{2+} from the cytosol back into the ER; (ii) plasma membrane Ca^{2+}-ATPases (PMCA) that pump Ca^{2+} from the cytosol out of the cell; and (iii) mitochondrial Ca^{2+} pumps (46). Mathematical models that combined all of these sources and sinks, and incorporated membrane potential and K^+ channel distributions, would allow precise studies of the effects of K^+ channels on regulating Ca^{2+}-signaling.

While most recent literature has focused on the role of K^+-channels in Ca^{2+}-signaling, one of the earliest proposed roles K^+-channels was to regulate cellular volume (47, 48). With the finding that Kv1.3 ion channel activity is regulated pathways traditionally associated with T cell growth and proliferation (Chapters 2, 3), it would be interesting to revisit the roles of Kv1.3 ion channels in regulating volume. For example, it would be interesting to measure regulatory volume decrease (RVD) in different phenotypes of T cells both before and after stimulation. Such studies would also explore the effects of blockers of Kv1.3 activity on RVD in different T cell phenotypes, which has not been determined. For example, a potential role of the greatly increased Kv1.3 activity in activated T_{em} cells might be to enhance the ability of these T cells to regulate

volume. Such increased RVD might aid these cells in rapidly homing to peripheral tissues to fight infection, thus linking Kv1.3 activity to cellular migration.

5.10. Concluding remarks

Ion channels are fascinating proteins that are strongly implicated in the pathogenesis of several human diseases (23). The work presented in this thesis provides a novel methodology that enables new experimental possibilities to study these ion channels in cells of the immune system. We explored several of these possibilities, including immunological studies of the pathways that regulate Kv1.3 activity in human T cells, and clinical studies profiling the distributions of Kv1.3 activity in patients with autoimmune disease. The resulting insights from this work suggest that Kv1.3 activity is a useful and sensitive marker of active T cell mediated inflammation in human diseases such as MS and RA. While future experiments must be performed to establish high-throughput measurements of ion channel activity as an effective clinical test, the methods presented in this thesis may have significant impact as a quantitative tool to diagnose and monitor human autoimmune diseases.

Chapter 5 References

1. Wolinsky, J. S., P. A. Narayana, P. O'Connor, P. K. Coyle, C. Ford, K. Johnson, A. Miller, L. Pardo, S. Kadosh, and D. Ladkani, **2007**, Glatiramer acetate in primary progressive multiple sclerosis: results of a multinational, multicenter, double-blind, placebo-controlled trial, *Ann. Neurol.*, 61: 14-24.

2. Frohman, E. M., M. K. Racke, and C. S. Raine, **2006**, Multiple sclerosis--the plaque and its pathogenesis, *N. Engl. J. Med.*, 354: 942-955.

3. Constable, T. J., R. A. Crockson, A. P. Crockson, and B. McConkey, **1975**, Drug treatment of rheumatoid arthritis. A systematic approach, *Lancet*, 1: 1176-1180.

4. Olsen, N. J., and C. M. Stein, **2004**, New drugs for rheumatoid arthritis, *N. Engl. J. Med.*, 350: 2167-2179.

5. O'Dell, J. R., **2004**, Therapeutic strategies for rheumatoid arthritis, *N. Engl. J. Med.*, 350: 2591-2602.

6. Edwards, J. C., L. Szczepanski, J. Szechinski, A. Filipowicz-Sosnowska, P. Emery, D. R. Close, R. M. Stevens, and T. Shaw, **2004**, Efficacy of B-cell-targeted therapy with rituximab in patients with rheumatoid arthritis, *N. Engl. J. Med.*, 350: 2572-2581.

7. Roll, P., T. Dorner, and H. P. Tony, **2008**, Anti-CD20 therapy in patients with rheumatoid arthritis: Predictors of response and B cell subset regeneration after repeated treatment, *Arthritis Rheum.*, 58: 1566-1575.

8. Wulff, H., H. G. Knaus, M. Pennington, and K. G. Chandy, **2004**, K+ channel expression during B cell differentiation: Implications for immunomodulation and autoimmunity, *J. Immunol.*, 173: 776-786.

9. Poulopoulou, C., Z. Papadopoulou-Daifoti, A. Hatzimanolis, K. Fragiadaki, A. Polissidis, E. Anderzanova, P. Davaki, C. G. Katsiari, and P. P. Sfikakis, **2008**, Glutamate levels and activity of the T cell voltage-gated potassium Kv1.3 channel in patients with systemic lupus erythematosus, *Arthritis Rheum.*, 58: 1445-1450.

10. Dalton, C. M., P. A. Brex, K. A. Miszkiel, S. J. Hickman, D. G. MacManus, G. T. Plant, A. J. Thompson, and D. H. Miller, **2002**, Application of the new McDonald criteria to patients with clinically isolated syndromes suggestive of multiple sclerosis, *Ann. Neurol.*, 52: 47-53.

11. McDonald, W. I., A. Compston, G. Edan, D. Goodkin, H. P. Hartung, F. D. Lublin, H. F. McFarland, D. W. Paty, C. H. Polman, S. C. Reingold, M. Sandberg-Wollheim, W. Sibley, A. Thompson, S. van den Noort, B. Y. Weinshenker, and J. S. Wolinsky, **2001**, Recommended diagnostic criteria for multiple sclerosis: guidelines from the International Panel on the diagnosis of multiple sclerosis, *Ann. Neurol.*, 50: 121-127.

12. Filippi, M., M. Bozzali, M. Rovaris, O. Gonen, C. Kesavadas, A. Ghezzi, V. Martinelli, R. I. Grossman, G. Scotti, G. Comi, and A. Falini, **2003**, Evidence for widespread axonal damage at the earliest clinical stage of multiple sclerosis, *Brain*, 126: 433-437.

13. Kuhlmann, T., G. Lingfeld, A. Bitsch, J. Schuchardt, and W. Bruck, **2002**, Acute axonal damage in multiple sclerosis is most extensive in early disease stages and decreases over time, *Brain*, 125: 2202-2212.

14. Bielekova, B., M. H. Sung, N. Kadom, R. Simon, H. McFarland, and R. Martin, **2004**, Expansion and functional relevance of high-avidity myelin-specific CD4+ T cells in multiple sclerosis, *J. Immunol.*, 172: 3893-3904.

15. Wulff, H., P. A. Calabresi, R. Allie, S. Yun, M. Pennington, C. Beeton, and K. G. Chandy, **2003**, The voltage-gated Kv1.3 K+ channel in effector memory T cells as new target for MS, *J. Clin. Invest.*, 111: 1703-1713.

16. Beeton, C., H. Wulff, N. E. Standifer, P. Azam, K. M. Mullen, M. W. Pennington, A. Kolski-Andreaco, E. Wei, A. Grino, D. R. Counts, P. H. Wang, C. J. LeeHealey, S. A. B, A. Sankaranarayanan, D. Homerick, W. W. Roeck, J. Tehranzadeh, K. L. Stanhope, P. Zimin, P. J. Havel, S. Griffey, H. G. Knaus, G. T. Nepom, G. A. Gutman, P. A. Calabresi, and K. G. Chandy, **2006**, Kv1.3 channels are a therapeutic target for T cell-mediated autoimmune diseases, *Proc. Natl. Acad. Sci. U. S. A.*, 103: 17414-17419.

17. Whiting, P., R. Harbord, C. Main, J. J. Deeks, G. Filippini, M. Egger, and J. A. Sterne, **2006**, Accuracy of magnetic resonance imaging for the diagnosis of multiple sclerosis: systematic review, *BMJ*, 332: 875-884.

18. DeCoursey, T. E., K. G. Chandy, S. Gupta, and M. D. Cahalan, **1984**, Voltage-gated K+ channels in human T lymphocytes: a role in mitogenesis?, *Nature*, 307: 465-468.

19. Schroeder, K., B. Neagle, D. J. Trezise, and J. Worley, **2003**, IonWorks (TM) HT: A new high-throughput electrophysiology measurement platform, *J. Biomol. Screen.*, 8: 50-64.

20. Uram, J. D., K. Ke, A. J. Hunt, and M. Mayer, **2006**, Label-free affinity assays by rapid detection of immune complexes in submicrometer pores, *Angew. Chem. Int. Ed. Engl.*, 45: 2281-2285.

21. Dunlop, J., M. Bowlby, R. Peri, D. Vasilyev, and R. Arias, **2008**, High-throughput electrophysiology: an emerging paradigm for ion-channel screening and physiology, *Nat. Rev. Drug Discov.*, 7: 358-368.

22. Sakmann, B., and E. Neher, **1995**, *Single-Channel Recording*; Plenum Press: New York.

23. Beeton, C., and K. G. Chandy, **2005**, Potassium channels, memory T cells, and multiple sclerosis, *Neuroscientist*, 11: 550-562.

24. Chandy, K. G., H. Wulff, C. Beeton, M. Pennington, G. A. Gutman, and M. D. Cahalan, **2004**, K+ channels as targets for specific immunomodulation, *Trends Pharmacol. Sci.*, 25: 280-289.

25. Schmitz, A., A. Sankaranarayanan, P. Azam, K. Schmidt-Lassen, D. Homerick, W. Hansel, and H. Wulff, **2005**, Design of PAP-1, a selective small molecule Kv1.3 blocker, for the suppression of effector memory T cells in autoimmune diseases, *Mol. Pharmacol.*, 68: 1254-1270.

26. Chandy, G., H. Wulff, C. Beeton, P. Calabresi, G. A. Gutman, and M. Pennington, **2006**, The Kv1.3 potassium channel: physiology, pharmacology, and therapeutic indications, In: *Voltage-Gated Ion Channels as Drug Targets*; Triggle, D. J., M. Gopalakrishnan, D. Rampe, and W. Zheng, Eds.; Wiley-VCH: Weinheim, Germany, pp 214-252.

27. Vennekamp, J., H. Wulff, C. Beeton, P. A. Calabresi, S. Grissmer, W. Hansel, and K. G. Chandy, **2004**, Kv1.3-blocking 5-phenylalkoxypsoralens: a new class of immunomodulators, *Mol. Pharmacol.*, 65: 1364-1374.

28. Abbas, A. K., and A. H. Lichtman, **2005**, *Cellular and Molecular Immunology*, 5th Ed. ed.; Elsevier Saunders: Philadelphia, PA.

29. Kiss, L., P. B. Bennett, V. N. Uebele, K. S. Koblan, S. A. Kane, B. Neagle, and K. Schroeder, **2003**, High throughput ion-channel pharmacology: planar-array-based voltage clamp, *Assay Drug Dev. Technol.*, 1: 127-135.

30. Estes, D. J., S. Memarsadeghi, S. K. Lundy, F. Marti, D. D. Mikol, D. A. Fox, and M. Mayer, **2008**, High-throughput profiling of ion channel activity in primary human lymphocytes, *Anal. Chem.*, 80: 3728-3735.

31. Estes, D. J., S. K. Lundy, F. Marti, D. A. Fox, and M. Mayer, **2008**, Functional regulation of Kv1.3 ion channels in human T lymphocytes, *In preparation*.

32. Ghanshani, S., H. Wulff, M. J. Miller, H. Rohm, A. Neben, G. A. Gutman, M. D. Cahalan, and K. G. Chandy, **2000**, Up-regulation of the IKCa1 potassium channel during T-cell activation. Molecular mechanism and functional consequences, *J. Biol. Chem.*, 275: 37137-37149.

33. Grissmer, S., A. N. Nguyen, and M. D. Cahalan, **1993**, Calcium-activated potassium channels in resting and activated human T lymphocytes. Expression levels, calcium dependence, ion selectivity, and pharmacology, *J. Gen. Physiol.*, 102: 601-630.

34. Grissmer, S., R. S. Lewis, and M. D. Cahalan, **1992**, Ca(2+)-activated K+ channels in human leukemic T cells, *J. Gen. Physiol.*, 99: 63-84.

35. Lewis, R. S., and M. D. Cahalan, **1995**, Potassium and calcium channels in lymphocytes, *Annu. Rev. Immunol.*, 13: 623-653.

36. Bruggemann, A., S. Stoelzle, M. George, J. C. Behrends, and N. Fertig, **2006**, Microchip technology for automated and parallel patch-clamp recording, *Small*, 2: 840-846.

37. Kudlacz, E., B. Perry, P. Sawyer, M. Conklyn, S. McCurdy, W. Brissette, M. Flanagan And, and P. Changelian, **2004**, The novel JAK-3 inhibitor CP-690550 is a potent immunosuppressive agent in various murine models, *Am J Transplant*, 4: 51-57.

38. El-Kholy, W., P. E. Macdonald, J. H. Lin, J. Wang, J. M. Fox, P. E. Light, Q. Wang, R. G. Tsushima, and M. B. Wheeler, **2003**, The phosphatidylinositol 3-kinase inhibitor LY294002 potently blocks K(V) currents via a direct mechanism, *FASEB J.*, 17: 720-722.

39. Goffinet, C., and O. T. Keppler, **2006**, Efficient nonviral gene delivery into primary lymphocytes from rats and mice, *Faseb J*, 20: 500-502.

40. McManus, M. T., B. B. Haines, C. P. Dillon, C. E. Whitehurst, L. van Parijs, J. Chen, and P. A. Sharp, **2002**, Small interfering RNA-mediated gene silencing in T lymphocytes, *J. Immunol.*, 169: 5754-5760.

41. Marodon, G., E. Mouly, E. J. Blair, C. Frisen, F. M. Lemoine, and D. Klatzmann, **2003**, Specific transgene expression in human and mouse CD4+ cells using lentiviral vectors with regulatory sequences from the CD4 gene, *Blood*, 101: 3416-3423.

42. Peer, D., P. Zhu, C. V. Carman, J. Lieberman, and M. Shimaoka, **2007**, Selective gene silencing in activated leukocytes by targeting siRNAs to the integrin lymphocyte function-associated antigen-1, *Proc Natl Acad Sci U S A*, 104: 4095-4100.

43. Lewis, R. S., and M. D. Cahalan, **1989**, Mitogen-induced oscillations of cytosolic Ca2+ and transmembrane Ca2+ current in human leukemic T cells, *Cell Regul.*, 1: 99-112.

44. Agrawal, N. G. B., and J. J. Linderman, **1995**, Calcium Response of Helper T-Lymphocytes to Antigen-Presenting Cells in a Single-Cell Assay, *Biophys. J.*, 69: 1178-1190.

45. Dolmetsch, R. E., R. S. Lewis, C. C. Goodnow, and J. I. Healy, **1997**, Differential activation of transcription factors induced by Ca2+ response amplitude and duration, *Nature*, 386: 855-858.

46. Lewis, R. S., **2001**, Calcium signaling mechanisms in T lymphocytes, *Annu. Rev. Immunol.*, 19: 497-521.

47. Grinstein, S., and J. D. Smith, **1990**, Calcium-independent cell volume regulation in human lymphocytes. Inhibition by charybdotoxin, *J. Gen. Physiol.*, 95: 97-120.

48. Lewis, R. S., P. E. Ross, and M. D. Cahalan, **1993**, Chloride channels activated by osmotic stress in T lymphocytes, *J. Gen. Physiol.*, 101: 801-826.